Distributed Source Seeking with Formation Control of Multi-Agent Systems

Vom Promotionsausschuss der
Technischen Universität Hamburg
zur Erlangung des akademischen Grades

Doktor-Ingenieur (Dr.-Ing.)

genehmigte Dissertation

von

Siavash Ahmadi Barogh

aus

Zandschan, Iran

2023

1. Gutachter:
Prof. Dr. Herbert Werner

2. Gutachter:
Prof. Dr. Uwe Weltin

Vorsitzende des Promotionsverfahrens:
Prof. Dr.-Ing. Robert Seifried

Tag der mündlichen Prüfung: 15. Dezember 2022

Author: https://orcid.org/0009-0003-5334-1458

ISBN: 978-3-8439-5290-3

DOI: https://doi.org/10.15480/882.5125

Dedicated to my lovely wife, Shabnam and my cute daughter, Sevda

Acknowledgments

I use this opportunity to express my sincere gratitude to my supervisor Prof. Dr. Herbert Werner who gave me a chance to come to Germany and be his student. I appreciate him for his strong support and leadership during my research time at the Institute of Control Systems (ICS) of the Hamburg University of Technology (TUHH). He led me through my Ph.D. and I used his advice and encouragement and his rich knowledge during my research so much. Also at the Institute of Control Systems, I had an opportunity to take part in some enhanced lectures that were taught by Prof. Werner such as Optimal and Robust Control and Neural Network and also I participated in his seminars which opened my academic knowledge in my field of research.

I am exactly thankful to Prof. Dr. Uwe Weltin for being an examiner of my doctoral thesis, and special thanks to Prof. Dr.-Ing. Robert Seifried for chairing the doctoral committee. Also, I would like to have special thanks to the former secretary of the Institute of Control Systems, Ms. Bettina Schrieber, and Mrs. von Dewitz, who made so much effort during my Ph.D. time also special thanks go to Ms. Christine Kopf, the current secretary of the ICS, she not only did so many efforts during my research time but also she helped so much in the submission procedure of my thesis. I am also thankful to Dr. Esteban Rosero for the helpful discussions and his useful ideas during my Ph.D. I would also like to express my thankfulness to Mr. Herwig Meyer and Mr. Klaus Baumgart and Mr. Uwe Jahns for their technical support and friendly helps.

The experimental results of this work were not achieved without the contributions and help of numerous students, who worked on this research with their Bachelor's or Master's thesis or project work. They enthusiastically and with interest made many efforts to do well and complete the implementation part of this research and used their scientific power and creative intelligence. I should mention Oliver Menck and Martin Kiefer who especially did a great job with their valuable contributions. I am thankful to them.

I would like to express my gratitude to my wife, Shabnam Moeini for her constant rich support and helps during my research and study. She stood strongly beside me and I could rely on her as a standing pillar during the whole process of my Ph.D. from the beginning until the end. I am truly thankful for having her in my life. She has always been supportive, and patient all over the times of discomfort or failure. She worked during my research time and based on her financial support, I could spend the whole of my time researching and my mind could be free from all other issues except research. I am a lucky guy who has a wife that cares me for everything and is patient in all difficulties. Also special dedication to my daughter Sevda who is the love and brightness in my life and

also special warm thanks to my parents, Maliheh and Rasoul and Shabnams' parents, Soudabeh and Ali, and my sisters, Mehrnosh and Solmaz, and Shabnam's brothers, Reza and Hossein, for all of their support and good energy and mood during the Ph.D. time.

Summary

Distributed control of multi-agent systems is a research area that has been receiving considerable attention for many years. Collaboration between a group of autonomous agents can be a key element for solving complex problems in a variety of applications. In this work, novel solutions to the formation control problem are proposed and applied to the source seeking problem.

The agents considered in this work are autonomous dynamic systems that are capable of sensing, moving, changing direction and speed, and of exchanging information with neighbors. It is assumed that agents are moving in two dimensional space. Physical representations of such agents can be e.g. wheeled robots, spinning objects or four-wheel vehicles.

The formation control problem is a fundamental problem in cooperative control – a group of agents is required to arrange themselves in a specified geometric pattern relative to each other, and to maintain this shape. Control schemes need to be implemented in a distributed manner, and an important aspect is the scalability of the associated analysis and synthesis problems. In this work, analysis and synthesis results with complexity corresponding to the size of a single are presented for novel formation control strategies. These strategies include both displacement-based methods and distance-based methods, where an advantage of the latter is that it does not require a common coordinate system for all agents. A displacement-based strategy is proposed for non-holonomic agents, and a novel approach to distance-based formation control is presented that includes angle information and facilitates the generation of rigid formations and can be applied to agents with single integrator dynamics, double integrator dynamics and to non-holonomic agents. All proposed approaches are capable of collision avoidance.

The proposed formation control schemes are then applied to the source seeking problem, where the source (extremum) of an unknown but measurable scalar field is to be located. For this purpose, gradient-based source seeking is combined with distance-based formation control to yield a novel distance-based source seeking strategy. Lyapunov stability of this approach is established for single and double integrator agents as well as for kinematic and dynamic non-holonomic agents.

The practicality of the proposed methods is illustrated in simulation studies and experimental validation with a group of wheeled robots.

Contents

List of Figures

List of Tables

Chapter 1

Introduction

1.1 Multi-Agent Systems

In recent years, the field of multi-agent systems control is receiving increasing attention. In many fields a group of agents equipped with suitable sensors is used to perform a complicated mission. In hazardous environments where there is a high probability of danger for the presence of humans, a multi-agent system with cooperative agents can collect enough data from the environment. In comparison with a single agent, the multi-agent system can collect more info from the environment in several multiple spots with simple agents while a single agent needs to be equipped with enhanced sensors and can not catch data from several different points simultaneously. Also single agents have restrictions. The sensor range is limited therefore to capture enough data, a single agent needs sharp and fast maneuvering, which would be complicated in the actual environment.

In this work, we assume that each agent is an autonomous dynamic system that can fulfill different actions together such as sensing, moving, changing the direction and speed, and communicating with each other. Agents are assumed to move in a $2D$ plane and without any boundary, The size of each agent and the number of all agents are not limited in this work. In real environments, wheeled robots, spinning objects, or four-wheel vehicles would be some physical representations of agents.

A multi-agent system (MAS) can be implemented in two formats: Centralized and distributed. In a centralized format, all information that is gathered from all agents is processed in one processor. The result of processing is transferred to each agent to steer the agent through the defined objective. This method has an advantages and disadvantages. The main advantage of this method is the availability of all information to make the best decision. In other words according to accessing all gathering data by the central processor, this processor can apply the best algorithm to achieve the best results. But besides these advantages, some disadvantages arise. The computation power in central processors needs to be high enough to analyze a huge amount of data. The performance of computation is strongly dependent on the number of agents. Due to collecting all data in the common center, the communication delay is another important issue that affects the centralized multi-agent system's functionality. The security of centralized sys-

tems is always problematic because of the vulnerability of a system to the failure of the computation center.

In contrast to the centralized format, there would be distributed format multi-agent systems. In the distributed multi-agent system the information data is distributed through all agents and the calculation is done inside each agent. The communication platform can be predefined or adaptive. There is no center of computation and all agents are collecting data from their neighbors and their local sensors. The distribution control is applied between distributed multi-agent systems, which means all agents calculate the control law based on their collecting data (from sensors or neighbors via communication). The reliability of the system increased and in a case of failure in one or more agents the multi-agent system can keep its existence and still other agents can follow the mission. The calculation effort in each agent is less and so the processors can be simpler than the processor in the centralized method.

Biological systems in nature are good examples of multi-agent distributed systems that can cooperatively handle a task. cooperation between animals inside the group to find a path or to find a source of seeds or foodstuffs. A group of animals such as flocks of ducks or gooses cooperates to find a path in their migration over thousands of kilometers. They employ strategic techniques in a special formation to find the direction of flying and also to save energy and to use air streams during a long trip. The cooperative geometrical shape with multiple agents is denoted by Formation.

1.2 Formation Control

Formation control of mobile agents is one of the main problems in this context, where formation control means to maintain a group of agents (e.g. mobile robots) in a specified geometric formation (Chen and Wang [2005]). distributed approaches to cooperative control involving analysis and synthesis problems of the size of a single agent are of interest, regardless of the number of agents. There are numerous applications related to formation control such as control of vehicle platoons, wheeled robots, satellites etc (Ren [2006]).

The nature of cooperative control in multi-agent systems is distributed, therefore, control laws depend on the information flow among agents. Communication graphs are used to represent this information flow. The designer assigns references to individual agents, and all agents try to achieve their desired reference as a local goal. Achieving a specified formation is to be guaranteed by covering local references (Oh et al. [2012]).

The concept of formation control has a strong relationship with the consensus problem (Olfati-Saber et al. [2007]), (Jadbabaie et al. [2003]). Control laws are based on information exchange between agents and relative distances among agents. Agents try to achieve agreement on values of a subset of their state variables, referred to as consensus. Attaining a given formation can be seen as reaching consensus (Olfati-Saber and Murray [2004]).

Formation control for agents with non-holonomic constraints is significantly more complex than for agents with linear time-invariant models. Some work has been done on non-holonomic agents control by time varying mission control (Yamaguchi [2002]) or by input-

output linearisation (Lawton et al. [2003]). Other researchers have studied leader follower techniques (Chen et al. [2010]), (Consolini et al. [2008]). In (Dong and Farrell [2008]) control laws are designed in two parts. First the purpose is to reach some stationary points, and in the second part they propose control laws to achieve a formation and also to track a desired trajectory. In (Kostić et al. [2010]) the formation can be time-varying but the reference trajectory for all agents defines the formation shape. So it is always needed to take a trajectory to maintain the formation for all agents. In (Sadowska et al. [2011]) formation control is implemented by designing a virtual structure for each mutual couple of agents. The design of a virtual structure for any couple of agents requires heavy calculation, too. In (Dimarogonas and Kyriakopoulos [2007]) control laws are presented to achieve rendezvous among non-holonomic agents in terms of position or orientation. In (Lin et al. [2005]) necessary and sufficient graphical conditions for formation control of uni-cycle agents are analyzed and evaluated.

1.3 Formation Control Formats

Research related to formation control can be divided into two groups, displacement approaches, and distance-based approaches. The main difference between both approaches is the availability of a common coordinate system for agents(Oh et al. [2015]). Special attention is given to distance-based formation control due to its entirely distributed structure. Agents do not need to share a common coordinate system and the main objective for each agent is to control its position using the information taken from local sensors. The absence of a common coordinate systems makes distance-based formation control schemes more challenging

Formation control research based mainly on distributed approaches (Oh et al. [2015]), meaning that "global sensing information" was used to achieve the desired formation. Lately, however, research has moved to analyzing distributed approaches. Distributed approaches only use local sensing information to achieve the desired formation.

Most existing formation control approaches can be categorized into three types (Oh et al. [2015]):

- **Position-based approaches** are based on positions with respect to a global coordinate system. The description of the desired formation as well as the measured positions of the agents are all based on this global coordinate system, relative to which the agents' positions are controlled. This approach is shown in Fig. 1.3.1 for three agents i, j and k (Verginis et al. [2017]).

- **Displacement-based approaches** are still based on a global coordinate system in which now the displacements between agents are measured. The description of the desired formation then only uses these displacements and the agents' formation is achieved merely by controlling the displacements. Unlike in position-based approaches, the actual positions of the agents are not used for the control law. Fig. 1.3.1 depicts an example where displacements are measured relative to agent i

(Ahmadi Barogh et al. [2015]). Due to the use of the same coordinate system between all agents, this format of formation control is also called "global frame" formation control (Montijano et al. [2014]).

- **Distance-based approaches** remove the need for a global coordinate system completely, being based only on the relative positions between pairs of agents with respect to their local coordinate systems. The formation is achieved only by controlling these distances without any information about the agents' position with respect to some global coordinate system. This approach is illustrated in Fig. 1.3.1 in which distances are determined with respect to agent i's local coordinate system. The angle between agents also can be added as an extra factor to improve the rigidity of formation achievement as well (Ahmadi Barogh and Werner [2016a]). In some works the term 'local frame' is used instead of distance-based but it has the same meaning (Gonzlez et al. [2019]).

In (Baillieul and Suri [2003]) Baillieul and Suri propose a control law for distance-based formation control, and prove the stability within a minimally persistent graph. Local and global stability of formation control by the distance-based strategy is investigated in (Dimarogonas and Johansson [2008]) (Krick et al. [2008]) (Dorfler and Francis [2010]). In (Oh and Ahn [2014]) the local asymptotic stability of single and double integrator agents is analyzed and proved for rigid formations. In (Bishop [2011]) (Eren [2012]) (Zhaoa et al. [2014]) control laws are proposed for formation control using inter-neighbor bearing information. In (Zhao and Zelazo [2015]) stabilizing target formations specified by inter-neighbor bearings are investigated. In (Gouvea et al. [2010]) the formation control of unicycle agents with unknown dynamic parameters is addressed.

In (Bishop et al. [2013]) combining directions and distances is proposed. The hierarchical formation control of a group of non-holonomic agents is investigated in (Consolini et al. [2009]). The distance and angle between the orientations of agents are used to define a control law. Agents need to know the direction and speed of the leaders and should follow in the same coordinate system. In (Fidan et al. [2013]), single-view distance estimation-based formation control is proposed for multi-agent systems; agents have single-integrator or non-holonomic dynamics and are equipped with cameras to detect distances between themselves. In (Tran and Lee [2011]) agents use angles and distances to define a formation between themselves. In the control law which was proposed, each agent knows the direction of its leader with respect to a common x axis.

The conventional distance-based formation controllers only stabilize the the formation shape while the orientation of whole formation is not considered. In some recent works orientation control is studied. The distance-based formation control with orientation control is studied in (Sun and Anderson [2015]) (Park and Hyo-Sung [2015]). In these works the agent model is a single integrator, and if the initial formation shape and the desired formation shape are close enough and the initial orientation of agents and the desired orientation are close enough also then the agents achieve the desired formation and the desired orientation. In (Park and Hyo-Sung [2015]) the position of formation centroid should be preserved but in (Sun and Anderson [2015]) this condition is not needed.

There are some approaches that have been proposed for large-scale systems. In such

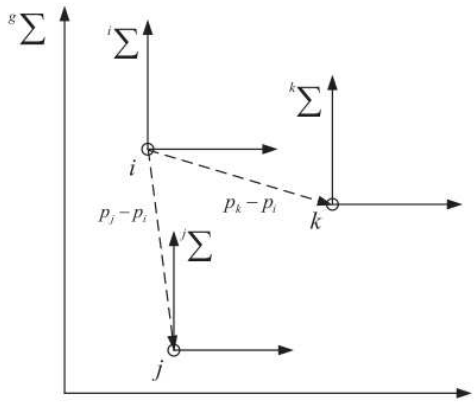

(a) Displacement-based setup.

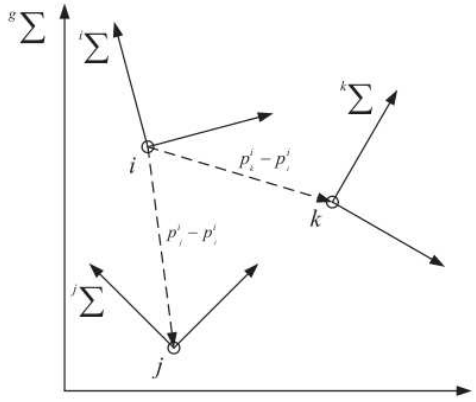

(b) Distance-based setup.

Figure 1.3.1: Types of formation control approaches. (Oh et al. [2012])

systems, the individual positions are not important but the density of agents that are located in a specific area or sphere in space is taken into account. Bandyopadhyay et al., use the idea of the probability of agent location and its distribution to specify the formation (Bandyopadhyay et al. [2017]). In swarm-based formation approaches the exact absolute position of each agent is not important but the global distribution of all agents needs to be defined for all in the common coordinate system (Li et al. [2019]). In (Queralta et al. [2019a]), the authors proposed a method that requires only one-way communication and also they assumed that agents have the same orientation reference therefore they need some kind of sensors to define configurations with a predefined orientation. In (Queralta et al. [2019b]) a formation algorithm for a swarm of agents is proposed that enables different configurations with communication-free and index-free implementation. Absolute positioning is still needed in their approach. In (Mateo et al. [2017]) the relationship between the number of connections and effectiveness in static networks of swarm robots is investigated.

1.4 Source Seeking

Source seeking means to localize the source extremum of a scalar field. Localizing and detecting the source with a cooperative multi-agent system is effective in a wide range of applications. Cooperative source seeking can be used in environmental monitoring (Ogren et al. [2004]), oil pollution management (Senga et al. [2007]), environmental disaster monitoring, rescue cases sound source localization, chemical spill searching etc; cases when for a single agent estimating the gradient would be hard. Usually, all agents are equipped with relevant sensors to detect the concentration of the scalar field. Cooperative source seeking with a distance-based formation strategy is implemented in situations when common coordinates are not available, for example in indoor areas.

On top of formation control, in this work we use source seeking to locate the source of a measured scalar field in a plane. This means the agents moving in the plane will attempt to find the local maximum of a scalar field. Source seeking in general is the process of finding the source of some substance or signal, which can be heat, light, a chemical substance or something else. It is found in nature, where animals among other things locate the source of sound and use odor or chemical signals to reach the source of some distributed substance (Fabbiano [2015]). From a technical perspective, source seeking is specifically helpful to operate autonomous agents in hazardous environments, such as fire spots, chemical spill belts or for conducting environmental studies (Rosero and Werner [2014]).

There are various proposed approaches to deal with the source seeking problem. Several approaches are focused on behavior-based source seeking methods (Farrell et al. [2005]), (Spears et al. [2004]). In behavior-based source seeking approaches, a set of behaviors and their combinations are defined. A group of behaviors is activated and caused to drive a single agent or a multi-agent system to the source direction. However, the main difficulty of behavior-based methods is ignoring the local dynamics of agents. Other approaches concentrate on control-based source seeking and unlike the behavioral-based methods, in control-based methods, the dynamics of agents is entirely considered in the proposed control laws (Gazi and Passino [2004]), (Zhang et al. [2007]). In (Rabbat and Nowak [2004]), sensors are distributed all over the testing environment in constant positions without moving. A centralized optimization algorithm uses the information obtained via sensors to solve the problem of source seeking. In (Biyik and Arcak [2007]), (Zhang and Leonard [2010]), a number of algorithms are proposed to deal with source seeking in multi-agent systems. In most of these algorithms all-to-all communication is required also the center of mass of formation is a key to estimating the gradient and steer the group of agents to the source. In (Wu and Zhang [2012]) not only immediate real-time measurements are used to estimate the gradient but also the off-time series of measurement data are included. In (Brinon-Arranz et al. [2016]) the problem of source seeking is addressed for a group of agents via locating them in a cicular formation. Agents are spinning around the center of mass of formation and the gradient is estimated at the center. In (Li et al. [2014]) for both all-to-all and limited communication appropriate control laws are proposed. In the limited communication case, several consensus filters are assumed and therefore achieving consensus through those filters takes a long time and the control laws

act slowly. In (Rosero and Werner [2014]), a new approach is proposed to locating the scalar field's unknown source. The communication is undirected and constrained. Each agent uses the neighbors' signal strength and absolute position to estimate the gradient direction, and with a distributed controller a specified formation shape is maintained. In (Moore and Canudas-de Wit [2010]), (Brinon-Arranz et al. [2011]), (Brinon-Arranz et al. [2014]) a collaborative control law to lead a group of underwater vehicles to the source by organizing a circular formation for vehicles is studied. Formation control laws to achieve and maintain a circular formation are investigated. In (Atanasov et al. [2014]), two algorithms based on gradient estimation at the center of the formation are proposed; they use stochastic approximation to achieve convergence in the estimation of the gradient at the center. The control laws are based on relative positioning with respect to neighbor agents and the center of mass of formation. In (Fabbiano et al. [2014]) a circular formation and source seeking are combined as a two objectives. Both objectives are included in the control law and convergence is achieved. In (Fabbiano et al. [2018]) a distributed algorithm to estimate the gradient of the scalar field is proposed and this information is used to drive a group of rotating sensors towards the source, without using full position information. Sensors are rotating around the circular formation. Lazna and others proposed cooperative source seeking in (Lazna et al. [2018]) and localization of gamma-radiation in outdoor environments. In their approach there is a cooperation between a human operator, an unmanned aerial vehicle, and an unmanned ground vehicle. Al-Abri and Zhang in (Al-Abri et al. [2018]) and (Al-Abri and Zhang [2022]) proposed a distributed algorithm that enables swarms of agents to perform source seeking and level curve tracking without estimation of the field gradient or sharing the scalar field measurements. They need to use a common coordinate system. In (Al-Abri et al. [2019]) the authors used a leader-based consensus algorithm in a sphere shape to achieve the common movement direction with the assumption that agents can detect the velocity and its direction of their neighbors. In (Wang et al. [2019]), a cooperative distributed control law is developed for a group of two agents. One of those estimates the gradient of a scalar field and the other agents follow it.

In (Hutchinson et al. [2017]) a review of techniques used to gain information about atmospheric events and the review has resulted in a discussion on the current limitations of source term estimation. In (Turgeman and Werner [2017]) a distributed control scheme based on hierarchy formation and reduced topology is proposed. The agents, equipped with sensors, navigate by using an estimated gradient method and their neighbors' shared measurements. In (Turgeman et al. [2019]) an approach is proposed for source seeking without gradient estimation and global localization. They used a flocking approach which is combined with a technique inspired by glowworm swarm optimization.

Most of the above approaches need the absolute position with respect to a common coordinate system. In (Fabbiano et al. [2018]), (Fabbiano et al. [2014]) the position information is not necessary but sensors are constantly spinning in the circular formation. In (Atanasov et al. [2014]) the relative localization with respect to the center of formation is required.

Source seeking studied in this work is achieved by using gradient estimation, using data points from several agents in the plane. Although source seeking is possible using merely

a single agent, multi-agent source seeking has been an increasingly researched because it offers multiple advantages, such as more robustness and increased efficiency in comparison to single-agent systems (Rosero and Werner [2014]). In experiments carried out as part of this work, the source to be found is a light bulb. Agents measure the infrared intensity at their position to locate the light bulb while retaining the desired formation.

1.5 Preliminaries

1.5.1 Notation

A formation of N mobile agents is described in terms of graph theory. Therefore some of the basic concepts in graph theory are reviewed briefly (Mesbahi and Egerstedt [2010]). Note in this work we consider two graphs associated with agents: a formation graph $\mathcal{G}_f$ and a source seeking communication graph $\mathcal{G}_s$. A formation directed graph with N vertices and M_f edges is denoted by $\mathcal{G}_f = (\mathcal{V}, \mathcal{E}_f)$ where $\mathcal{V} = \{1, \cdots, N\}$ and $\mathcal{E}_f \subset \mathcal{V} \times \mathcal{V}$, $|\mathcal{E}_f| = M_f$. The neighbor agent set of agent i is denoted by $\mathcal{N}_{fi} = \{j \in \mathcal{V} : (i,j) \in \mathcal{E}_f\}$. We consider $(i,j) \in \mathcal{E}_f$ a directed edge if the distance between agent i and j is considered to be controlled. We Let $p_i(t) \in \mathbb{R}^n$ represent the position of vertex (agent) i in n-dimensional space at time t for all $i \in \mathcal{V}$ and the vector $p = \begin{bmatrix} p_1^T & \cdots & p_N^T \end{bmatrix}^T \in \mathbb{R}^{nN}$ is the position vector of all agents. The framework $(\mathcal{G}_f, p)$ represents a graph $\mathcal{G}_f$ in $\mathbb{R}^n$. Two frameworks $(\mathcal{G}_f, p)$ and $(\mathcal{G}_f, p')$ from the same graph are equivalent if $\|p_i - p_j\| = \|p'_i - p'_j\|$ for all $(i,j) \in \mathcal{E}_f$ and are congruent if $\|p_i - p_j\| = \|p'_i - p'_j\|$ for all $i, j \in \mathcal{V}$. A sequence of edges $(i_1, i_2), (i_2, i_3), \cdots, (i_{k-1}, i_k)$ where $i_1, i_2, \cdots i_k \in \mathcal{V}$, is defined as a directed path in $\mathcal{G}_f$ and i_1 and i_k are the start and the end vertex of the directed path. If the start and the end vertices of the directed path are the same, the directed path is referred to as a cycle. A directed graph which has no directed cycle is referred to as an acyclic (cycle free) directed graph (Biggs et al. [1993]).

The graph $\mathcal{G}_s = (\mathcal{V}, \mathcal{E}_s)$ is an undirected graph to model the interaction among agents, where $\mathcal{V} = \{1, ..., N\}$ is the set of nodes and $\mathcal{E}_s \subseteq \mathcal{V} \times \mathcal{V}$ is the set of edges. Every edge corresponds to a bidirectional information exchange channel. An edge $(i,j) \in \mathcal{E}_s$ indicates that agent i and j exchange information. The adjacency matrix $A_s = [a_{ij}] \in \mathbb{R}^{N \times N}$ of a graph $\mathcal{G}_s$ with N nodes specifies the interconnection topology of the network. Here $a_{ij} = 1$ if $(i,j) \in \mathcal{E}_s$, else $a_{ij} = 0$. We let $\mathcal{N}_{si} = \{i \in \mathcal{V} : a_{ij} \neq 0\}$ denote the set of neighbors of node i that exchanges information with node i.

The adjacency matrix $\mathcal{A}_{\{} = [a_{ij}] \in \mathbb{R}^{N \times N}$ of a graph $\mathcal{G}_f = (\mathcal{V}, \mathcal{E}_f)$ with N nodes specifies the interconnection topology of the network. Here $a_{ij} = 1$ if $(i,j) \in \mathcal{E}$, else $a_{ij} = 0$. The Laplacian matrix L of the graph $\mathcal{G}$ is defined as $L = \Delta - \mathcal{A}$, where Δ =diag$(\mathcal{A} \cdot \mathbf{1})$ is a diagonal matrix with the nodes' degrees on its diagonal, i.e., $\Delta_{ii} = d_i = \sum_j a_{ij}$. Here $\mathbf{1} = [1\ 1\ 1\ ...\ 1]^T \in \mathbb{R}^N$ denotes the vector of ones, which is a right eigenvector of L corresponding to $\lambda_1 = 0$, i.e., $\mathcal{L} \cdot \mathbf{1} = 0$. The second smallest eigenvalue λ_2 determines the speed of convergence of the algorithm.

Remark 1.5.1. *In this thesis, we assume that $\mathcal{G}_f$ in all Theorems is connected, directed*

and also cycle free. Without loss of generality, we assume that vertices of $\mathcal{G}_f$ are ordered as all neighbors of agent i are indexed with $j < i$, otherwise we reorder the indices of all agents. Graph $\mathcal{G}_s$ is undirected and connected and $|\mathcal{N}_{si}| \geq n$, $N \geq n+1$ and the agent i and their neighbors are not collinear.

Definition 1.5.1. *As mentioned in (Ahmadi Barogh and Werner [2016a]), in formation graph $\mathcal{G}_f$ the neighbor set of agent i, $\mathcal{N}_{fi}$ where $i > 2$ is divided into two subsets: the distance neighbor set and the angle neighbor set. One of the neighbors of agent i is selected as distance neighbor which is considered to control the distance between it and agent i. The distance neighbor set is denoted by $\mathcal{D}_{fi}$ and contains the distance neighbor of agent i. In this thesis, we assume that the agent which has the greatest index among neighbors of agent i is considered as a distance neighbor of it. The remaining neighbors of agent i are referred to as angle neighbors, they are in $\mathcal{A}_{fi}$.*

In the following, $\|.\|$ and $\|.\|_1$ denote the Euclidean norm and 1-norm respectively. The global coordinate system denoted by ${}^{g}\sum$ and the local coordinate system for agent i represents with ${}^{i}\sum$ and n denotes the dimension of space.

1.5.2 Graph Rigidity

Definition 1.5.2. *: Let $\mathcal{G}$ be a graph with N vertices and its realization p. Let $\mathcal{K}$ be the complete graph with the same vertex set of $\mathcal{G}$. The framework $(\mathcal{G}, p)$ is rigid in $\mathbb{R}^2$ if there exists a neighborhood $\mathcal{U}$ of p in $\mathbb{R}^{2N}$ such that $g_{\mathcal{G}}^{-1}(g_{\mathcal{G}}(p)) \cap \mathcal{U}_p = g_{\mathcal{K}}^{-1}(g_{\mathcal{K}}(p)) \cap \mathcal{U}_p$. (Oh et al. [2012])*

Rigid formations can be achieved by combining the angles and distances between vertices. As shown in Fig. 1.5.1(a) to determine a rigid formation with three vertices, three distances are needed. Instead of three distances, if it is possible to use two distances (d_{12} and d_{23}) in addition to $\angle 321 = \alpha$ the framework rigidity is maintained. The advantage of the angle instead of a third distance is the sign of the angle (clockwise or counterclockwise) that prevents the flip ambiguity, which means preventing agent 3 from reflecting to another side of d_{12}, because of $\alpha = -\alpha'$ while the distance $d_{13} = d_{13'}$. In normal distance-based formation controllers, agent 3 in Fig. 1.5.1(a), can be stabilized in both of points 3 or 3′ while using angle and distance as constraints, regarding the value and sign of the desired angle, one of the points 3 or 3′ is uniquely determined. Thus, the flip ambiguity and also the flex ambiguity are avoided.

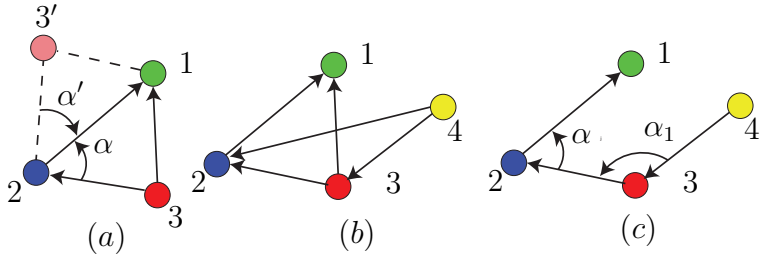

Figure 1.5.1: Rigid formation

1.5.3 Agent Models

Consider N identical agents in n-dimensional space. In this thesis three types of agent model are considered: single integrator and double integrator and non-holonomic model. For single integrators, each agent follows the integrator model represented by

$$\dot{p}_i(t) = u_i(t), \forall i \in \{1 \cdots N\}, \tag{1.5.1}$$

where $p_i \in \mathbb{R}^n$ denotes the coordinates of the position of agent i in n-dimensional space and $u_i \in \mathbb{R}^n$ is the control input velocity vector for steering the agent. For double integrator agents, the model is given by

$$\begin{aligned} \dot{p}_i(t) &= v_i(t), \forall i \in \{1 \cdots N\}, \\ \dot{v}_i(t) &= \frac{u_i(t)}{m_i}, \end{aligned} \tag{1.5.2}$$

where $p_i \in \mathbb{R}^n$, $v_i \in \mathbb{R}^n$ and $u_i \in \mathbb{R}^n$ denote the position, velocity and the control input of agent i respectively. The positive value, m_i is representing the mass of agent i. All quantities are calculated with respect to ${}^g\sum$. We assume that the agents do not necessarily use a common coordinate system, but each agent maintains its own local coordinate system. Superscripts on p_i^i, u_i^i, v_i^i are references to the local coordinate system of agent i.

The kinematic model of the non-holonomic agent is represented by

$$\begin{aligned} \dot{q}_i(t) &= R_i(\theta_i)u_i(t), \\ u_i(t) &= \begin{bmatrix} v_i(t) & \omega_i(t) \end{bmatrix}^T, i = 1 \cdots N, \end{aligned} \tag{1.5.3}$$

where

$$R_i = \begin{bmatrix} \cos(\theta_i(t)) & 0 \\ \sin(\theta_i(t)) & 0 \\ 0 & 1 \end{bmatrix},$$

and for non-holonomic model with dynamics

$$M_i\dot{u}_i(t) = \tau_i(t), i = 1 \cdots N, \tag{1.5.4}$$

where $M_i = \begin{bmatrix} m_i & 0 \\ 0 & l_i \end{bmatrix}$ and $\tau_i = \begin{bmatrix} \tau_{1i} & \tau_{2i} \end{bmatrix}^T \in \mathbb{R}^2$. In (1.5.4), $q_i = \begin{bmatrix} p_i^T & \theta_i \end{bmatrix}^T$, and $p_i = \begin{bmatrix} x_i & y_i \end{bmatrix}^T \in \mathbb{R}^2$, $\theta_i, v_i, \omega_i \in \mathbb{R}$, are the position, orientation, speed and angular velocity of agent i. The quantities m_i and l_i take positive values and represent the mass and the moment of inertia of agent i, respectively. The control inputs for agent i are the force input τ_{1i} and the torque input τ_{2i}.

All quantities are calculated with respect to the common Cartesian coordinate system ${}^g\sum$. We assume that the agents do not use a common coordinate system, but each agent maintains its own local coordinate system. We denote the local coordinate system of

agent i by ${}^{i}\sum$. Superscripts on p_i^i, u_i^i, v_i^i, ω_i^i, τ_{2i}^i, τ_{1i}^i are references to the local coordinate system of an agent i. By adopting this notation, the dynamics of agents can be written as

$$\begin{aligned} \dot{q}_i^i &= R_i(\theta_i^i)u_i^i, \\ M_i\dot{u}_i^i &= \tau_i^i, \end{aligned} \tag{1.5.5}$$

where $q_i^i = \begin{bmatrix} p_i^{iT} & \theta_i^i \end{bmatrix}^T$ and $p_i^i, u_i^i, \tau_i^i \in \mathbb{R}^2$.

The detecting topology is represented by a directed graph $\mathcal{G}_f = (\mathcal{V}, \mathcal{E}_f)$. Each agent uses its own local sensors to detect the relative position of its neighbors with respect to its own local coordinate system. Then for agent i, p_j^i is the position of agent j with respect to ${}^{i}\sum$. To analyze the stability of the system, it is better to represent the dynamics of all agents in a common coordinate system. Regarding the results of (Oh and Ahn [2014]) with an appropriate rotation and translation, all results from a common coordinate system are converted to the local coordinate system of agent i. In this thesis to prove stability and convergence the control laws and the agent dynamics are represented in a common coordinate system.

1.5.4 Scalar Field

The spatial distribution of a particular element (i.e. toxic gas, chemical pollution, etc) with scalar magnitude value can be represented by a scalar field. This scalar value allows for the analysis of the spatial distribution of that element by associating a corresponding value with each point in space. In this thesis a scalar field is represented as $\mu(p_i(t)) : \mathbb{R}^n \to \mathbb{R}^+$. We assume μ is a convex and twice continuously differentiable function with a global maximum $\bar{\mu}(p_s)$, when $p_s \in \mathbb{R}^n$

Remark 1.5.2. *Agents detect the instantaneous values of the scalar field with appropriate sensors. Considering the fact that each agent uses its local coordinate system so they detect the different values of the same function, μ in different positions with respect to their local coordinate. The scalar field value that is detected with agent i is denoted by μ_i.*

1.5.5 Distributed Gradient Estimation

Consider a group of mobile agents with a number of N spatially distributed members. The communication graph is $\mathcal{G}_s$. Each agent i measures the signal strength $\mu(p_i^i)$ In this thesis, we use the approach that was proposed in (Rosero and Werner [2014]) to estimate the gradient for each agent. The gradient and the Hessian matrix of scalar field is represented as follows.

$$\begin{aligned} \hat{g}_i^i(p_i^i) &= \bigtriangledown\mu(p_i^i), \\ \hat{H}_i^i(p_i^i) &= \bigtriangledown^2\mu(p_i^i). \end{aligned} \tag{1.5.6}$$

An estimate of the unweighted gradient proposed in (Rosero and Werner [2014]) is

$$R_i = \begin{bmatrix} (p_j^i - p_i^i)^T \\ \vdots \end{bmatrix}_{|\mathcal{N}_{si}| \times n},$$
$$b_i = \begin{bmatrix} \mu_j(p_j^i) - \mu_i(p_i^i) \\ \vdots \end{bmatrix}_{|\mathcal{N}_{si}| \times n}, j \in \mathcal{N}_{si}$$
$$\hat{g}_i^i(p_i^i) = (R_i^T R_i)^{-1} R_i^T b_i, \tag{1.5.7}$$

where $\hat{g}_i^i$ is the estimated gradient in agent i with respect to its own local coordinate system. The matrix R_i must have full column rank and thus the rank$(R_i = n)$ and this is satisfied if and only if the agent i and its neighbors are not collinear. Since $R_i \in \mathbb{R}^{|\mathcal{N}_{si}| \times n}$, we thus need $|\mathcal{N}_{si}| \geq n$.

1.5.6 Assumptions about a Scalar Field Scenario

For the scalar field $\mu(p_i)$ the following assumptions are considered.

Assumption 1.5.1. *The Hessian matrix of $\mu(p_i)$ satisfies $\lambda_{max}(H) \leq \eta_1$ and $\lambda_{min}(H) \geq \eta_2$ where $\eta_1, \eta_2 < 0$.*

Assumption 1.5.2. *The estimated gradient that is calculated by (1.5.7) has a bounded error. $\|\hat{g}_i^i - g_i^i\| \leq e_g$, where e_g is a positive constant and g_i^i is the true value of the gradient in the location of agent i with respect to ${}^i\sum$.*

Assumption 1.5.3. *Agents can only detect the value of the scalar field at its own current location.*

Assumption 1.5.4. *The scalar field is not time variant. Scalar field has one global maximum without local maximums.*

1.6 Contribution of This Thesis

In this thesis we consider multi-agent systems with N agents who are moving in the space R^2 and there is communication among agents represented by an undirected communication graph G_s. The following problems are addressed here:

- **Formation control with displacement format:** Displacement formation control for non-holonomic agents is proposed. The control laws consist of collision avoidance as well. Agents need to have access to relative displacement between themselves and their neighbors. The communication graph represents the cooperation topology among the agents. The graph needs to be connected but fully connected. To have a collision avoidance capability the gradient of an avoidance function is added to the control scheme. The stability of whole the cooperated formation control is shown with the Lyapunov-based method (Ahmadi Barogh et al. [2015]).

- **Formation control with distance-based format:** Distance-based formation control with a combination of distance and angle is proposed. The proposed formation control scheme consists of collision avoidance as well. Agents only detect their distances with neighbors and there is no communication among the agents. Each agent has its local coordinate system and based on its coordinate system generates the control law. The dynamic of agents is a single and double integrator (Ahmadi Barogh and Werner [2016a]), non-holonomic kinematic, and non-holonomic dynamic model (Ahmadi Barogh and Werner [2016b]). The stability of the distributed control law is proven with Lyapunov based methods.

- **Source seeking with formation control:** A source seeking scheme is integrated with the distance-based formation control. To solve the problem of source seeking, a cooperative distributed source seeking approach for each agent is proposed. The dynamic model of the agents is singe and double integrator, non-holonomic kinematic, and dynamic model. The control scheme consists of three parts: formation control, collision avoidance, and source seeking. The approach which is proposed does not need to use a particular formation shape (e.g. circular) and it is neither necessary to know the center of formation nor to use the spinning formation format. A global coordinate system is not needed and each agent uses its own local coordinates, therefore in indoor cases without access to global positioning, the proposed approach can work without crashing (Ahmadi Barogh and Werner [2017b]), (Ahmadi Barogh and Werner [2017a]).

1.7 Structure of This Thesis

The thesis is structured in these chapters:

In Chapter 2 a control scheme with displacement formation control for a group of agents with non-holonomic dynamics is proposed. Agents communicate with their neighbors and the communication topology is defined with a communication graph. Agents will achieve the desired formation and the stability of the whole formation structure is proved.

In Chapter 3 a new method with a combination of distance and angle is proposed for formation control of a group of agents with single integrator and double integrator dynamics. In comparison with the control scheme which was proposed in the previous chapter, in this chapter agents have no communication with their neighbors. Based on the measurements captured from their local sensors each agent follows the formation.

In Chapter 4 the control scheme which was proposed in the previous chapter is extended for non-holonomic kinematic and dynamic models. In both models, the stability of formation is proven with Lyapunuv based method.

In Chapter 5 the distance-angle based formation which was proposed in Chapter 3 extended to have source seeking capability. The gradient-based source seeking control law is proposed for the single integrator and double integrator model agents and the stability of whole formation close to the scalar filed maximum value is shown.

In Chapter 6 the control scheme which was proposed in the previous chapter is extended for non-holonomic kinematic and dynamic models. In both models, the stability of the whole formation close to the scalar field maximum value is shown.

In Chapter 7 to show the effectiveness and practical functionality of the proposed approach for source seeking with distance-based formation, the results of implementation on a group of wheeled robots are presented in this chapter. All implementation results were obtained at the Institute of Control Systems, Hamburg University of Technology in Master projects.

In the end, there is a Conclusions and Outlook chapter to summarize the results of this thesis and to give future directions for the next works.

Chapter 2

Formation Control with Displacement Formation

In this chapter a distributed formation control law to achieve a desired formation and to avoid collision between agents and obstacles for non-holonomic multi-agent systems is proposed. It is assumed that each agent knows its relative position and can detect any object within the sensor range. The controllers are implemented locally on each agent. Stability conditions for achieving desired formation and for avoiding collision are provided. Simulation results to illustrate the proposed controllers are presented. The control schemes and mathematical analysis that are proposed in this chapter were published in (Ahmadi Barogh et al. [2015]).

2.1 Introduction

Formation control of multi-agents with displacement formation received much attention in recent years. Some relevant work on non-holonomic agents is reviewed here. In (Mastellone et al. [2008]) a control law for tracking and target-following by non-holonomic agents is introduced. Results are extended to formation control. In the formation case, all agents operate individually. They need a leader to define a trajectory for them. A trajectory is defined for every agent with respect to a virtual center of mass of the desired formation. In (Gonzalez and Werner [2014]) LPV controller is proposed for formation control of non-holonomic agents. Here in this work, we extend the idea of (Mastellone et al. [2008]) to formation control and propose new formation control laws for non-holonomic agents. Our proposed control laws are simpler, and in comparison with results in (Listmann et al. [2009]) and (Sadowska et al. [2012]), our controller is faster and has a lower complexity.

The main contributions of this chapter are the design of distributed controllers using only neighbors' information which guarantees formation control and avoid collisions between agents and obstacles for a group of agents with non-holonomic dynamics.

The rest of this chapter is organised as follows: In Section 2.2 three control laws for a

group of non-holonomic agents are proposed. Simulation results are shown in Section 2.3. Conclusions are given in Section 2.4.

2.2 Distributed Control Strategy

Consider a group of N non-holonomic mobile agents with kinematic models given by

$$\begin{aligned} \dot{x}_i(t) &= v_i \cos(\theta_i(t)), \\ \dot{y}_i(t) &= v_i \sin(\theta_i(t)), \\ \dot{\theta}_i(t) &= \omega_i(t), \end{aligned} \tag{2.2.1}$$

where $i = 1, \ldots, N$, $r_i = [x_i \ y_i]^T \in \mathbb{R}^2$ describes the position of agent i in the plane $\mathbb{R}^2$, $\theta_i \in [0, \ 2\pi)$ is the orientation of agent i with respect to x coordinate, $v_i \in \mathbb{R}$ and $\omega_i \in \mathbb{R}$ are the linear and angular velocity inputs, respectively. The desired formation is defined as

$$\begin{aligned} X_f &= \begin{bmatrix} x_{F1} & \cdots & x_{FN} \end{bmatrix}^T, \\ Y_f &= \begin{bmatrix} y_{F1} & \cdots & y_{FN} \end{bmatrix}^T, \end{aligned} \tag{2.2.2}$$

where X_f and Y_f are vectors of desired positions. Regarding the consensus problem in (Olfati-Saber and Murray [2004]) and (Olfati-Saber et al. [2007]), the desired formation is achieved when

$$e = \begin{bmatrix} \vdots \\ a_{ij} \begin{bmatrix} (x_{Fi} - x_{Fj}) - (x_i - x_j) \\ (y_{Fi} - y_{Fj}) - (y_i - y_j) \end{bmatrix} \\ \vdots \end{bmatrix}_{2N(N-1)\times 1} = 0, \tag{2.2.3}$$

where $1 \leq i \leq N$ and $1 \leq j \leq N$ and $i \neq j$.

2.2.1 Formation Control

To achieve a consensus in the desired position, the following control law is proposed

$$\begin{aligned} v_i(t) &= k_v D_i(t) \cos(e_{\theta i}(t)), \\ \omega_i(t) &= -k_\theta e_{\theta i}(t) + \dot{\theta}_{di}(t), \end{aligned} \tag{2.2.4}$$

with

$$e_{\theta i} = \theta_i - \theta_{di}, \tag{2.2.5a}$$

$$D_i = \sqrt{e_{xi}^2 + e_{yi}^2}, \tag{2.2.5b}$$

$$e_{xi} = \sum_{j \in \mathcal{N}_i} a_{ij} \left[(x_{Fi} - x_{Fj}) - (x_i - x_j) \right], \tag{2.2.5c}$$

$$= \sum_{j=1}^{N} l_{ij}(x_{Fj} - x_j),$$

$$e_{yi} = \sum_{j \in \mathcal{N}_i} a_{ij} \left[(y_{Fi} - y_{Fj}) - (y_i - y_j) \right], \tag{2.2.5d}$$

$$= \sum_{j=1}^{N} l_{ij}(y_{Fj} - y_j),$$

$$\theta_{di} = \operatorname{atan}\left(\frac{e_{yi}}{e_{xi}}\right), \tag{2.2.5e}$$

where $k_\theta > 0$ and $k_v > 0$ are tuning parameters, l_{ij} are the elements of Laplacian matrix L, $e_{\theta i}$ defines the orientation error of agent i and θ_{di} defines the desired orientation of agent i.

Assumption 2.2.1. *It is assumed that $e_{\theta i} \neq k\frac{\pi}{2}$ for all agents, for all odd integers k. It implies that $\cos(e_{\theta i}) \neq 0$ for all agents at all times. In a case where $e_{\theta i} = k\frac{\pi}{2}$ for an agent, the orientation error can be replaced by $e_{\theta i} = e_{\theta i} + \epsilon$, where ϵ is a small value.*

Let us define E_{ey} and E_{ex} as

$$E_{ex} = \begin{bmatrix} e_{x1} & e_{x2} & \cdots & e_{xN} \end{bmatrix}^T,$$
$$E_{ey} = \begin{bmatrix} e_{y1} & e_{y2} & \cdots & e_{yN} \end{bmatrix}^T. \tag{2.2.6}$$

Lemma 2.2.1. *A necessary and sufficient condition for $e = 0$ is $E_{ex} = 0$ and $E_{ey} = 0$.*

Proof: First assume $e = 0$, then according to Equations (2.2.5c) and (2.2.5d), all $e_{xi} = 0$ and $e_{yi} = 0$, therefore $E_{ex} = 0$ and $E_{ey} = 0$.

Equations (2.2.5c) and (2.2.5d) can be rewritten as

$$E_{ex} = L \begin{bmatrix} (x_{F1} - x_1) & (x_{F2} - x_2) & \cdots & (x_{FN} - x_N) \end{bmatrix}^T,$$
$$E_{ey} = L \begin{bmatrix} (y_{F1} - y_1) & (y_{F2} - y_2) & \cdots & (y_{FN} - y_N) \end{bmatrix}^T. \tag{2.2.7}$$

On the other hand $E_{ex} = 0$ and $E_{ey} = 0$ implies

$$L \begin{bmatrix} (x_{F1} - x_1) & (x_{F2} - x_2) & \cdots & (x_{FN} - x_N) \end{bmatrix}^T = 0,$$
$$L \begin{bmatrix} (y_{F1} - y_1) & (y_{F2} - y_2) & \cdots & (y_{FN} - y_N) \end{bmatrix}^T = 0. \tag{2.2.8}$$

Since the graph $\mathcal{G}$ is connected, then L only has one zero eigenvalue and the eigenvector corresponding to zero eigenvalue is $\mathbf{1}$, therefore

$$x_{F1} - x_1 = x_{F2} - x_2 = \cdots \qquad = x_{FN} - x_N,$$
$$y_{F1} - y_1 = y_{F2} - y_2 = \cdots \qquad = y_{FN} - y_N, \tag{2.2.9}$$

thus $e = 0$. ■

Theorem 2.2.1. *Consider the multi-agent system (2.2.1) with the distributed control law (2.2.4). Suppose that Assumption 2.2.1 is fulfilled. Then, for all* $r_i(0) \in \mathbb{R}^2$ *and* $t \geq 0$, *the agents achieve a desired formation and* $\lim_{t\to\infty} e(t) = 0$.

Proof: Consider the Lyapunov candidate function

$$\begin{aligned} V =& \frac{1}{4}\sum_{i=1}^{N}\sum_{j=1}^{N} a_{ij}\left[(x_{Fi}-x_{Fj})-(x_i-x_j)\right]^2 \\ &+ \frac{1}{4}\sum_{i=1}^{N}\sum_{j=1}^{N} a_{ij}\left[(y_{Fi}-y_{Fj})-(y_i-y_j)\right]^2 \\ &+ \frac{1}{2}\sum_{i=1}^{N} e_{\theta i}^2, \end{aligned} \tag{2.2.10}$$

where V is a continuously differentiable function, $V(0) = 0$ and $V > 0$ for $e \neq 0$. The derivative of V along the trajectories of the system is given by

$$\begin{aligned} \dot{V} =& -\sum_{i=1}^{N}\dot{x}_i\sum_{j=1}^{N} l_{ij}(x_{Fj}-x_j) \\ &-\sum_{i=1}^{N}\dot{y}_i\sum_{j=1}^{N} l_{ij}(y_{Fj}-y_j) + \sum_{i=1}^{N} e_{\theta i}\dot{e}_{\theta i}. \end{aligned} \tag{2.2.11}$$

Substituting Equations (2.2.5c) and (2.2.5d) into the derivative of V, and taking the derivative of $e_{\theta i}$, it is possible to write

$$\dot{V} = -\sum_{i=1}^{N}\dot{x}_i e_{xi} - \sum_{i=1}^{N}\dot{y}_i e_{yi} - k_\theta\sum_{i=1}^{N} e_{\theta i}^2. \tag{2.2.12}$$

Since $\theta_i = e_{\theta i} + \theta_{di}$ and replacing the control law (2.2.4) in the model of agent i (2.2.1), it is possible to obtain

$$\begin{aligned} \dot{x}_i &= v_i\cos(e_{\theta j}+\theta_{dj}) \\ &= v_i\left(\cos(e_{\theta i})\cos(\theta_{di}) - \sin(e_{\theta i})\sin(\theta_{di})\right), \\ \dot{y}_i &= v_i\sin(e_{\theta j}+\theta_{dj}) \\ &= v_i\left(\sin(e_{\theta i})\cos(\theta_{di}) + \cos(e_{\theta i})\sin(\theta_{di})\right). \end{aligned} \tag{2.2.13}$$

Using the expressions $\cos(\theta_{dj}) = \frac{e_{xj}}{D_j}$ and $\sin(\theta_{dj}) = \frac{e_{yj}}{D_j}$, and replacing Equation (2.2.13) in Equation (2.2.12) and from control law (2.2.4), the derivative of Lyapunov equation can be finally written as

$$\dot{V} = -k_v\sum_{i=1}^{N}\cos^2(e_{\theta i})(e_{xi}^2+e_{yi}^2) - k_\theta\sum_{i=1}^{N} e_{\theta i}^2, \tag{2.2.14}$$

hence $\dot{V} \leq 0$, and we have $e \to 0$ for $k_\theta > 0$ and $k_v > 0$. From Assumption 2.2.1, it is obvious that $\cos^2(e_{\theta i}) \neq 0$ and hence $\dot{V} = 0$ in case of all $e_{xi} = 0$, all $e_{yi} = 0$ and all $e_{\theta i} = 0$. According to Lemma 2.2.1, $e \to 0$ means that the desired formation is achieved. ■

2.2.2 Formation Control and Collision Avoidance

To avoid collision between agents and obstacles, usually an avoidance function is used. In this work the avoidance function proposed by (G. Leitmann and Skowronski [1977]) is applied. The avoidance function is defined as

$$V_{aij} = \left(\min \left\{ 0, \frac{d_{ij}^2 - R^2}{d_{ij}^2 - r^2} \right\} \right)^2, \tag{2.2.15}$$

where $d_{ij} = \sqrt{(x_i - x_j)^2 + (y_i - y_j)^2}$ and $\begin{bmatrix} x_j & y_j \end{bmatrix}$ are coordinates of another agent or a static obstacle which are in contact with agent i. We define

$$V_{ai} = \sum_{j=1, j\neq i}^{N_{oi}} V_{aij}, \tag{2.2.16}$$

where N_{oi} is the number of obstacles that agent i encountered in the same time. Assume $R > r > 0$. Regarding Fig. 2.2.1, R and r are the radii of protection and detection areas around each agent, respectively.

The avoidance function takes infinity value when the distance achieves r, and it is zero when the distance is greater than R.

Assumption 2.2.2. *In this work, we assume all obstacles have a cylindrical shape. Also, the radius of each obstacle and its location is known to all agents.*

By taking partial derivatives of V_{aij} with respect to x_i and y_i, it is possible to compute

$$\begin{aligned}
\frac{\partial V_{aij}}{\partial x_i} &= \begin{cases} 0 & \text{if} \quad d_{ij} \geq R, \\ 4\frac{(R^2 - r^2)(d_{ij}^2 - R^2)}{(d_{ij}^2 - r^2)}(x_i - x_j) & \text{if} \quad R > d_{ij} > r, \\ 0 & \text{if} \quad d_{ij} < r, \end{cases} \\
\frac{\partial V_{aij}}{\partial y_i} &= \begin{cases} 0 & \text{if} \quad d_{ij} \geq R, \\ 4\frac{(R^2 - r^2)(d_{ij}^2 - R^2)}{(d_{ij}^2 - r^2)}(y_i - y_j) & \text{if} \quad R > d_{ij} > r, \\ 0 & \text{if} \quad d_{ij} < r, \end{cases} \\
\frac{\partial V_{ai}}{\partial y_i} &= \sum_{j=1, j\neq i}^{N_{oi}} \frac{\partial V_{aij}}{\partial y_i}, \\
\frac{\partial V_{ai}}{\partial x_i} &= \sum_{j=1, j\neq i}^{N_{oi}} \frac{\partial V_{aij}}{\partial x_i}.
\end{aligned} \tag{2.2.17}$$

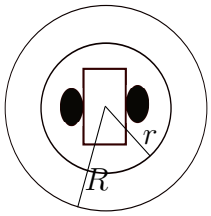

Figure 2.2.1: Protection and detection area around the agent

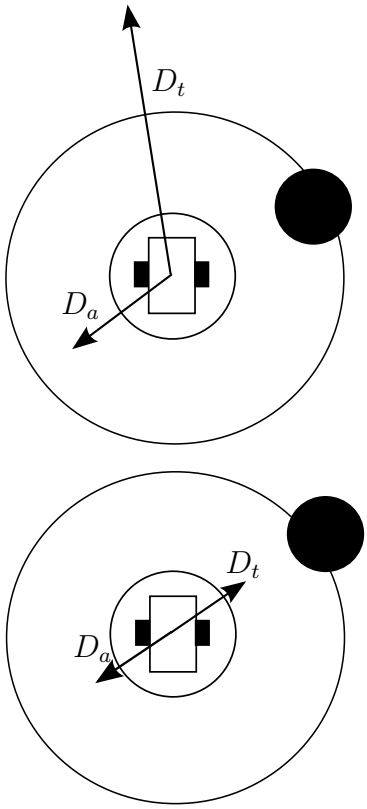

Figure 2.2.2: Examples of admissible (top) and non-admissible trajectories (bottom) which shows the trajectory force (D_t) and repulsive force (D_a)

Let us define

$$E_{xi} = e_{xi} - \left(\frac{\partial V_{ai}}{\partial x_i}\right), \tag{2.2.18a}$$

$$E_{yi} = e_{yi} - \left(\frac{\partial V_{ai}}{\partial y_i}\right), \tag{2.2.18b}$$

$$\theta_{di} = \text{atan}\left(\frac{E_{yi}}{E_{xi}}\right), \tag{2.2.18c}$$

where e_{xi} and e_{yi} are obtained in the same way as Equations (2.2.5c) and (2.2.5d). $\frac{\partial V_{ai}}{\partial x_i}$ and $\frac{\partial V_{ai}}{\partial y_i}$ are obtained from Equation (2.2.17).

As depicted in Fig. 2.2.2, when an agent encounters an obstacle and the obstacle is inside the protection area of the agent, two forces influence the agent. Force D_t directs the agent to the desired formation and D_a is a repulsive force to avoid a collision. As shown in Fig. 2.2.2 bottom, it is possible that these two forces eliminate the effect of each other. In this case the agent stops while there is a obstacle inside the protection area of corresponding agent.

Remark 2.2.1. *$E_{xi} = E_{yi} = 0$ can occur in the following two cases. The first case occurs outside the protection area where*

$$\frac{\partial V_{ai}}{\partial x_i} = \frac{\partial V_{ai}}{\partial y_i} = 0,$$

which corresponds to $e_{xi} = e_{yi} = 0$ and in this case the agent i achieves its desired position in a formation without collision. The second case occurs inside the protection area as in Fig. 2.2.2 bottom. We assume that if agent i is inside the protection area of each obstacle, we have $E_{xi} \neq 0$ or $E_{yi} \neq 0$. In a case that both $E_{xi} = 0$ and $E_{yi} = 0$ we can add small ϵ value to one of them.

Theorem 2.2.2. *Consider the multi-agent system (2.2.1) and suppose that Assumption 2.2.1 and Remark 2.2.1 are fulfilled. Then, for all $r_i(0) \in \mathbb{R}^2$ and $t \geq 0$, the agents achieve the desired formation without any collision in the presence of obstacles if the following distributed controllers are applied*

$$\begin{aligned} v_i(t) &= k_v D_i(t) \cos(e_{\theta i}(t)), \\ \omega_i(t) &= -k_\theta e_{\theta i}(t) + \dot{\theta}_{di}(t), \end{aligned} \tag{2.2.19}$$

where $D_i = \sqrt{Ex_i^2 + Ey_i^2}$ and Ex_i , Ey_i are calculated as in (2.2.18a) and (2.2.18b), respectively, and $e_{\theta i}$ is defined in (2.2.5a).

Proof: Consider the Lyapunov function candidate

$$V_c = V + \sum_{i=1}^{N} V_{ai}, \tag{2.2.20}$$

where V is defined as in Equation (2.2.10) and V_{ai} is calculated as Equation (2.2.16). $V_c \geq 0$ is a continuously differentiable function except at a measure zero set on the boundary of the detection area where $d_{ij} = r$. $V_c = 0$ means $\sum_{i=1}^{N} V_{ai} = 0$ and $V = 0$. If $\sum_{i=1}^{N} V_{ai} = 0$ obviously all agents are outside of the protection area of all obstacles, and $V = 0$ means that $e = 0$ and all agents achieve a desired formation. By taking the derivative of V_c and using Equation (2.2.12) we obtain

$$\dot{V}_c = -\sum_{i=1}^{N} \dot{x}_i e_{xi} - \sum_{i=1}^{N} \dot{y}_i e_{yi} + \sum_{i=1}^{N} \frac{\partial V_{ai}}{\partial x_i} \dot{x}_i + \sum_{i=1}^{N} \frac{\partial V_{ai}}{\partial y_i} \dot{y}_i - k_\theta \sum_{i=1}^{N} e_{\theta i}^2,$$

$$= -\sum_{i=1}^{N} \dot{x}_i \left(e_{xi} - \frac{\partial V_{ai}}{\partial x_i} \right) - \sum_{i=1}^{N} \dot{y}_i \left(e_{xi} - \frac{\partial V_{ai}}{\partial x_i} \right) - k_\theta \sum_{i=1}^{N} e_{\theta i}^2.$$

From Equations (2.2.18a) and (2.2.18b) if is clear that

$$\dot{V}_c = -\sum_{i=1}^{N} \dot{x}_i E_{xi} - \sum_{i=1}^{N} \dot{y}_i E_{yi} - k_\theta \sum_{i=1}^{N} e_{\theta i}^2. \tag{2.2.21}$$

By substitution of $\cos(\theta_{dj}) = \frac{E_{xj}}{D_j}$ and $\sin(\theta_{dj}) = \frac{E_{yj}}{D_j}$ in Equation (2.2.13) and from the control law (2.2.19) it is possible to obtain

$$\begin{aligned} \dot{x}_i &= k_v \left(\cos^2(e_{\theta i}) E_{x_i} - \cos(e_{\theta i}) \sin(e_{\theta i}) E_{y_i} \right), \\ \dot{y}_i &= k_v \left(\cos(e_{\theta i}) \sin(e_{\theta i}) E_{x_i} + \cos^2(e_{\theta i}) E_{y_i} \right). \end{aligned} \tag{2.2.22}$$

Therefore using Equation (2.2.22) in Equation (2.2.21) and after some calculations, we obtain

$$\dot{V}_c = -k_v \sum_{i=1}^{N} \cos^2(e_{\theta i})(E_{xi}^2 + E_{yi}^2) - k_\theta \sum_{i=1}^{N} e_{\theta i}^2, \tag{2.2.23}$$

hence $\dot{V}_c \leq 0$, and $E_{ex} = 0$ and $E_{ey} = 0$ for $i = 1 \cdots N$ and $k_\theta 0$ and $k_v > 0$. According to Assumption 2.2.1, if $\dot{V}_c = 0$ we have $E_{xi} = 0$ and $E_{yi} = 0$. According to Remark 2.2.1 all agents are outside of the protection area of the obstacles and collision avoidance for all agents is guaranteed, we have for all agents $e_{xi} = 0$ and $e_{yi} = 0$. From Lemma 2.2.1, it is concluded that $e = 0$ and all agents achieve the desired formation. ■

2.2.3 Formation Control and Collision Avoidance with Bounded Speed

The control law (2.2.19) has no limitation in magnitude value of v_i. This means the speed of every agent can be increased without any bound. In practice, wheeled robots have velocity limits according to their mechanical specifications. To apply bounds on speed of agent v_i we propose the control law

$$v_i = \frac{k_v D_i \cos(e_{\theta i})}{D_i + k_b}, \tag{2.2.24}$$

where $k_b \geq 0$ and the speed is bounded by $-k_v \leq v_i \leq k_v$. The control law for angular velocity ω_i is the same as the control law for angular velocity defined in Equation (2.2.19).

By substituting the control law with bounded speed (2.2.24) instead of control law (2.2.19), and repeating the process of the proof of Theorem 2.2.2, it is possible to write

$$\dot{V}_c = -k_v \sum_{i=1}^{N} \frac{\cos^2(e_{\theta i})(E_{xi}^2 + E_{yi}^2)}{D_i + k_b} - k_\theta \sum_{i=1}^{N} e_{\theta i}^2, \tag{2.2.25}$$

hence $\dot{V}_c \leq 0$, and $E_{ex} = 0$ and $E_{ey} = 0$ for all $k_\theta > 0$, $k_v > 0$ and $k_b > 0$. We conclude that the agents achieve the desired formation and avoid the collision between agents and obstacles. The control law (2.2.24) improves the performance of the group of agents because it bounds the speed and avoids to increase the velocity's magnitude to unrealistic values.

2.3 Simulation Results

In this section, simulations to verify the effectiveness of the proposed distributed control laws are presented. Consider a group of $N = 5$ agents with the communication graph $\mathcal{G}$ defined by the Laplacian matrix as

$$L = \begin{bmatrix} 2 & -1 & -1 & 0 & 0 \\ -1 & 2 & -1 & 0 & 0 \\ 0 & -1 & 2 & -1 & 0 \\ 0 & 0 & -1 & 2 & -1 \\ -1 & 0 & 0 & -1 & 2 \end{bmatrix}.$$

The desired formation is defined as a pentagon formation with

$$X_F = \begin{bmatrix} 9 & -9 & 5 & -5 & 0 \end{bmatrix}^T,$$
$$Y_F = \begin{bmatrix} 0 & 0 & 10 & 10 & -9 \end{bmatrix}^T.$$

The initial positions and directions of agents are defined as $[x_{10}\ y_{10}\ \theta_{10}] = [-23\ 15\ \pi/2]$, $[x_{20}\ y_{20}\ \theta_{20}] = [-20\ -16\ \pi/6]$, $[x_{30}\ y_{30}\ \theta_{30}] = [35\ 10\ 3\pi/2]$, $[x_{40}\ y_{40}\ \theta_{40}] = [50\ 45\ -2\pi/3]$, $[x_{50}\ y_{50}\ \theta_{50}] = [-32\ 18\ \pi/2]$.

The static obstacles are placed at $[x_{o1}\ y_{o1}] = [-15\ -10]$, $[x_{o2}\ y_{o2}] = [40\ 40]$ and $[x_{o3}\ y_{o3}] = [30\ 8]$. The protection and detection areas are defined by the radii $R = 5$ and $r = 3$. The tuning parameters are selected as $k_v = 0.5$, $k_\theta = 0.5$ and $k_b = 1$.

Three scenarios are simulated: only formation control, formation control with collision avoidance and formation control with collision avoidance using a bounded speed.

2.3.1 Formation Control

In this scenario collision avoidance between agents and obstacles is not considered. The trajectories of the group of agents applying the control law (2.2.4) is given by Fig. 2.3.1. The formation error (E_{xi} and E_{yi}) and the orientation error $e_{\theta i}$ for each agent are represented in Fig. 2.3.2.

Fig. 2.3.1 shows that the agents achieve the desired formation in a pentagon shape, while the Fig. 2.3.2 shows that the relative errors converge to zero.

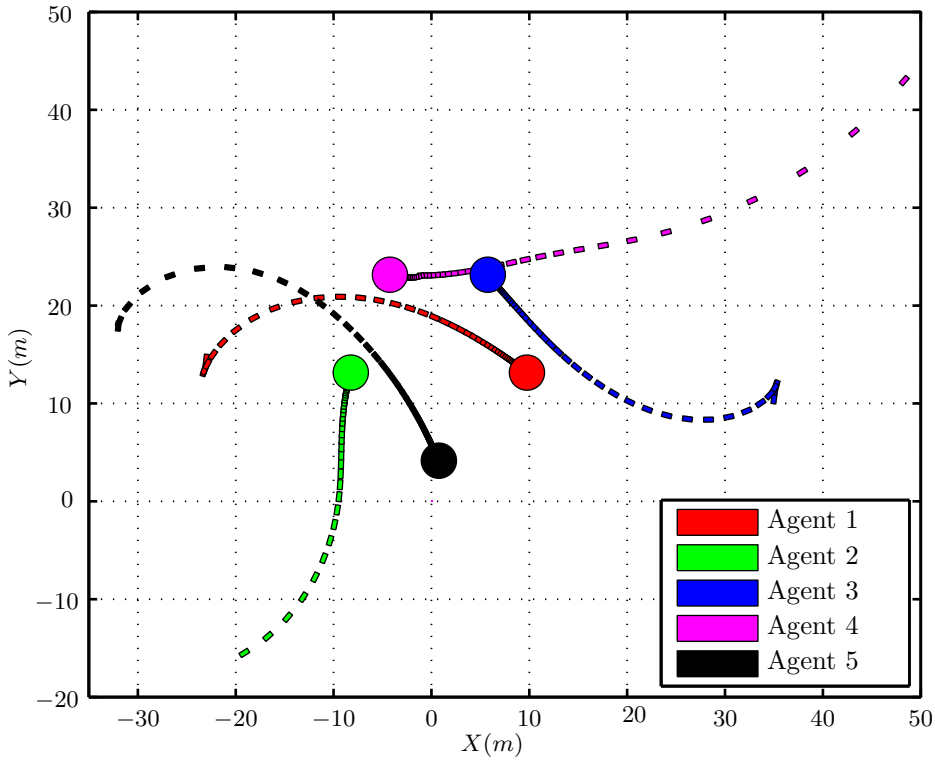

Figure 2.3.1: Formation control without collision avoidance

2.3.2 Formation Control with Collision Avoidance

In this scenario static obstacles in the plane are included. After applying the control law (2.2.19), the trajectories of the group of agents are represented in Fig. 2.3.3. When one agent or an obstacle is inside a protection area of another agent, the avoidance function is activated, as a consequence, the agents change the trajectories to avoid the collisions.

Fig. 2.3.4 shows that the relative errors converge to zero when agents achieve the desired formation. Note that when one agent detect an obstacle, the errors increase or decrease depending on the direction of the repulsive force.

Fig. 2.3.5 shows the speed of agents with the distributed control law 2.2.19. When agents achieve the desired formation, all velocities converge to zero.

2.3.3 Formation Control with Collision Avoidance Using a Bounded Speed

Fig. 2.3.6 shows the trajectories of the group of agents after applying the control law (2.2.24). Note that the agents avoid the obstacles and achieve the desired formation.

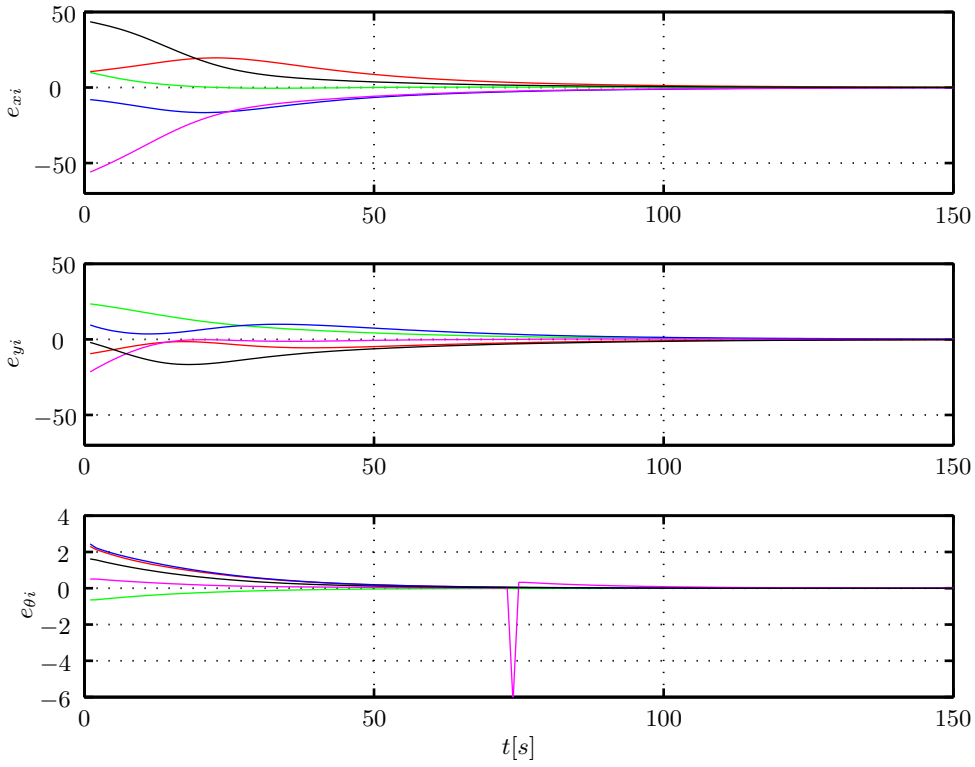

Figure 2.3.2: Errors for formation control

Fig. 2.3.7 shows that the formation and orientation errors converge to zero. Since the speed of agents is bounded by $-0.5 \leq v_i \leq 0.5$, the agents spend more time to achieve the desired formation. It can be seen comparing Fig. 2.3.7 and 2.3.4.

Fig. 2.3.8 shows the speed of agents with the distributed control law 2.2.24. When agents achieve the desired formation, all velocities converge to zero.

Figs. 2.3.5 and 2.3.8 compare the speed of the group of non-holonomic agents when the control laws (2.2.19) and (2.2.24) are applied. When the control law (2.2.19) is implemented, the magnitudes of linear velocities are larger than the the magnitudes of linear velocities implementing the control law (2.2.24). Fig. 2.3.8 also shows that the speed is bounded by $-0.5 \leq v_i \leq 0.5$, which is given by the tuning parameter $k_v = 0.5$.

2.4 Conclusions

In this chapter simple distributed control laws for formation control and collision avoidance between agents and obstacles of a group of non-holonomic agents with limited communication are presented. The proposed algorithms enable agents to achieve consensus in the desired formation and also avoid collision between agents and obstacles. The controllers are assumed to run locally on each agent. They require information only from its

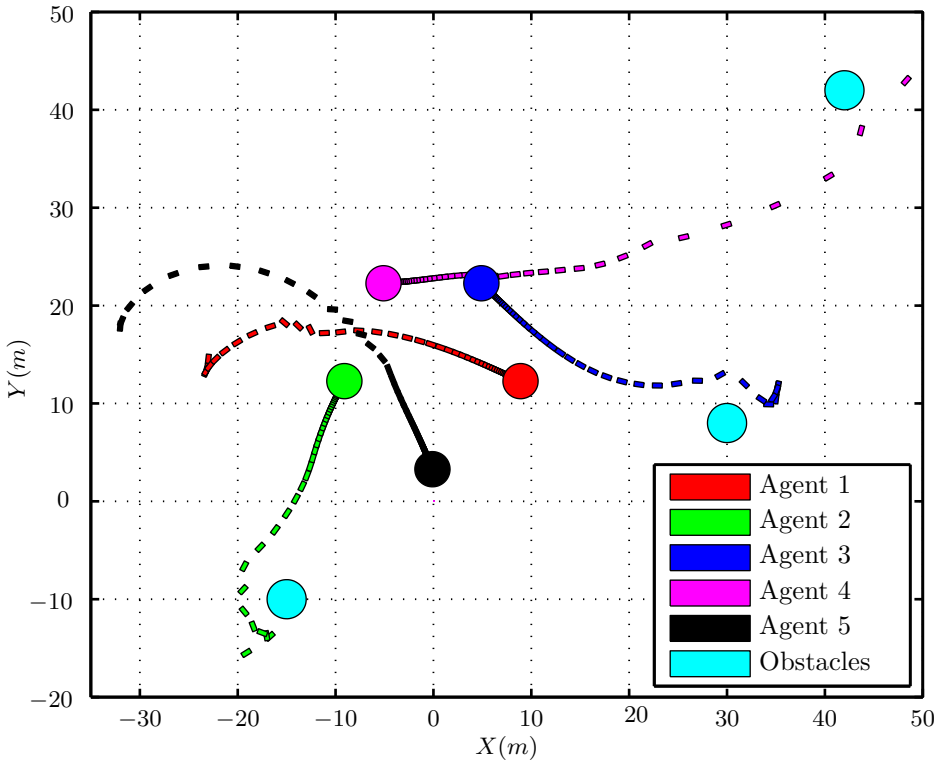

Figure 2.3.3: Formation control with collision avoidance

local neighbors. Stability analysis shows that the dynamics of group of agents is stable. Simulations confirm the effectiveness of the proposed algorithms.

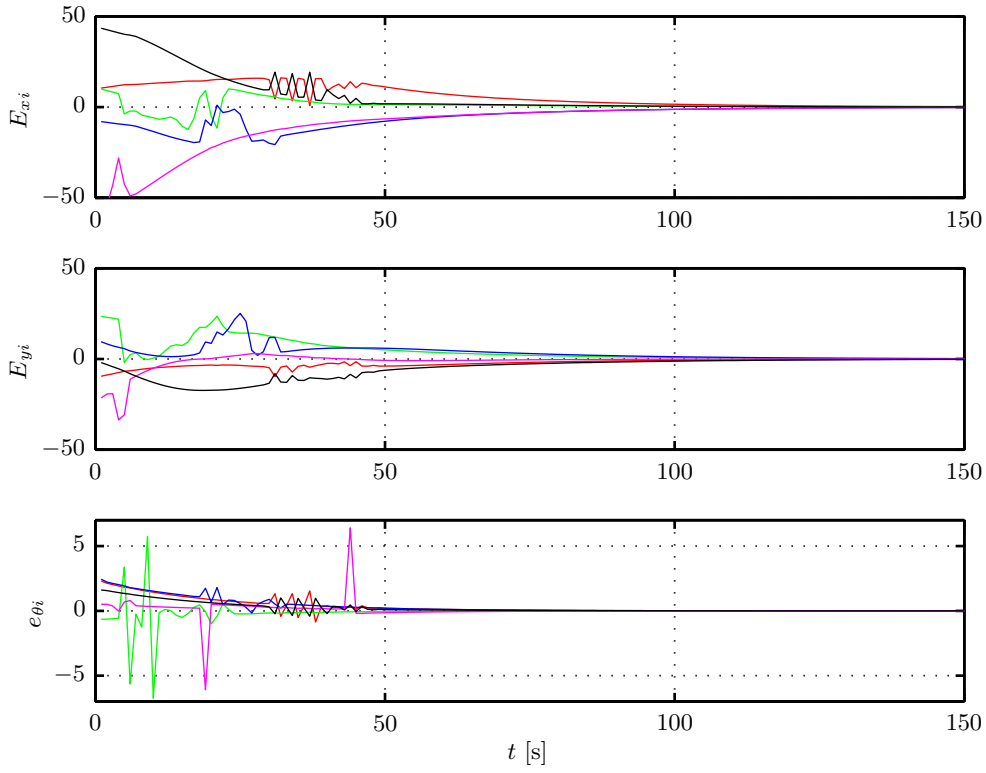

Figure 2.3.4: Errors in formation control with collision avoidance

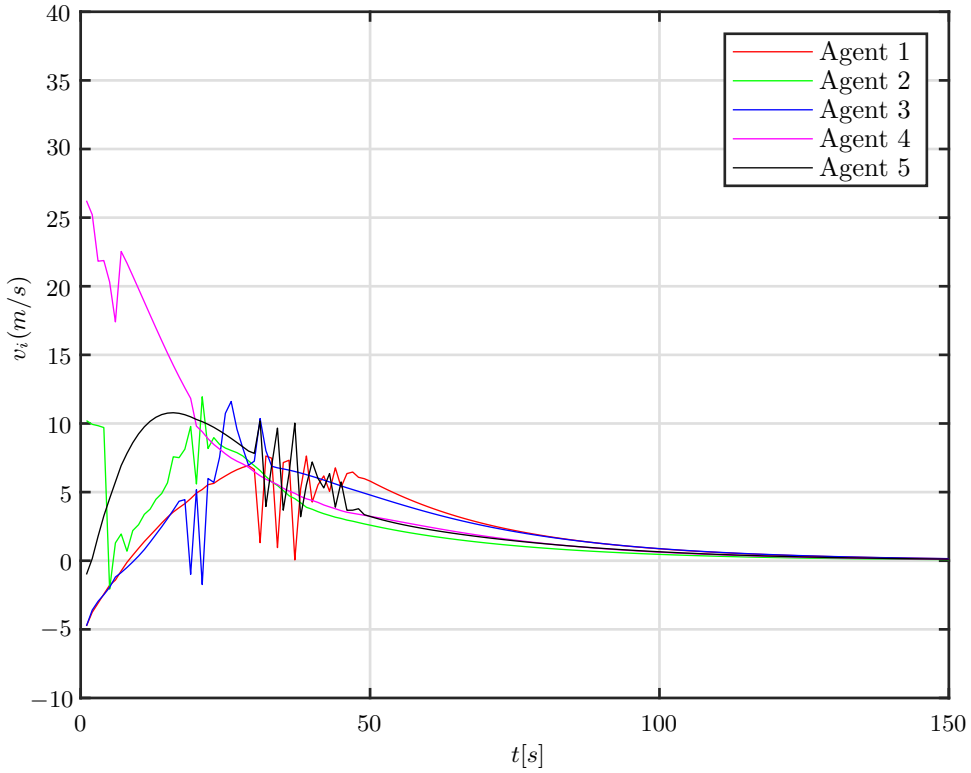

Figure 2.3.5: Velocities in formation control with collision avoidance

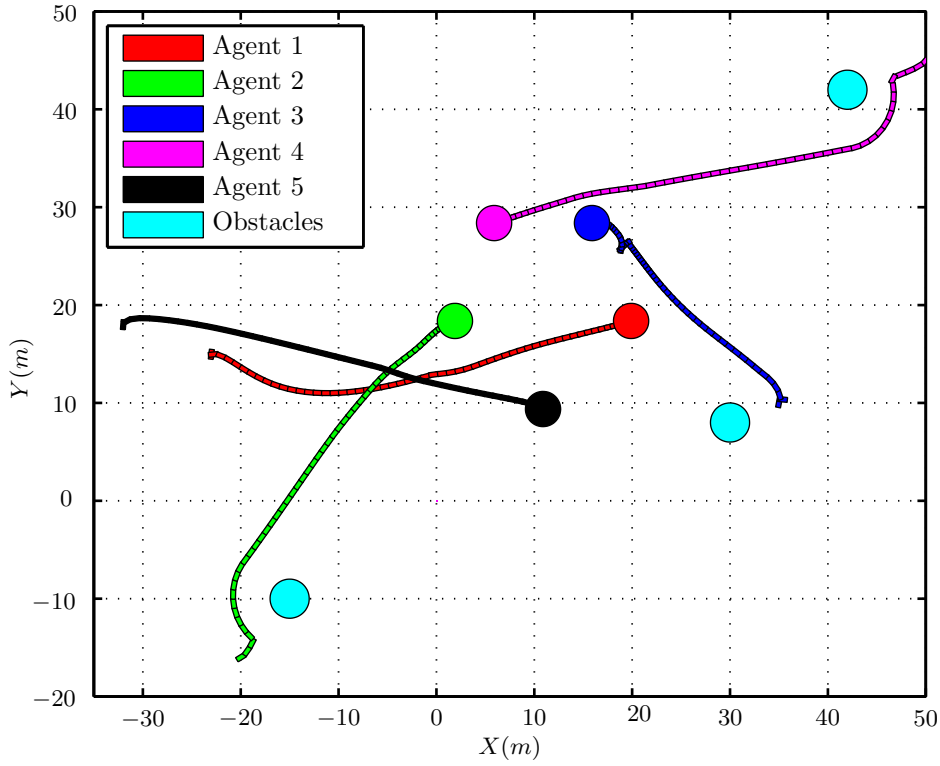

Figure 2.3.6: Formation control with collision avoidance and bounded speed

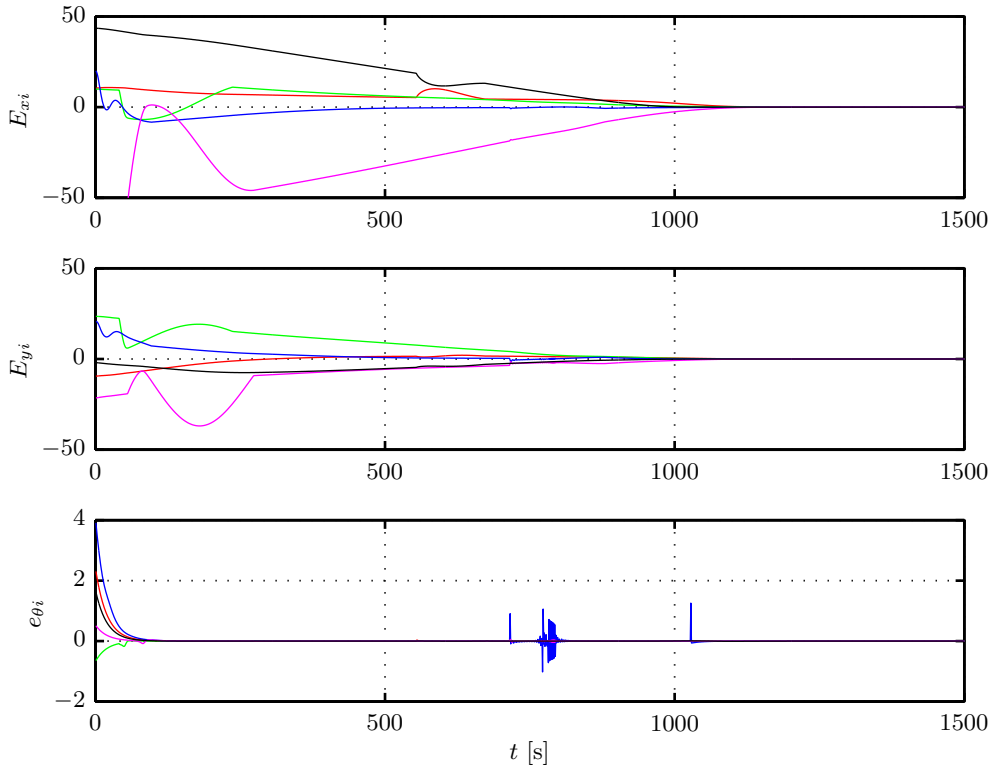

Figure 2.3.7: Errors in formation control with collision avoidance and bounded speed

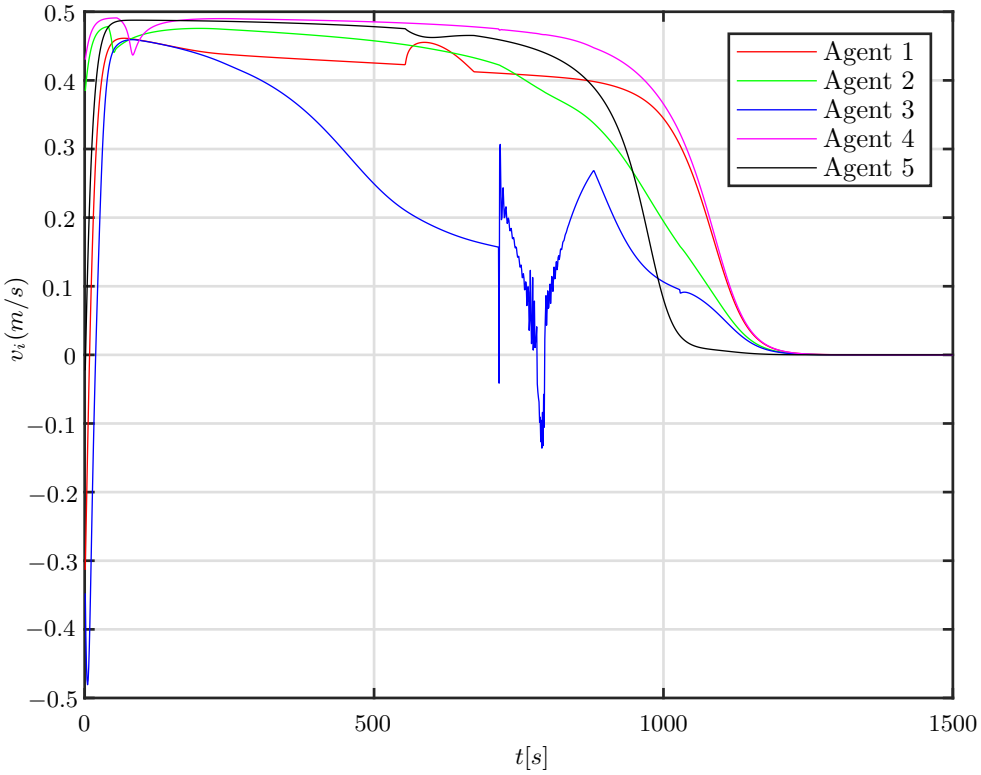

Figure 2.3.8: Bounded speed in formation control with collision avoidance

Chapter 3

Distance-Angle Based Formation Control for Single and Double Integrator Agents

In this chapter a new distance-based formation control approach with combination of distance and angle is proposed. In this method a stable leader-following formation control for multi-agent systems with obstacle collision avoidance and orientation control is considered. In this method a cascaded distributed control law that uses information about the angle and distance between agents to achieve a persistent formation is proposed. The control scheme with collision avoidance for groups of agents with a single integrator or double integrator model is provided. For both dynamic models, asymptotic stability of the formation under a gradient control law is shown. The proposed control law includes a distance-angle-based controller for shape stabilization and distance-based formation control of certain leader agents to control the direction of the whole formation. The control schemes and mathematical analysis that are proposed in this chapter were published in (Ahmadi Barogh and Werner [2016a]).

3.1 Introduction

The chapter is structured as follows: Section 3.2 provides preliminary definitions and mathematical background review of formation control problems. In Section 3.3, we propose a control law that achieves the desired formation and orientation, and we show the stability of the closed-loop system for single integrator and double integrator agents in the presence of obstacles. Section 3.4 shows simulation results, and Section 3.5, concludes with a summary.

3.2 Preliminary

The neighbor set of agent i, where $i > 2$ is divided in two subsets: a distance neighbor and the angle neighbor set. One of the neighbors of agent i is selected as distance neighbor which is considered to control the distance between it and agent i. In this work we assume that the agent which has the greatest index among all neighbors of agent i is considered the distance neighbor of it. The remaining neighbors of agent i are referred to as angle neighbors, they are in $\mathcal{A}_i$. Regarding the angle neighbors, the objective is controlling the angle between agent i, its distance neighbor and an angle neighbor. In the example shown in Fig. 3.2.1(c) we have $\mathcal{D}_3 = \{2\}$, $\mathcal{D}_4 = \{3\}$ and $\mathcal{A}_3 = \{1\}$, $\mathcal{A}_4 = \{2\}$

Assumption 3.2.1. *In this work we assume that the communication graph is cycle free. For each agent i with $i > 2$ and $\mathcal{N}_i > 2$, there is at least one angle neighbor and if that agent detects more angle neighbors, it can increase the neighbor angles set.*

Lemma 3.2.1. *In a digraph $\mathcal{G} = (\mathcal{V}, \mathcal{E})$, with representation $(\mathcal{G}, p)$ in $\mathbb{R}^2$, for each agent i with $i > 2$, satisfying one desired distance and the related desired angle between itself and its neighbors is sufficient to maintain the rigidity of the formation.*

Proof: As depicted in Fig. 3.2.1(a) for agent 3, if agents 1 and 2 are in the desired formation, satisfying one desired distance (d_{32}) and one desired angle (α) is sufficient to maintain the rigidity. If one more agent is added to the formation (Fig. 3.2.1(c)), by achieving the desired distance (d_{43}) and the corresponding angle (α_1), the formation shape stays rigid and congruent with the desired rigid formation shape (Fig. 3.2.1(b)). Therefore for each agent i with $i > 2$, satisfying one desired distance and the related desired angle is sufficient to achieve rigidity. ■

The sensing topology is represented by a directed graph $\mathcal{G} = (\mathcal{V}, \mathcal{E})$. Each agent uses its own local sensors to detect the relative position of its neighbors with respect to its own local coordinate system. Then for agent i, $p_j^i = \begin{bmatrix} x_j^i & y_j^i \end{bmatrix}^T$ is the position of agent j with respect to ${}^i\sum$. The formation control law which is presented below, is distributed and can be implemented with respect to the local coordinate system of the agents. To analyze the stability of the system, it is better to represent the dynamics of all agents in a common coordinate system. Regarding the results of (Oh and Ahn [2014]) with an appropriate rotation and translation, all results from a common coordinate system are converted to the local coordinate system of agent i

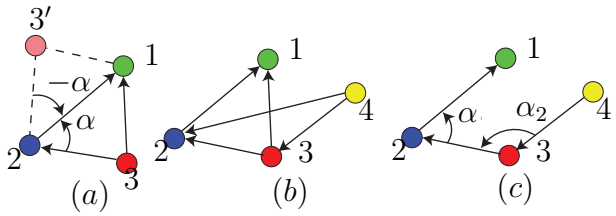

Figure 3.2.1: Formation control of group of four agents

3.2.1 Information Topology

All agents are assigned constant predefined index numbers $i \leq N$. Without loss of generality, assume agents 1 and 2 are leaders. As depicted in Fig. 3.2.1(b), arrows show the relationship. The head of the arrow points to the neighbor in each sensing relationship.

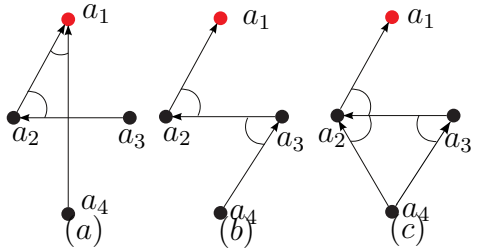

Figure 3.2.2: Formation control of group of four agents

3.2.2 Problem Statement

Given $p^* \in \mathbb{R}^{2N}$ as instance of a formation with graph $\mathcal{G}$, in the plane, the desired formation of a group of single integrator agents is represented by the set

$$E_p = \left\{ p \in \mathbb{R}^{2N} : \|p_j - p_i\| = \left\|p_j^* - p_i^*\right\|, \forall i, j \in \mathcal{V} \right\}. \tag{3.2.1}$$

For double integrator agents the desired formation is represented by

$$E_{p,v} = \left\{ \begin{bmatrix} p \\ v \end{bmatrix} \in \mathbb{R}^{4N} : \|p_j - p_i\| = \left\|p_j^* - p_i^*\right\|, \\ v = 0, \forall i, j \in \mathcal{V} \right\}, \tag{3.2.2}$$

where $v = [v_1^T, \cdots, v_N^T]$. Therefore E_p and $E_{p,v}$ are the sets of all formations congruent to p^*. The desired distance between agent i and j is denoted by $d_{ij}^* = \left\|p_j^* - p_i^*\right\|$. The formation control problem which is addressed in this chapter is formulated as follows.

Problem 3.2.1. *Given an N agent group with formation directed graph $\mathcal{G}_f = (\mathcal{V}, \mathcal{E}_f)$ and a desired realization p^* of $\mathcal{G}_f$, all agents are modeled by identical single integrators (1.5.1) or by double integrators (1.5.2). Assuming that the graph $\mathcal{G}_f = (\mathcal{V}, \mathcal{E}_f)$ is cycle free and rigid, design a controller to achieve a formation that is congruent with the desired formation and E_p or $E_{p,v}$, is asymptotically stable.*

3.3 Cascaded Formation Fontrol

To illustrate the above strategies, consider a group of four agents in a plane and assume the desired formation shape is square. Agents 1 and 2 are the leaders. The initial positions of agents and the desired formation are given as depicted in Fig. 3.3.1(a). The directed formation graph is depicted in Fig. 3.3.1(a1). First agent 1 and agent 2 use tracking to

achieve a desired distance, d^*_{12}. Agent 3 has two neighbors: agent 1 and agent 2. Then agent 3 selects agent 2 as a distance neighbor and agent 1 as an angle neighbor and uses tracking to satisfy two objectives: the distance d_{32} is equal to the desired distance and the angle $\angle 321$ is equal to the desired angle. Agent 4 has two neighbors: agent 2 and agent 3. Then agent 4 selects agent 3 as a distance neighbor and agent 2 as an angle neighbor. We assume that agents do not know whether their neighbors achieve a formation or not. Agents always follow their neighbors, regardless of whether their neighbors achieve the desired formation or not. The graph is assumed cycle-free and so in the cascade structure, all agents achieve the desired formation step by step. In Fig. 3.3.1(b), agent i and its neighbors are shown. Agent k is a distance neighbor of agent i and agent j is an angle neighbor of it. The desired angle and desired distance between agent i and agent k and j are defined by α^*_{ikj} and d^*_{ki}, respectively, and α_{ikj} and d_{ki} are the real angle and distance between agent i and agent k and j. From Fig. 3.3.1(b) define:

$$\begin{aligned}
\alpha^*_{ikj} &= \arccos\left(\frac{d^{*2}_{ki} + d^{*2}_{kj} - d^{*2}_{ji}}{2d^*_{ki}d^*_{kj}}\right), \\
\alpha_{ikj}(t) &= \arccos\left(\frac{d^2_{ki}(t) + d^2_{kj}(t) - d^2_{ji}(t)}{2d_{ki}(t)d_{kj}(t)}\right), \\
\sigma_{ikj}(t) &= (\alpha_{ikj}(t) - \alpha^*_{ikj})sign(S_i), \\
S_i &= (x^i_i(t) - x^i_k(t))(y^i_j(t) - y^i_k(t)) \\
&\quad - (y^i_i(t) - y^i_k(t))(x^i_j(t) - x^i_k(t)),
\end{aligned} \tag{3.3.1}$$

and $-\pi < \alpha_{ikj}, \alpha^*_{ikj} \leq \pi$.

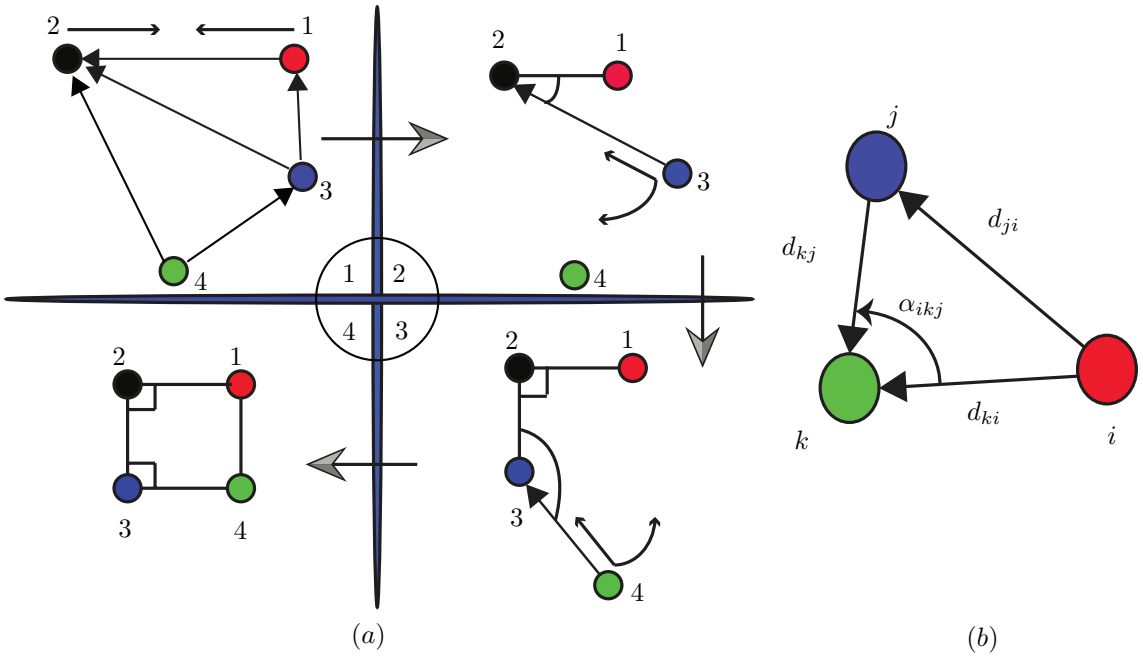

Figure 3.3.1: (a) Cascaded formation control of a group of four agents with square-shaped desired formation. (b) Angle and distances

The control law consists of two parts, to achieve the desired distance and the desired angle. To achieve these goals the following two functions are defined as formation errors

$$\begin{aligned}\phi_{ij}(t) &= (\alpha_{ikj}(t) - \alpha^*_{ikj})^2,\\ \phi_i(t) &= \sum_{j\in\mathcal{A}_i} \phi_{ij}(t),\\ \psi_i(t) &= (d_{ki}(t) - d^*_{ki})^2,\end{aligned} \tag{3.3.2}$$

where k is the index of the distance neighbor for agent i and also ϕ_i and ψ_i are errors of angle and distance for agent i respectively. Then agent i achieves the desired formation if $\phi_{ij} = 0$ for all $j \in \mathcal{A}_i$ and $\psi_i = 0$. By taking gradients of ψ_{ki} and ϕ_{ki} with respect to p^i_i, we obtain:

$$\begin{aligned}\Phi^i_{ij}(t) &= -\frac{1}{2}\nabla_{p^i_i}\phi_{ij}(t) =\\ &= \begin{bmatrix} -\frac{\sigma_{ikj}(y^i_i - y^i_k)}{d^2_{ki}} & \frac{\sigma_{ikj}(x^i_i - x^i_k)}{d^2_{ki}}\end{bmatrix}^T,\\ \Psi^i_i(t) &= -\frac{1}{2}\nabla_{p^i_i}\psi_i(t) = \frac{(d^*_{ki} - d_{ki})}{d_{ki}}(p_i - p_k),\\ \Phi^i_i(t) &= \sum_{j\in\mathcal{A}_i}\Phi^i_{ij}(t),\end{aligned} \tag{3.3.3}$$

where σ_{ikj} is obtained from (3.3.1). The vectors Φ^i_i and Ψ^i_i for each agent are always orthogonal. Therefore in case that $\Phi^i_i + \Psi^i_i = 0$ it follows that both $\Phi^i_i = 0$ and $\Psi^i_i = 0$.

Remark 3.3.1. *Based on Lemma 3.2.1, it is clear that satisfying one distance and one angle condition for each agent is sufficient to achieve a desired formation in the cascade formation. Each agent has one distance neighbor and $\mathcal{N}_i - 1$ angle neighbors. However, choosing more than one angle neighbor is useful for making the control law more robust against loosing a neighbor. According to Assumption 3.2.1, to calculate Φ^i_i as far as adding new angle neighbors does not cause $\Phi^i_i = 0$ we can choose more angle neighbors. In the worst case, each agent just uses one angle neighbor to reach the desired formation.*

3.3.1 Collision Avoidance

To achieve obstacle collision avoidance, usually an avoidance function is used. The collision avoidance function is already explained in Section 2.2.2 and that is the same here.

3.3.2 Control Law

In this section, a control law to achieve a formation and to maintain it will be introduced. In addition, asymptotic stability of the formation is proved.

3.3.3 Control law for Single Integrator Agents

The control law for agent i can be designed as

$$u_i^i(t) = \begin{cases} k_v \Psi_i^i - k_o \frac{\partial V_{ai}}{\partial p_i^i} & if \quad i < 3 \\ k_\alpha \Phi_i^i + k_v \Psi_i^i - k_o \frac{\partial V_{ai}}{\partial p_i^i} & if \quad i \geq 3, \end{cases}, \tag{3.3.4}$$

where $k_\alpha > 0$, $k_v > 0, k_o > 0$ and Ψ_i^i and Φ_i^i are obtained from (3.3.3). The control law (3.3.4) is completely distributed in the sense that each agent can implement it in its local coordinate system by using only local measurements. As mentioned already, to study stability it is more convenient to represent the control law and the dynamics of agents with respect to ${}^g\sum$. On the basis of the results of (Oh and Ahn [2014]), by a suitable coordinate transformation, the control law (3.3.4) with respect to ${}^g\sum$ is represented as

$$u_i(t) = \begin{cases} k_v \Psi_i - k_o \frac{\partial V_{ai}}{\partial p_i} & if \quad i < 3 \\ k_\alpha \Phi_i + k_v \Psi_i - k_o \frac{\partial V_{ai}}{\partial p_i} & if \quad i \geq 3, \end{cases}, \tag{3.3.5}$$

where $\Psi_i = -\frac{1}{2}\nabla_{p_i}\psi_i$ and $\Phi_i = \sum_{j\in\mathcal{A}_i} -\frac{1}{2}\nabla_{p_i}\phi_{ij}$. The following Lemma establishes stability.

Lemma 3.3.1. *Consider agent i, where $i > 2$ in a multi-agent system with agents modeled as (1.5.1), and assume all neighbors of agent i are in the desired formation. Applying control law (3.3.5) leads to $\psi_{ki} \to 0$ and $\phi_{ki} \to 0$ as $t \to \infty$*

Proof: Consider the Lyapunov function candidate

$$V_k(p_i) = \frac{1}{2}\sum_{k\in\mathcal{A}_i} k_\alpha \phi_{ki} + \frac{1}{2} k_v \psi_i + k_o V_{ai}. \tag{3.3.6}$$

By taking the derivative of (3.3.6) and substituting from (1.5.1) and (3.3.5) yields

$$\dot{V}_k = -\left\| k_\alpha \Phi_i + k_v \Psi_i - k_o \frac{\partial V_{ai}}{\partial p_i} \right\|^2. \tag{3.3.7}$$

We have $\dot{V}_k \leq 0$, which shows stability of formation errors of agent i. To show asymptotic stability, the equilibrium point of $\dot{V}_k = 0$ is analyzed. $\dot{V}_k = 0$ implies that $u_i = 0$ and from Remark 2.2.1 it is concluded that in the equilibrium points $\frac{\partial V_{ai}}{\partial p_i} = 0$. Then $\dot{V}_k = 0$ leads to $\Phi_i + \Psi_i = 0$. Φ_i and Ψ_i are perpendicular and thus $\dot{V}_k = 0$ implies that $\Psi_i = 0$ and $\Phi_i = 0$. Then from $\Psi_i = 0$ it is concluded that $\frac{(d_{ki}^* - d_{ki})}{d_{ki}}(p_i - p_k) = 0$ and therefore $d_{ki} = d_{ki}^*$. From $\Phi_i = 0$ we obtain

$$\frac{(y_i - y_k)\sum_j \sigma_{ikj}}{d_{ki}^2} = 0, \frac{(x_i - x_k)\sum_j \sigma_{ikj}}{d_{ki}^2} = 0.$$

If agent i uses one angle neighbor to calculate Φ_i, then from $\Phi_i = 0$ it follows that $\frac{(\alpha_{ki}^* - \alpha_{ki})^2}{d_{ki}^2} = 0$ and $\alpha_{ki} = \alpha_{ki}^*$. On the basis of Remark 3.3.1, increasing the number of angle neighbors in the calculation of Φ_i is done as long as it does not create undesired equilibrium points for $\Phi_i = 0$. Therefore from $\dot{V}_k = 0$ it is concluded that $\psi_{ki} = 0, \phi_{ki} = 0$ and asymptotic stability of formation errors of agent i is proved. ■

Asymptotic stability of of a group of agents is ensured on the basis of Lemma 3.3.1 as follows.

Theorem 3.3.1. *Given a multi-agent system with N single integrator agents (1.5.1), and the distributed control law (3.3.4). Suppose that all Assumptions are fulfilled. Then, for all $p_i(0) \in \mathbb{R}^2$ and $t \geq 0$, the agents achieve a desired formation that is congruent with p^*, without collision and the system is asymptotically stable.*

Proof: Regarding (3.3.5), for agents 1 and 2, the control law only contains the avoidance function and the distance error. Take $V_{12}(t) = k_v\psi_1 + k_oV_{a1} + k_oV_{a2}$ as Lyapunov candidate function. From (3.3.2) we conclude that $\psi_1 = \psi_2$. By taking the derivative of V_{12} and substituting from (1.5.1) and (3.3.5),

$$\dot{V}_{12} = -\left\| k_v\Psi_1 - k_o\frac{\partial V_{a1}}{\partial p_1}\right\|^2 - \left\| k_v\Psi_2 - k_o\frac{\partial V_{a2}}{\partial p_2}\right\|^2$$

is obtained. From Remark 2.2.1 it is concluded that in equilibrium $\dot{V}_{12} = 0$ we have $\frac{\partial V_{a1}}{\partial p_1} = 0$ and $\frac{\partial V_{a2}}{\partial p_2} = 0$, and the collision avoidance is guaranteed. $\dot{V}_{12} = 0$ yields that $d_{12} = d_{12}^*$ and asymptotic stability of the formation errors of agent 1 and 2 is proved. Agent 3 uses agent 1 as distance neighbor and agent 2 as angle neighbor. The control law for agent 3 consists of distance and angle errors and from Lemma 3.3.1, it follows that the formation error of agent 3 converges to zero. By induction agent i converges to the desired formation and the whole system is asymptotically stable. Therefore $p \in E_p$ when $t \to \infty$. ■

3.3.4 Control Law for Double Integrator Agents

In this section, the above results are extended to double integrator agents. Each agent measures its own velocity and the relative distances to its neighbors. The control law for agent i is proposed as

$$u_i^i(t) = \begin{cases} k_v\Phi_i^i - k_o\frac{\partial V_{ai}}{\partial p_i^i} - k_dv_i^i & if \quad i < 3 \\ k_\alpha\Phi_i^i + k_v\Psi_i^i - k_o\frac{\partial V_{ai}}{\partial p_i^i} - k_dv_i^i & if \quad i \geq 3, \end{cases} \tag{3.3.8}$$

where $k_\alpha > 0$, $k_v > 0, k_o > 0, k_d > 0$ and Ψ_i^i and Φ_i^i are obtained from (3.3.3).

Lemma 3.3.2. *Consider agent i, where $i > 2$ in a multi-agent system with agents modeled as (1.5.2), and assume all neighbors of agent i are in the desired formation. Applying control law (3.3.8) leads to $v_i, \psi_{ki}, \phi_{ki} \to 0$ as $t \to \infty$.*

Proof: As mentioned already, the control law (3.3.8) is distributed and implemented based on the local coordinate system of each agent, but to analyze the stability of the system, the control law is represented with respect to the common coordinate system. To show asymptotic stability we use the following Lyapunov function candidate

$$V_k(p_i, v_i) = \frac{1}{2}\sum_{k\in\mathcal{A}_i} k_\alpha\phi_{ki} + \frac{1}{2}k_v\psi_i + k_oV_{ai} + \frac{m_i}{2}k_d\left\|v_i\right\|^2. \tag{3.3.9}$$

Taking the derivative of (3.3.9) and substituting from (3.3.8) and (1.5.2) yields

$$\dot{V}_k = -v_i^T \left(k_\alpha \Phi_i + k_v \Psi_i - k_o \frac{\partial V_{ai}}{\partial p_i} \right) + k_d v_i^T u_i. \tag{3.3.10}$$

Substituting from (3.3.8) leads to

$$\dot{V}_k = -k_d \left\| v_i \right\|^2. \tag{3.3.11}$$

Thus $\dot{V}_k \leq 0$, which shows stability of the formation error of agent i. To show asymptotic stability, an equilibrium point of $\dot{V}_k = 0$ is analyzed. $\dot{V}_k = 0$ implies that $v_i = 0$ and so from (1.5.2) it follows that $u_i = 0$. Then from Remark 2.2.1 it is concluded that in equilibrium point $\frac{\partial V_{ai}}{\partial p_i} = 0$. Then $\dot{V}_k = 0$, from (3.3.8) leads to, $\Phi_i + \Psi_i = 0$. Φ_i and Ψ_i are orthogonal and thus $\dot{V}_k = 0$ implies that $\Psi_i = 0$ and $\Phi_i = 0$. Then from $\Psi_i = 0$ it is concluded that $(d_{ki}^* - d_{ki})^2 = 0$ and therefore $d_{ki} = d_{ki}^*$. From Remark 3.3.1 and similar to the proof of Lemma 3.3.2, it follows that $\phi_{ki} \to 0$ and asymptotic stability of the system is concluded. Thus in the equilibrium points of $\dot{V}_k = 0$ we have $v_i, \psi_{ki}, \phi_{ki} = 0$ and the proof is completed. ■

Theorem 3.3.2. *Given a multi-agent system with N double integrator agents modeled as (1.5.2). By applying the control law (3.3.8) to all $p_i(0) \in \mathbb{R}^2$, the desired formation without collision is achieved and the system is asymptotically stable.*

Proof: The proof is similar to that of Theorem 3.3.1. ■

3.3.5 Formation and Orientation Control

In this section, the results of sections 3.3.3 and 3.3.4 are extended to achieve both formation and orientation. By assuming the rigid formation as a solid body and by specifying the direction of one edge, the orientation of the whole formation can be controlled. The edge between agent 1 and 2 is considered as an orientation edge. The desired orientation vectors are defined as $\hat{p}_{12} = \hat{p}_1 - \hat{p}_2$ and $\hat{p}_1$ and $\hat{p}_2$ are defined with respect to a common coordinate system. The relative difference between agent 1 and 2 is denoted by $p_{12} = p_1 - p_2$ with respect to the common coordinates.

Remark 3.3.2. *To achieve an orientation control, only in this section we assume agents* 1 *and* 2 *use the common coordinate system, whereas the other agents do not.*

The formation error for agents 1 and 2 is obtained by the formation error function used in (Ahmadi Barogh et al. [2015]) for the distance-based formation control as

$$V_o(t) = \begin{bmatrix} V_{o1} & V_{o2} \end{bmatrix}^T = \frac{1}{2}(p_{12} - \hat{p}_{12})^T (L \otimes I_2)(p_{12} - \hat{p}_{12}), \tag{3.3.12}$$

where $L = \begin{bmatrix} 1 & -1 \\ -1 & 1 \end{bmatrix}$ is a Laplacian matrix and I_2 is the identity matrix.

Then the gradient of formation error and avoidance function, for agent 1 and 2 is defined as

$$e_{ri} = -k_v \frac{\partial V_{oi}}{\partial p_i} - k_o \frac{\partial V_{ai}}{\partial p_i}, \tag{3.3.13}$$

where $i = 1, 2$ and $k_o, k_v > 0$ and V_{ai} is calculated from Equation (2.2.15). The control law for a single integrator dynamic model for agent 1 and 2 is given by

$$u_i = e_{ri}. \tag{3.3.14}$$

The control law for a double integrator dynamic model for agent 1 and 2 is given by

$$u_i = e_{ri} - k_d v_i, \tag{3.3.15}$$

where $k_d > 0$. The control law derived for agent i when $i > 2$ is the same as (3.3.4) for a single integrator dynamic models and (3.3.8) for a double integrator dynamic model. Agents $i > 2$ follow agent 1 and 2 in a cascade manner. In the next theorem, we show the proposed control law is asymptotically stable and the desired formation and orientation are obtained.

Theorem 3.3.3. *Suppose N identical agents with single integrator dynamics as in (1.5.1). The desired orientation is prescribed by $\hat{p}_1$ and $\hat{p}_2$. Then by the control law (3.3.14) for agent 1 and 2 and (3.3.4) for the other agents, the formation is asymptotically stable and the desired formation is achieved with desired orientation.*

Proof: A Lyapunov candidate function for agents 1 and 2 is

$$V_{12}(t) = k_v (p_{12} - \hat{p}_{12})^T (L \otimes I_2)(p_{12} - \hat{p}_{12}) + k_o V_{a1} + k_o V_{a2}.$$

By taking the derivative of V_{12} and substituting from (3.3.14) and (1.5.1), one can conclude that

$$\dot{V}_{12} = -\left\| k_v \frac{\partial V_{o1}}{\partial p_1} + k_o \frac{\partial V_{a1}}{\partial p_1} \right\|^2 - \left\| k_v \frac{\partial V_{o2}}{\partial p_2} + k_o \frac{\partial V_{a2}}{\partial p_2} \right\|^2 \leq 0$$

which implies that the gradient of formation errors of agent 1 and agent 2 are stable. In the equilibrium point $\dot{V}_{12} = 0$, using Remark 2.2.1, $\frac{\partial V_{ai}}{\partial p_i} = 0$ and collision avoidance is guaranteed. Therefore $\dot{V}_{12} = 0$ implies that $(L \otimes I_2)(p_{12} - \hat{p}_{12}) = 0$. The Laplacian matrix L has a zero eigenvalue with corresponding eigenvector equal to $\mathbf{1}_2 = \begin{bmatrix} 1 & 1 \end{bmatrix}^T$. So $\dot{V}_{12} = 0$ implies that $p_1 - p_2 = \hat{p}_1 - \hat{p}_2$ and the agent 1 and 2 achieve a desired formation with desired orientation and asymptotic stability of the desired formation and orientation of agent 1 and 2 is concluded. The distance neighbor of agent 3 is agent 1 and the angle neighbor of it is agent 2; from Lemma 3.3.1 it follows that agent 3 converges to the desired formation and in the cascade structure all agents achieve the desired formation, thus asymptotic stability of the formation is proved and therefore $p \in E_p$ when $t \to \infty$. Considering the rigidity of the whole formation, the edge between agents 1 and 2 is in the direction of desired orientation so the whole formation is at the desired orientation. ■

Remark 3.3.3. *In this chapter, all results in all Theorems and Lemmas are based on Remark 2.2.1. Remark 2.2.1 may not always true. For example, if obstacles are located very close to the desired position of follower agents. In that case, an incorrect equilibrium point is created and the formation errors do not converge to zero. Hence, our results on asymptotic stability are valid only in a local sense .*

3.4 Simulation Results

In this section, simulation results are presented to verify the functionality and effectiveness of the proposed control laws in the previous section. Experimental results will be provided in the last chapter of this thesis. Consider five single integrator agents in a plane. The aim is to achieve a desired formation with five sides equal to 30 and angles in the set $A = \{\pi/3 \quad 5\pi/6 \quad \pi/2 \quad \pi/2 \quad 5\pi/6\}$. In Table I all initial positions and all gain values are shown. As listed in Table I the initial formation shape of agents is not close to the desired formation shape. As shown in the simulation results, the final formation shape is congruent to the desired formation shape. In all following simulations we assume agents 1 and 2 are the leaders and the distance neighbor and the angle neighbor of agent i with $i > 2$ are agent $i-1$ and agent $i-2$, respectively. The desired orientation is represented by $\hat{p}_1 = \begin{bmatrix}100 & 100\end{bmatrix}^T$ and $\hat{p}_2 = \begin{bmatrix}73 & 91\end{bmatrix}^T$. Three scenarios are simulated

Table 3.1: Initial position of agents and gain parameters.

x	y
40	180
12	120
60	80
-60	100
-40	80

k_α	k_v	k_o	k_d	R	r	m
10	0.151	0.1	0.951	10	5	1

3.4.1 Formation Control of Single Integrator Agents with Orientation Control

In this scenario, the control law (3.3.14) is applied to agent 1 and 2 and all other agents use (3.3.4) in the plane with obstacles. The trajectories are shown in Fig. 3.4.1. The distance and angle errors (ψ_i and ϕ_i) for each agent are shown in Fig. 3.4.2. Note that when one agent or an obstacle is inside the detection area of another agent, the avoidance function is activated; as a consequence, the agents change the trajectories to avoid the collisions and the distance and angle errors increase or decrease depending on the direction of the repulsive force. As depicted in Fig. 3.4.1, the desired formation and orientation are achieved.

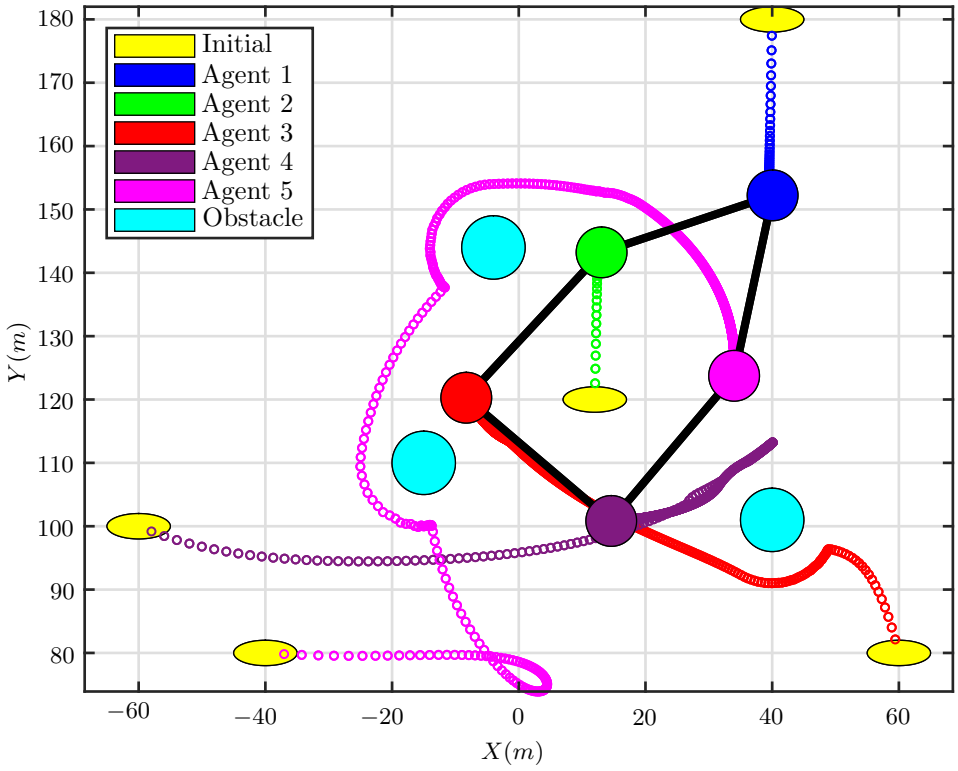

Figure 3.4.1: Simulation results of single integrator agents with orientation control

3.4.2 Formation Control of Double Integrator Agents

In this scenario orientation control is not considered. The control law (3.3.8) is applied to a group of agents with double integrator dynamic as in (1.5.2). The trajectories are depicted in Fig. 3.4.3. The distance, angle errors and the velocity norm (ψ_i, ϕ_i, v_i) for each agent are shown in Fig. 3.4.4.

3.4.3 Formation Control of Double Integrator Agents with Orientation

In this scenario the control law (3.3.15) is is applied to agent 1 and 2 and all other agents use the proposed controller (3.3.8). All agents are described by identical double integrator dynamics as (1.5.2). The trajectories are shown in Fig. 3.4.5 and the formation errors are shown in Fig. 3.4.6. As observed in Fig. 3.4.5 the desired formation and orientation are achieved.

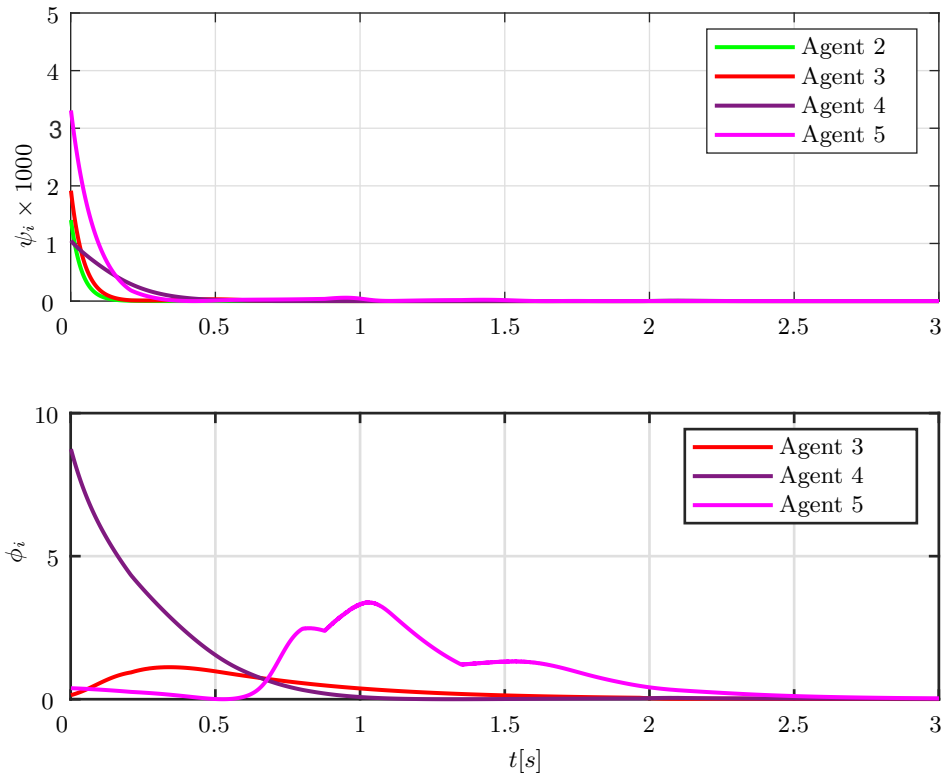

Figure 3.4.2: Distance (ψ_i) and angle (ϕ_i) errors for single integrator agents with orientation control

3.5 Conclusion

In this chapter, a new method for distance-angle-based formation control is proposed. In this approach, a combination of angle and distance approach is used to design a control law. A combination of angles and distances can avoid a flip and flex ambiguity in distance-based formation approaches. A common coordinate system is not required to be implemented on all agents. Unlike normal distance-based formation controls, in our approach for all initial positions of agents, the final formation shape is congruent to the desired formation shape and closeness of the initial formation to the desired formation is not necessary. We prove asymptotic stability of the cascaded system by using Lyapunov-like functions for single integrator and double integrator agents in the presence of obstacles. The control laws have the capability of preventing collision between agents, or agents and static obstacles. Finally, we improve the controller to achieve the desired formation, and the desired orientation. For orientation control, the distance-based approach is used for a small number of agents which are forced to control the relative positions. All other agents follow the orientation agents based on distance-angle cascaded formation control. Simulations confirm the effectiveness of the proposed approach.

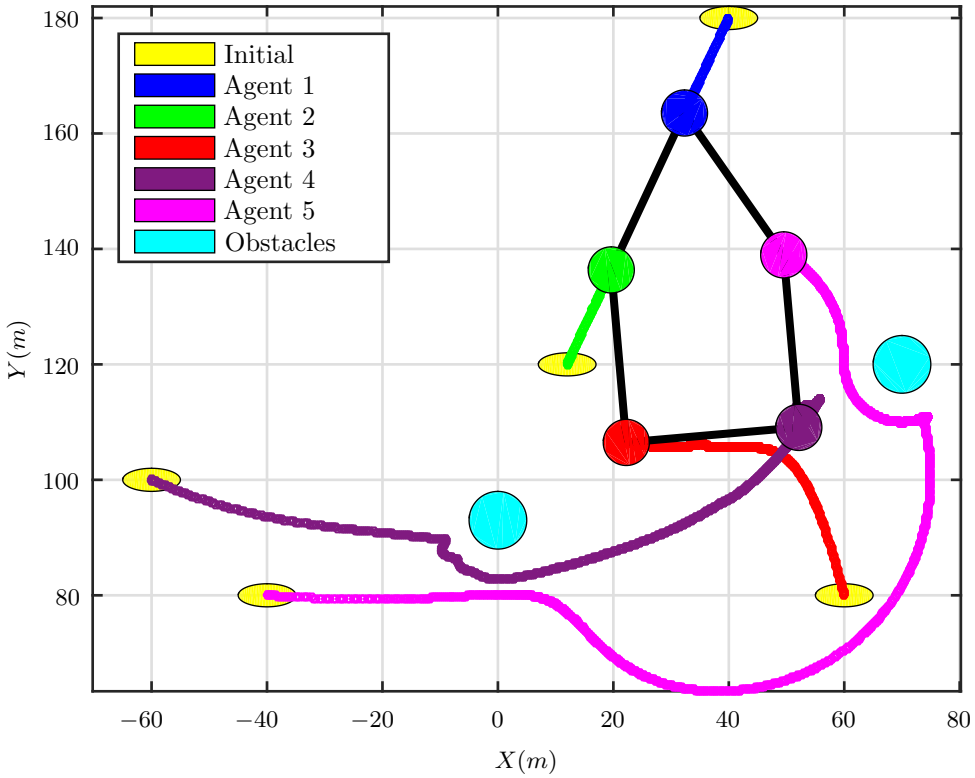

Figure 3.4.3: Simulation result of double integrator agents without orientation control

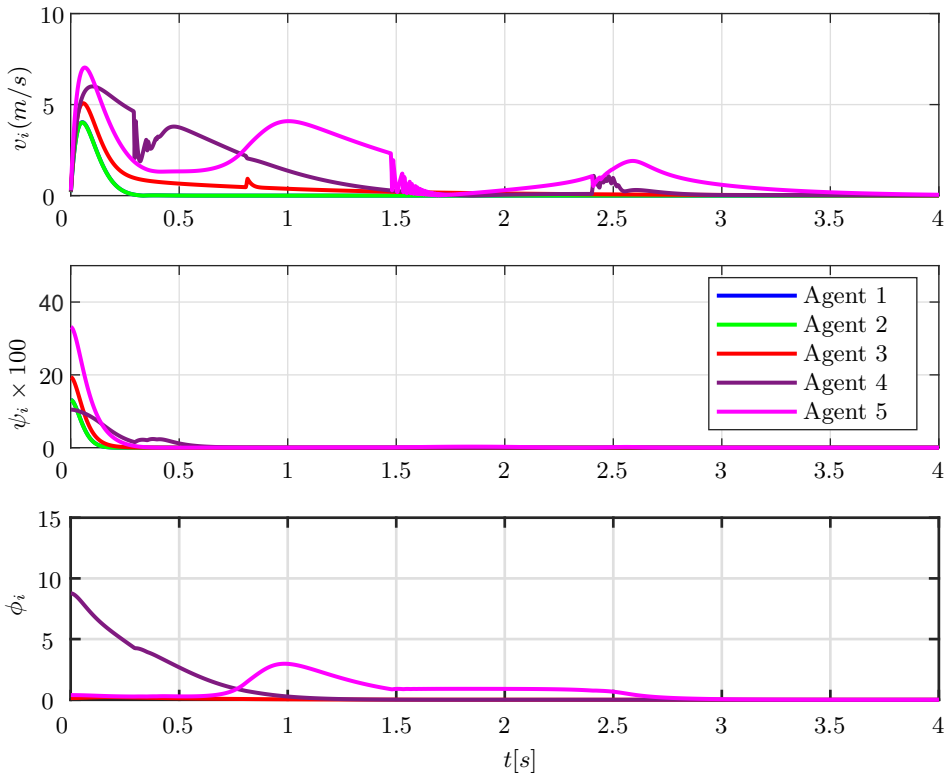

Figure 3.4.4: Distance (ψ_i) and angle (ϕ_i) errors and v_i for double integrator agents without orientation control

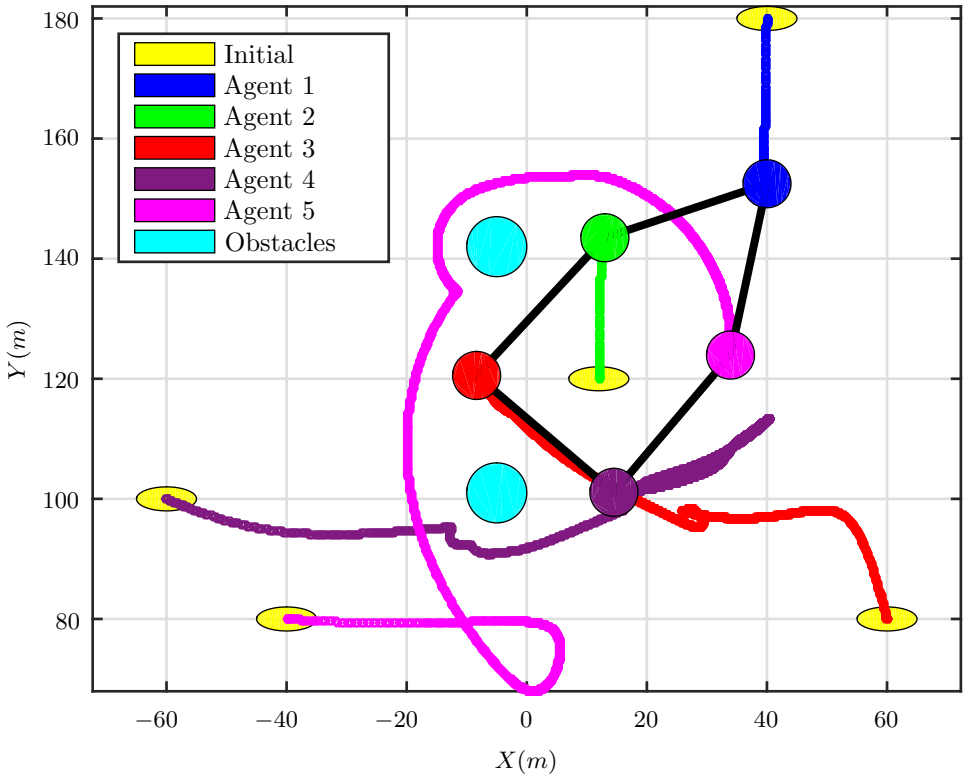

Figure 3.4.5: Simulation result of double integrator agents with orientation control

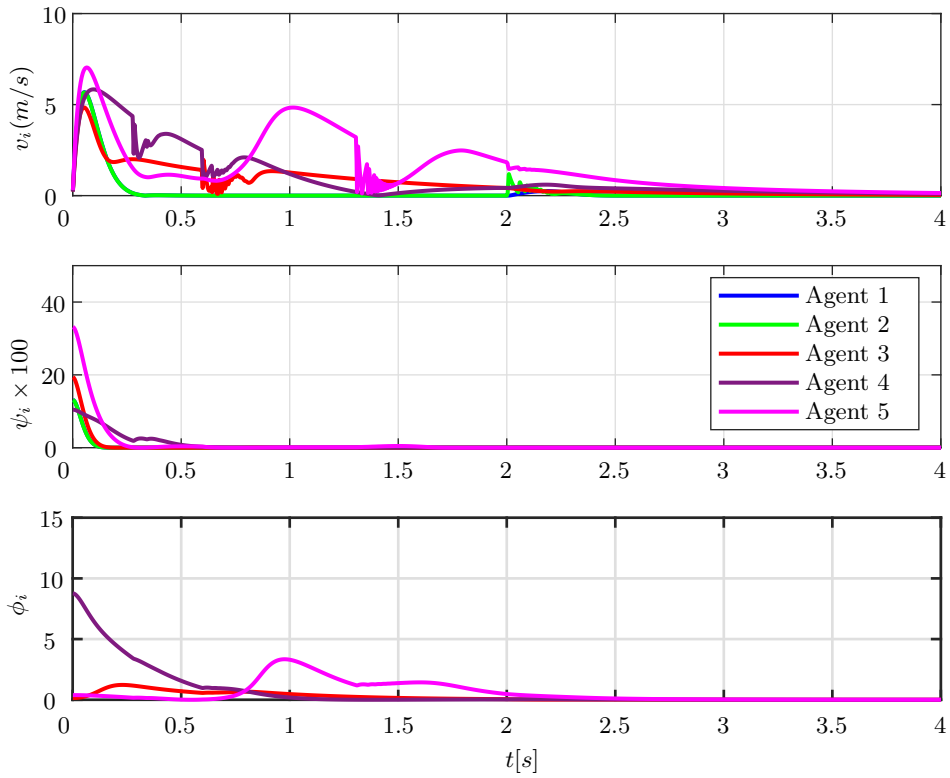

Figure 3.4.6: Distance (ψ_i) and angle (ϕ_i) errors and v_i for double integrator agents with orientation control

Chapter 4

Distance-Angle Based Formation Control for Non-Holonomic Agents

In this chapter, multi-agent formation control with obstacle collision avoidance for distance angle-based formations with orientation control for non-holonomic dynamics is considered. This chapter is an extension of the method that was proposed in Chapter 3 to non-holonomic dynamics. We propose an approach that uses information about the angle and distance between agents to achieve a leader-follower formation. First, we provide a sequential control law with collision avoidance for groups of agents with unicycle models and prove asymptotic stability of the formation. The non-holonomic unicycle model includes both dynamic and kinematic equations. Second, the proposed control law is combined with distance-based formation control. The shape of the formation is controlled by distance-angle-based formation control and the orientation of a group of agents is controlled to the desired orientation by a distance-based control law. Simulation results are presented to illustrate the proposed controllers. The control schemes and mathematical analysis that are discussed in this chapter were published in (Ahmadi Barogh and Werner [2016b]).

4.1 Introduction

In Chapter 2, we proposed a formation control scheme for non-holonomic agents based on displacement. In the main part of this chapter, an alternative approach to distance-angle-based formation control is considered and a novel way of combining the distances and angles between agents to achieve a formation is proposed. One phenomenon in distance-based formation control is the flip ambiguity, which can prevent a unique shape of a formation (Anderson et al. [2008]). A combination of angles and distances provides additional benefits to formation control in distance-based approaches to avoid flip ambiguity and flex ambiguity. Regarding this issue, with the proposed control law the closeness between initial positions of agents and desired formation is not necessary, which is a major advantage of our control law compared to other distance-based formation controllers. We assume all agents have a distinct local coordinate system. Each agent detects at least one

distance and one angle at the same time: using these two quantities, a rigid formation can be achieved. We assume a group of agents has one main leader. In comparison with (Tran and Lee [2011]) our new approach has the advantage that in order to achieve a formation it is not necessary to know the orientation of the leader. In comparison with distance-based formations, here a rigid formation is achieved with less information.

In the second part of this chapter, we aim to force the orientation of the whole formation to converge to the desired orientation. To reach this goal, certain agents (two agents) are chosen as orientation agents. The desired orientation is achieved by controlling the direction of the edge between orientation agents based on a distance approach. The orientation agents use a common coordinate system. The other agents follow the orientation agents with a distance-based approach to achieve the desired formation.

The rest of this chapter is arranged in four sections: In Section 4.2, the problem statement is established. In Section 4.3, we propose a control law that achieves the desired formation and orientation and establish the stability of the closed-loop system for non-holonomic agents in the presence of obstacles. Section 4.4 shows simulation results, and Section 4.5 concludes with a summary.

4.2 Problem Statement

Given N mobile agents in the plane, a directed formation graph $\mathcal{G}_f = (\mathcal{V}, \mathcal{E}_)$ and $p^* \in \mathbb{R}^{2N}$ as a desired representation of $\mathcal{G}_f$ in the plane. The desired formation of group of agents is defined as

$$E_p = \left\{ p \in \mathbb{R}^{2N} : \|p_j - p_i\| = \left\|p_j^* - p_i^*\right\|, \forall i, j : (i,j) \in \mathcal{E} \right\}. \tag{4.2.1}$$

Therefore E_p is the set of all formations congruent to p^*. The desired distance between agent i and j is denoted by $l_{ij} = \left\|p_j^* - p_i^*\right\|$ The formation control problem which is addressed in this chapter is formulated as follows.

Problem 4.2.1. *Given an N agent group with formation graph $\mathcal{G}_f = (\mathcal{V}, \mathcal{E}_f)$ and a desired realization p^* of $\mathcal{G}_f$, all agents are represented by identical non-holonomic models (1.5.3) or (1.5.4). Design a controller to achieve a formation that is congruent with the desired formation.*

4.3 Sequential Cascaded Formation Control

The sequential formation control strategy that is used here is the same as sequential formation control which was developed in Chapter 3 Section 3.3. Also, the collision avoidance function which is considered in the control law here is the same as the collision avoidance that is used already in Chapter 3 Section 3.3.

4.3.1 Control Law

In this section, a control law to achieve a formation and to maintain it will be introduced. In addition, the asymptotic stability of the formation is proved.

4.3.2 Control Law for Non-Holonomic Agents

The potential function for a group of agents with formation graph $\mathcal{G}_f = (\mathcal{V}, \mathcal{E}_f)$ is proposed as

$$V_i = \begin{cases} \psi_i(t) & i < 3 \\ \phi_i(t) + \psi_i(t) & i \geq 3, \end{cases} \tag{4.3.1}$$

where ψ_i and ϕ_i are obtained from (3.3.2). The formation errors are defined as

$$\begin{aligned} e_{ri} &= \begin{bmatrix} e_{xi} & e_{yi} \end{bmatrix}^T = -\frac{\partial V_i}{\partial p_i} - \frac{\partial V_{ai}}{\partial p_i} \\ \theta_{di} &= \arctan(e_{yi}, e_{xi}) \\ e_{\theta i} &= \theta_i - \theta_{di}, \end{aligned} \tag{4.3.2}$$

Assumption 2.2.1 is assumed. The control law for non-holonomic model (1.5.3) is

$$\begin{aligned} v_{di} &= k_f \sqrt{e_{xi}^2 + e_{yi}^2} \cos(e_{\theta i}) \\ \omega_{di} &= -k_\theta e_{\theta i} \end{aligned} \tag{4.3.3}$$

where $k_f > 0$ and $k_\theta > 0$. The control law which is proposed is

$$\begin{aligned} \tau_{1i} &= k_1(v_{di} - v_i) \\ \tau_{2i} &= k_2(\omega_{di} - \omega_i), \end{aligned} \tag{4.3.4}$$

where $k_{1i}, k_{2i} > 0$. The error of the formation is

$$e_i = \begin{bmatrix} e_{1i} & e_{2i} \end{bmatrix}^T = \begin{bmatrix} v_i - v_{di} & \omega_i - \omega_{di} \end{bmatrix}^T \tag{4.3.5}$$

Substituting (4.3.5) and (4.3.4) in (1.5.4) we have

$$\begin{aligned} m_i \dot{e}_{1i} + k_1 e_{1i} &= -m_i \dot{v}_{di} \\ l_i \dot{e}_{2i} + k_2 e_{2i} &= -l_i \dot{\omega}_{di}. \end{aligned} \tag{4.3.6}$$

Then one has that

$$M_i \dot{e}_i + k e_i = -M_i \dot{u}_{di} \tag{4.3.7}$$

where $k = \begin{bmatrix} k_1 & k_2 \end{bmatrix}^T$, $M_i = \begin{bmatrix} m_i & 0 \\ 0 & l_i \end{bmatrix}$ and $u_{di} = \begin{bmatrix} v_{di} & \omega_{di} \end{bmatrix}^T$ From (4.3.3) and (1.5.4) by taking derivative we have $\dot{u}_{di}$ as follow

$$\begin{aligned} \dot{v}_{di} &= \frac{\partial v_{di}}{\partial p_i} R_i u_i \\ \dot{\omega}_{di} &= k_\theta(\dot{\theta}_{di} - \omega_i), \end{aligned} \tag{4.3.8}$$

$$\dot{\theta}_{di} = v_i D_i, \tag{4.3.9}$$

$$D_i = \frac{\left[\frac{\partial V_i}{\partial x_i}\left(\frac{\partial^2 V_i}{\partial y_i \partial r_i} C_i\right) - \frac{\partial V_i}{\partial y_i}\left(\frac{\partial^2 V_i}{\partial x_i \partial r_i} C_i\right)\right]}{\left(\frac{\partial V_i}{\partial x_i}\right)^2 + \left(\frac{\partial V_i}{\partial y_i}\right)^2} \tag{4.3.10}$$

and

$$C_i = \begin{bmatrix} \cos(\theta_i) & \sin(\theta_i) \end{bmatrix}^T. \tag{4.3.11}$$

From this we obtain

$$\dot{u}_{di} = G_i u_i, \tag{4.3.12}$$

where

$$G_i = \begin{bmatrix} \frac{\partial v_{di}}{\partial p_i} R_i \\ \begin{bmatrix} D_i & -1 \end{bmatrix} \end{bmatrix}. \tag{4.3.13}$$

Then, substituting (4.3.12) in (4.3.7) results in

$$M_i \dot{e}_i + k e_i = -M_i G_i u_i. \tag{4.3.14}$$

Lemma 4.3.1. *Consider agent i in a multi-agent system with agents modeled as (1.5.4). Applying control law (4.3.4) leads to $\psi_{ki}, \phi_{ki} \to 0$ as $t \to \infty$*

Proof: The candidate Lyapunov function which is proposed is

$$F = \beta F_1 + F_2, \tag{4.3.15}$$

where F_1 and F_2 are

$$\begin{aligned} F_1 &= V_i + \frac{1}{2}\alpha(\theta_i - \theta_{di})^2, \\ F_2 &= \frac{1}{2}(m_i e_{1i}^2 + l_i e_{2i}^2), \end{aligned} \tag{4.3.16}$$

with $\alpha, \beta > 0$. By taking the derivative, we have

$$\dot{F} = \beta \dot{F}_1 + \dot{F}_2, \tag{4.3.17}$$

Without loss of generality, we assume $k_f = 1$, $k_\theta = 1$ and therefore we have

$$\dot{F}_1 = -e_{ri}\dot{r}_i + \alpha(\theta_i - \theta_{di})(\dot{\theta}_i - \dot{\theta}_{di}). \tag{4.3.18}$$

Then the derivative of F_2 is obtained as

$$\dot{F}_2 = m_i e_{1i}\dot{e}_{1i} + l_i e_{2i}\dot{e}_{2i}, \tag{4.3.19}$$

From (4.3.14) we obtain

$$\dot{F}_2 = -e^T k e - e^T M_i G_i u_i, \tag{4.3.20}$$

and from (4.3.18),(4.3.11) and (4.3.5) we have

$$\dot{F}_1 = -e_{ri} C_i v_i + \alpha(e_{2i} - \omega_i). \tag{4.3.21}$$

thus

$$e_{ri} C_i = e_{xi}\cos(\theta_{di} + e_{\theta i}) + e_{yi}\sin(\theta_{di} + e_{\theta i}). \tag{4.3.22}$$

From (4.3.3) and (4.3.22) we get

$$e_{ri} C_i = \sqrt{e_{xi}^2 + e_{yi}^2}\cos(e_{\theta i}), \tag{4.3.23}$$

and from (4.3.5) we have that

$$-e_{ri} C_i = e_{1i} - v_i. \tag{4.3.24}$$

Then, substituting (4.3.24) in (4.3.21) resulted

$$\dot{F}_1 = e_{1i} v_i - v_i^2 + \alpha(\omega_i e_{2i} - \omega_i^2 - e_{2i}\dot{\theta}_{di} + \omega_i \dot{\theta}_{di}), \tag{4.3.25}$$

where

$$e_{2i}\dot{\theta}_{id} = e_i^T \begin{bmatrix} 0 & 0 \\ D_i & 0 \end{bmatrix} u_i. \tag{4.3.26}$$

Substituting (4.3.26) in (4.3.25) yields

$$\dot{F}_1 = -v_i^2 - \alpha\omega_i^2 + \alpha\omega_i D_i v_i + u_i^T \begin{bmatrix} 1 & -\alpha D_i \\ 0 & \alpha \end{bmatrix} e_i. \tag{4.3.27}$$

Then, we have

$$\dot{F}_1 = -u_i^T N_i u_i + u_i^T \begin{bmatrix} 1 & -\alpha D_i \\ 0 & \alpha \end{bmatrix} e_i \tag{4.3.28}$$

where $N_i = \begin{bmatrix} 1 & -\frac{1}{2}\alpha D_i \\ -\frac{1}{2}\alpha D_i & \alpha \end{bmatrix}$. After replacing (4.3.28) and (4.3.20) in (4.3.17), yields

$$\dot{F} = -Z^T \begin{bmatrix} k & B \\ B^T & \beta N \end{bmatrix} Z, \tag{4.3.29}$$

where $B = \frac{1}{2}\left[M_i G_i - \beta \begin{bmatrix} 1 & 0 \\ -\alpha D_i & \alpha \end{bmatrix}\right]$ and $Z^T = \begin{bmatrix} e_i^T & u_i^T \end{bmatrix}$

Then, by using the Schur complement is possible to show that $N_i > 0$ if $\alpha < \frac{4}{D_i^2}$. From the results of (Gouvea et al. [2010]), and (Pereira et al. [2011]), we conclude that $\exists\beta$ such that $\dot{F} < 0$. Therefore δ_i and u_i converge to zero and from (4.3.5) we see that $v_i = v_{di}$ and $\omega_i = \omega_{di}$. From (4.3.16) is concluded that $F_1 \to 0$ and $F_2 \to 0$ and so $V_i \to 0$ and $V_{ai} \to 0$. Therefore we conclude that $\omega_{di} \to 0$ and $e_{\theta_i} \to 0$ and $v_{di} \to 0$ which implies $e_{ri} \to 0$. From Remark 2.2.1 it follows that $\frac{\partial V_{ai}}{\partial p_i} = 0$ and so $\frac{\partial V_i}{\partial p_i} \to 0$, thus it is concluded that $d_{ki} = d_{ki}^*$, $\alpha_{ikj} = \alpha_{ikj}^*$ and $\psi_i, \phi_i \to 0$ as $t \to \infty$, which completes the proof. ■

Theorem 4.3.1. *Given a multi-agent system with N non-holonomic agents (1.5.4) with the distributed control law (4.3.4). Suppose that Assumption 2.2.1 and Remark 2.2.1 are fulfilled. Then, for all $r_i(0) \in \mathbb{R}^2$ and $t \geq 0$, the agents achieve a desired formation without collision and the the system is asymptotically stable*

Proof: Regarding (4.3.1), for agents 1 and 2 the potential function only contains the avoidance function and the distance error. From Lemma 4.3.1 one can conclude that the distance error between agent 1 and 4 converges to zero. Agent 3 uses agent 1 or 2 as a leader and the control law for agent 3 consists of distance and angle errors and from Lemma 4.3.1, it follows that the formation error of agent 3 converges to zero. By induction agent i converges to the desired formation and the whole system is asymptotically stable. ■

4.3.3 Formation and Orientation Control

In this section the results of the previous section are extended to achieve both formation and orientation. By assuming the rigid formation as a solid body and specifying certain directions of one edge, the orientation of the whole formation can be controlled. The edge between agent 1 and 2 is considered as orientation edge. The desired orientation vectors defined as $\hat{p}_{12} = \hat{p}_1 - \hat{p}_2$ and $\hat{p}_1$ and $\hat{p}_2$ are defined with respect to a global coordinate system. The relative difference between agent 1 and 2 is defined as $p_{12} = p_1 - p_2$ with respect to global coordinates. The potential function for agent 1 and 2 is obtained from the potential function used in (Ahmadi Barogh et al. [2015]) for distance-based formation control as

$$V_o(p) = \begin{bmatrix} V_{o1} & V_{o2} \end{bmatrix}^T = \frac{1}{2}(p_{12} - \hat{p}_{12})^T (L \otimes I_2)(p_{12} - \hat{p}_{12}), \tag{4.3.30}$$

where $L = \begin{bmatrix} 1 & -1 \\ -1 & 1 \end{bmatrix}$.

Thus the formation errors for agent 1 and 2 are defined as

$$e_{ri} = -\frac{\partial V_{oi}}{\partial p_i} - \frac{\partial V_{ai}}{\partial p_i} \tag{4.3.31}$$

where $i = 1, 2$. The control law which is used for agent 1 and 2 is (4.3.3) with formation errors (4.3.31). The control law derived for agent i when $i \geq 3$ is the same as (4.3.3) that means the agents $i \geq 3$ follow the agent 1 and 2 in a sequential cascade manner. We show the proposed control law is asymptotically stable and the desired formation and orientation are obtained.

Theorem 4.3.2. *Suppose N non-holonomic agents are described as (1.5.4) and the desired formation is rigid and the initial positions are $p_i(0) \in \mathbb{R}^2$. Then with control law (4.3.3) the formation is asymptotically stable and the desired formation is achieved with desired orientation.*

Proof: The Lyapunov candidate function for agent 1 and 2 is

$$V_{12} = \frac{1}{2}(p_{12} - \hat{p}_{12})^T (L \otimes I_2)(p_{12} - \hat{p}_{12}) + V_{oi}. \tag{4.3.32}$$

By Lemma 4.3.1 one can conclude that $\frac{\partial V_{12}}{\partial p_1} \to 0$ and $\frac{\partial V_{12}}{\partial p_2} =\to 0$ when $t \to \infty$. Therefore from the gradient of (4.3.31) it follows that $p_{12} - \hat{p}_{12} = 0$. Thus asymptotic stability of the desired formation and orientation for agent 1 and 2 is concluded. For agent i when $i \geq 3$ the the formation error (4.3.1) with control law (4.3.3) is applied. The leader of agent 3 is agent 2 and from Lemma 4.3.1 it is possible to show that agent 3 converges to the desired formation and in a cascade structure all agents achieve a desired formation, thus local asymptotic stability of the formation is proved. Considering the rigidity of the whole formation, since the edge between agents 1 and 2 is in the direction of the desired orientation, the whole formation is at the desired orientation. ■

4.4 Simulation Results

In this section, simulation results are presented to verify the functionality and effectiveness of the proposed control laws in the previous section. Consider five agents with model (1.5.4) in a plane. The aim is to achieve a pentagon formation with side length equal to 30 and angles in the values of set $A = \{\pi/3 \quad 5\pi/6 \quad \pi/2 \quad \pi/2 \quad 5\pi/6\}$ to $\frac{3}{5}\pi$. In Tables (4.1), (4.2) and (4.3) all initial positions and all gain values are shown. In all following simulations we assume agent 1 is the leader and the local leader for agent i is agent $i-1$. Each agent just uses one leader and $N_i = 1$ for all agents.

Two scenarios are simulated: formation control without orientation control, and formation control with orientation control.

Table 4.1: Initial position of agents

x	y	θ
120	90	$2\pi/5$
12	110	$3\pi/5$
-10	40	$\pi/5$
-40	40	$2\pi/5$
-50	100	$\pi/5$

Table 4.2: Gain parameters

k_α	k_v	k_o	k_l	k_θ	R	r	m	I
2	0.01	0.1	1	0.01	8	4	2	2

Table 4.3: Static obstacles

x	y
100	115
-25	80
-20	120

4.4.1 Formation Control without Orientation Control

The formation control law (4.3.4) is applied to a group of agents with non-holonomic dynamics (1.5.4), in the plane with obstacles. Note that when one agent or an obstacle is inside the detection area of another agent, the avoidance function is activated, as a consequence, the agents change the trajectories to avoid the collision and the distance and angle errors increase or decrease depending on the direction of the repulsive force. We apply the formation control law (4.3.3) with formation errors (4.3.5). The result of the simulation is presented in Fig. 4.4.1. All agents achieve the formation. Fig. 4.4.2 shows squared distance and angle errors.

4.4.2 Formation Control of Non-Holonomic Agents with Orientation Control

In this section we apply control law (4.3.3) with formation errors (4.3.31). The desired orientation is $\pi/4$ with respect to the global coordinate system. Results are shown in Fig. 4.4.3. All agents follow the leader while maintaining the formation. Fig. 4.4.4 shows squared distance and angle errors and as shown in the figure the distance and angle errors increase when one agent or an obstacle are inside a detection area of other agent.

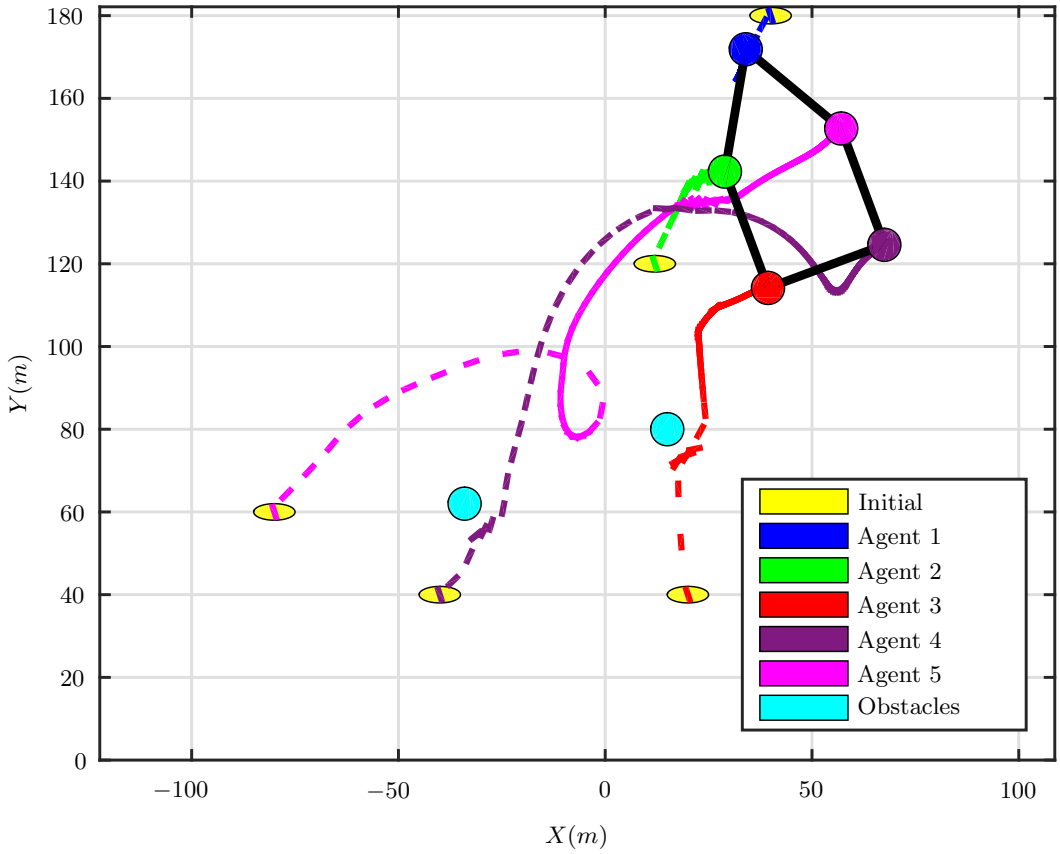

Figure 4.4.1: Simulation results of non-holonomic agents without orientation control.

4.5 Conclusion

In this chapter, a new method for distance-based formation control is proposed. In this approach, a combination of angle and distance approach is used to design a control law. A combination of angles and distances can avoid the flip ambiguity in the distance-based formation approaches. For all agents, the global coordinate system is not required to implement the formation control. We prove asymptotic stability of the cascaded system by using Lyapunov-like functions for non-holonomic agents with dynamic models in the presence of obstacles. The control law has the capability of preventing collision between agents, or agents and static obstacles. Finally we improve the controller to achieve a desired formation. For orientation control the distance-based approach is used for a small number of agents which are forced to control the relative positions. All other agents follow the orientation agents, based on distance-angle-based formation control. Simulations confirm the effectiveness of the proposed algorithms.

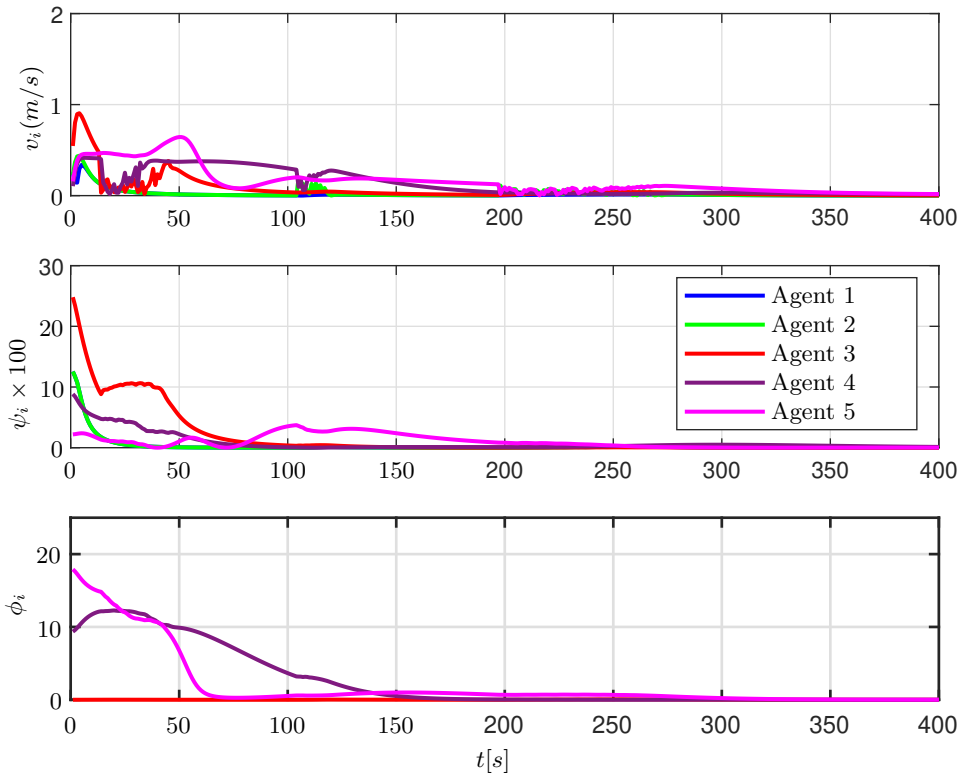

Figure 4.4.2: Squared distance (ψ_i) and angle (ϕ_i) errors and agent's speed v_i for non-holonomic agents without orientation control

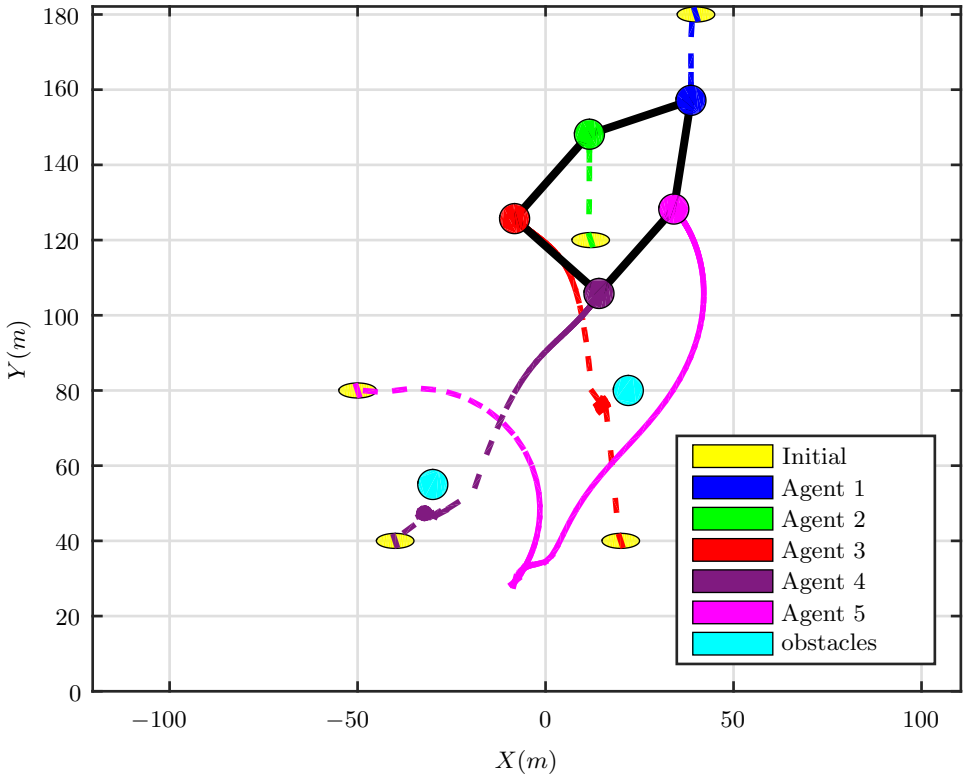

Figure 4.4.3: Simulation result of non-holonomic agents with orientation control.

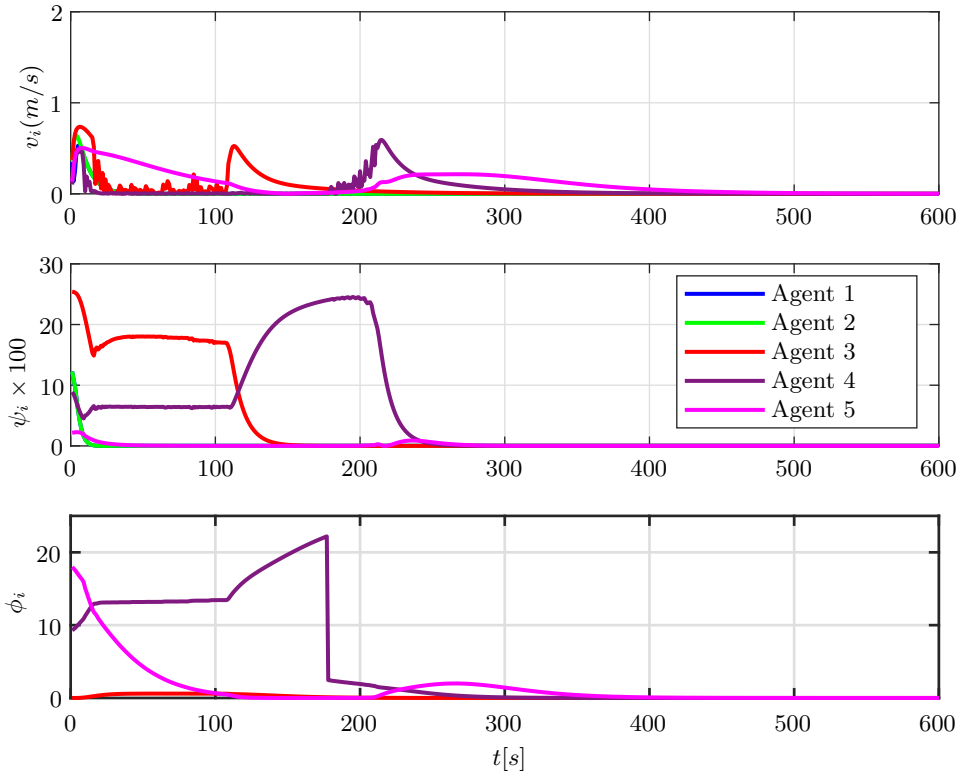

Figure 4.4.4: Squared distance and angle errors and speed with orientation control.

Chapter 5

Cooperative Source Seeking Using Agents with Integrator Dynamics

In this chapter the problem of source seeking with a group of agents in a distance-based formation is considered. Each agent is equipped with appropriate sensors to detect the distance between itself and its neighbors and to measure the strength of the signal. The task is to find a maximum point of the scalar field in the area. The multi-agent system cooperatively estimates the gradient of the scalar field and moves in the gradient direction, maintaining the specified formation in movement. In this chapter, a distributed controller for navigation of single and double integrator agents is proposed. We present a distance-angle-based formation controller to maintain a predefined formation when moving. In a distance-angle based formation agents do not need access to a common coordinate system. Conditions are provided for asymptotic stability of the system. Simulation results are presented to illustrate the effectiveness of the proposed approach. The control schemes and algorithm that are proposed in this chapter have been published in (Ahmadi Barogh and Werner [2017b]).

5.1 Introduction

Here we address the problem of source seeking using a formation of N identical agents with a distance-angle-based formation method without access to a common coordinate system. We assume each agent uses its own local coordinate system and is equipped with appropriate sensors to detect the distance and angle between itself and its neighbors. Each agent estimates the gradient direction with respect to its local coordinate system. To estimate the gradient direction each agent uses the neighbor's signal strength only and detects their position with respect to the local coordinate system of itself. A proposed distributed control law includes two parts: a formation control law and a source seeking trajectory control law. The first part of the control law guarantees that the group of agents achieves the formation and maintains it in the presence of obstacles, while the second part enforces the source seeking behavior.

5.2 Outline of This Chapter

This chapter covers the source localization with a distance-based formation control scheme for single integrator and double integrator agent models. In this work the control law neither needs the absolute position of agents nor to keep the agents in a specific circular rotating formation such as (Fabbiano et al. [2018]). Rotating agents in the circular geometric formation results in significant energy consumption in the system. When obstacles are in the area, the implementation of a circular rotating formation is difficult or might be impossible.

The rest of this chapter is arranged in five sections: Section 5.3 provides the background about distance based formation control and then the problem statement. In Section 5.4, a control law is proposed to locate the source and the desired formation. Stability of the closed-loop system is shown for single integrator and double integrator agents in the presence of obstacles. Section 5.5 shows simulation results, and Section 5.6, concludes with a summary.

5.3 Cascaded Formation Control

Cascaded formation control that is used in this chapter, was proposed in Chapter 3.

5.3.1 Problem Statement

Given $p^* \in \mathbb{R}^{nN}$ as a desired representation of $\mathcal{G}_f$ in n dimensional space. The scalar field is distributed in an environment and is represented with value μ. The communication graph used to estimate the gradients is represented to $\mathcal{G}_s$. The problem is design a control law to force the group of the agents to achieve the desired formation based on local information about the distance and angles, and to drive the center of the formation to the source p_s based on the estimated gradients. All agents are modeled by identical single integrators (1.5.1) or by double integrators (1.5.2). The desired formation of a group of single integrator agents is represented by the set

$$E_p = \left\{ p \in \mathbb{R}^{2N} : \|p_j - p_i\| = \left\|p_j^* - p_i^*\right\|, \forall i, j \in \mathcal{V} \right\}. \tag{5.3.1}$$

For double integrator agents the desired formation group is represented by

$$E_{p,v} = \left\{ \begin{bmatrix} p^T & v^T \end{bmatrix} \in \mathbb{R}^{4N} : \|p_j - p_i\| = \left\|p_j^* - p_i^*\right\| \\ , v = 0, \forall i, j \in \mathcal{V} \right\}, \tag{5.3.2}$$

where $v = [v_1^T, \cdots, v_N^T]$. Therefore E_p and $E_{p,v}$ are the sets of all formations congruent to p^*. The desired distance between agent i and j is denoted by $d_{ij}^* = \left\|p_j^* - p_i^*\right\|$.

Assumption 5.3.1. *Regarding that obstacles are scattered in random locations in an environment, the combination of obstacles can block the route of formation of agents to the source. The formation of agents tries to follow the estimated gradient direction of*

the scalar field and if this direction is completely blocked by a combination of obstacles, agents can not reach the source. In this work, we assume that the direction of gradient from the formation of agents to the source is not completely closed by the combination of obstacles and always there is a open route in the direction of gradient of scalar field from the formation of agents to the source.

Remark 5.3.1. *$\hat{g}_i^i$ denotes the estimate of the gradient of agent i with respect to ${}^i\sum$. To prove stability with the proposed control law, we assume all gradient vectors are transformed to ${}^g\sum$ with an appropriate rotation and transformation and denoted by $\hat{g}_i$. We define $\hat{g}_c = \frac{1}{N}\sum_{i=1}^{N}\hat{g}_i$ as an estimated gradient of a scalar field of the center of formation. In the following control laws, each agent only needs to calculate $\hat{g}_i^i$ and the gradient of the center is not required. We use $\hat{g}_c$ to prove stability and convergence. From Assumption 1.5.2 one can conclude that $\|\hat{g}_c - g_c\| \leq e_g$*

5.4 Control Law

In this section, a control law to achieve formation and source seeking will be introduced. In addition, asymptotic stability of the formation is proved.

Definition 5.4.1. *Define a function sign$\left(\begin{bmatrix} x & y \end{bmatrix}\right)$, where x and y are real numbers, which returns the vector $\begin{bmatrix} sgn(x) & sgn(y) \end{bmatrix}^T$ as a result where sgn(.) equal to 1, -1, 0 for positive, negative and zero inputs respectively.*

5.4.1 Control Law for Double Integrator Agents

The distributed control law for agent i can be designed as

$$u_i^i(t) = k_\alpha \Phi_i^i + k_v \Psi_i^i - k_o \frac{\partial V_{ai}}{\partial p_i^i} - k_d v_i^i + k_t \hat{g}_i^i(p_i^i) - k_s \cdot \text{sign}(v_i^i), \tag{5.4.1}$$

where $k_\alpha > 0,\ k_v > 0, k_o > 0, k_t > 0, k_d > 0, k_s > 0$ and Ψ_i^i and Φ_i^i are obtained from (3.3.3) and $\hat{g}_i^i$ comes from (1.5.7). For agent 1 and 2 in (5.4.1) $\Phi_i^i = 0$. The control law (5.4.1) is completely distributed in the sense that each agent can implement it in its local coordinate system by using only local measurements. As mentioned already, to study stability it is more convenient to represent the control law and the dynamics of agents with respect to ${}^g\sum$. The control law (5.4.1) with respect to ${}^g\sum$ is represented as

$$u_i(t) = k_\alpha \Phi_i + k_v \Psi_i - k_o \frac{\partial V_{ai}}{\partial p_i} - k_d v_i + k_t \hat{g}_i(p_i) - k_s \cdot \text{sign}(v_i), \tag{5.4.2}$$

where $\Psi_i = -\frac{1}{2}\nabla_{p_i}\psi_i$ and $\Phi_i = \sum_{j\in\mathcal{A}_{fi}} -\frac{1}{2}\nabla_{p_i}\phi_{ij}$.

In (5.4.1), $k_\alpha\Phi_i^i + k_v\Psi_i^i$ drives the agent to the desired formation, $k_o\frac{\partial V_{ai}}{\partial p_I^i}$ guarantees collision avoidance, $k_d v_i^i$ is a velocity damping that decreases the kinematic energy of the agent and $k_t\hat{g}_i(p_i)$ generates the gradient tracking.

The proposed control scheme in (5.4.2) is continuous but in actual implementation, sensors measure the values of a scalar-field, positions, and velocities of each agent and then transfer these values to the processor in every time interval. Therefore the implemented control scheme will be digital. On the other hand, the digitalized estimation (5.4.2) is implemented in the real environment. The proposed control scheme with digital estimation is stated in Algorithm 1.

Algorithm 1 Source seeking algorithm for agent i with distance-based formation

1: **repeat**
2: $\mu_i, p_i^i, v_i^i \Leftarrow$ Sensor readings.
3: $\forall \mu_j \Leftarrow$ Communication with neighbors $\forall j \in \mathcal{N}_{si}$
4: $p_j^i \Leftarrow$ Detecting the position of neighbors $\forall j \in \mathcal{N}_{si}$
5: Distributed gradient estimation $\hat{g}_i^i(p_i^i) \Leftarrow$ Equation (1.5.7)
6: Distributed control law $u_i^i(r_i) \Leftarrow$ Equation (5.4.1)
7: **until** $\|\hat{g}_i^i(r_i)\| < \epsilon$, where ϵ is a predefined positive constant.

The following theorem states the convergence of the proposed control law to the source.

Theorem 5.4.1. *Given a multi-agent system with N double integrator agents (1.5.2), and the distributed control law (5.4.1) under Algorithm 1. Suppose that Assumptions 1.5.1 to 1.5.4 and 5.3.1 about the scalar field and the location of obstacles and Remark 2.2.1 are fulfilled. Then, for all $p_i(0) \in \mathbb{R}^n$ and $t \geq 0$, the agents achieve a desired formation that is congruent with p^*, without collision, and the formation center ($p_c(t)$) satisfies $\hat{g}_c \to 0$ as $t \to \infty$ when $k_s \geq k_t\sqrt{2}e_g$. Then the center of formation is stabilized in a region with bounded distance from the source p_s as $\|(p_s - p_c)\| \leq \frac{-2e_g}{\eta_1}$*

Proof: As mentioned already, the control law (5.4.1) is distributed and implemented based on the local coordinate system of each agent, but to analyze the stability of the whole system, the control law is represented with respect to the common coordinate system. We will present the proof in two steps. First, the formation center's dynamic is presented and the stability is analyzed. Then source seeking is investigated. From (5.4.2) and (1.5.2) we obtain

$$\dot{v}_c = \frac{1}{N}\sum_1^N \dot{v}_i = \frac{1}{N}\left(k_v \sum_1^N \Psi_i + k_\alpha \sum_1^N \Phi_i - k_o \sum_1^N \frac{\partial V_{ai}}{\partial p_i} - k_d \sum_1^N v_i + k_t \sum_1^N \hat{g}_i(p_i)\right), \tag{5.4.3}$$

where $\dot{v}_c$ is the acceleration of the center of formation. To show asymptotic stability we use the Lyapunov function candidate

$$V(p_i, v_i) = \sum_{i=1}^N \left(\frac{1}{2}k_\alpha \phi_i + \frac{1}{2}k_v \psi_i + k_o V_{ai} + \frac{m_i}{2}\|v_i\|^2 + k_t(\bar{\mu}(p_s) - \mu(p_i)\right), \tag{5.4.4}$$

Taking the derivative of (5.4.4) and substituting from (1.5.2) yields

$$\dot{V} = \sum_{i=1}^N \left(- v_i^T \left(k_\alpha \Phi_i + k_v \Psi_i - k_o \frac{\partial V_{ai}}{\partial p_i} + k_t g_i\right) + v_i^T u_i\right), \tag{5.4.5}$$

Substituting from (5.4.2) leads to

$$\dot{V} = -k_d \sum_{i=1}^{N} \|v_i\|^2 + k_t \sum_{i=1}^{N} v_i^T (\hat{g}_i - g_i) - k_s \sum_{i=1}^{N} \|v_i\|_1 . \tag{5.4.6}$$

Note that the norm inequalities imply

$$v_i^T (\hat{g}_i - g_i) \leq \|v_i\|_1 \|\hat{g}_i - g_i\|_1 . \tag{5.4.7}$$

Thus in (5.4.6) using the properties of a vector norm, we obtain

$$\dot{V} \leq -k_d \sum_{i=1}^{N} \|v_i\|^2 + k_t \sum_{i=1}^{N} \|v_i\|_1 \|\hat{g}_i - g_i\|_1 - k_s \sum_{i=1}^{N} \|v_i\|_1 . \tag{5.4.8}$$

We have $\|\hat{g}_i - g_i\|_1 \leq \sqrt{2}\,\|\hat{g}_i - g_i\|$ and therefore from Assumption 1.5.2 we have

$$\|\hat{g}_i - g_i\|_1 \leq \sqrt{2} e_g.$$

Substituting in (5.4.8) yields

$$\dot{V} \leq -\sum_{i=1}^{N} \Big(k_d \|v_i\|^2 + \|v_i\|_1 (k_s - k_t \sqrt{2} e_g) \Big) . \tag{5.4.9}$$

In (5.4.9), by applying the condition that $k_s \geq k_t \sqrt{2} e_g$, we have $\dot{V} \leq 0$ and stability is proved. To show asymptotic stability, the equilibrium point of $\dot{V} = 0$ is analyzed. From $k_s \geq k_t \sqrt{2} e_g$ and (5.4.6) we have $\dot{V} = 0$ implies $v_i \to 0$ as time goes to infinity and so from (1.5.2) it follows that $u_i \to 0$. Then from Remark 2.2.1 and (5.4.2) it is concluded that in the equilibrium point $\frac{\partial V_{ai}}{\partial p_i} = 0$ and collision avoidance is guaranteed. Therefore $\Phi_i + \Psi_i \to 0$ as $t \to \infty$. Φ_i and Ψ_i are orthogonal and thus $\Psi_i \to 0$ and $\Phi_i \to 0$. Then from $\Psi_i \to 0$ it is concluded that $(d_{ki}^* - d_{ki})^2 \to 0$ and therefore $d_{ki} \to d_{ki}^*$. From $\Phi_i \to 0$ and after simplifications it is concluded that $\frac{(\alpha_{ki}^* - \alpha_{ki})^2}{d_{ki}^2} \to 0$ and so it follows that $\alpha_{ki} \to \alpha_{ki}^*$, $\phi_{ki} \to 0$ and asymptotic stability of system is established. Thus in the equilibrium points of $\dot{V} = 0$ we have $v_i, \psi_{ki}, \phi_{ki} = 0$. Consider $\dot{v}_i \to 0$ from (5.4.3) we have that $\dot{v}_c \to 0$ and therefore from (5.4.3), Remark 5.3.1 it is concluded that $\hat{g}_c \to 0$ as $t \to \infty$. Finally we will show that the distance between p_c and p_s is bounded. The Taylor expansion of $\bar{\mu}(p_s)$ around p_c is

$$\bar{\mu}(p_s) = \mu(p_c) + (p_s - p_c)^T \nabla \mu(p_c) + \frac{1}{2}(p_s - p_c)^T \nabla^2 \mu(p_c)(p_s - p_c) + \cdots . \tag{5.4.10}$$

Regarding Assumption 1.5.2, we have

$$\bar{\mu}(p_s) \leq \mu(p_c) + (p_s - p_c)^T \nabla \mu(p_c) + \frac{1}{2} \|(p_s - p_c)\|^2 \eta_1 + \cdots ,$$

and with respect to the norm inequality

$$\bar{\mu}(p_s) - \mu(p_c) \leq \big\|(p_s - p_c)^T \nabla \mu(p_c)\big\| + \frac{1}{2} \|(p_s - p_c)\|^2 \eta_1 + \cdots .$$

From Remark 5.3.1 and considering the fact that $\hat{g}_c \to 0$ it can be shown that $\|\nabla \mu(p_c)\| \leq e_g$ as $t \to \infty$. Note that according to the fact that $\bar{\mu}(p_s)$ is a global maximum we have $\bar{\mu}(p_s) - \mu(p_c) \geq 0$, and from Assumption 1.5.1 $\eta_1 < 0$ therefore $\|(p_s - p_c)\| \leq \frac{-2e_g}{\eta_1}$ ■

5.4.2 Control Law for Single Integrator Agents

The control law for agent i can be designed as

$$u_i^i(t) = k_\alpha \Phi_i^i + k_v \Psi_i^i - k_o \frac{\partial V_{ai}}{\partial p_i^i} + k_t \hat{g}_i^i(p_i^i) - k_s \cdot \text{sign}(u_i^i) \tag{5.4.11}$$

where $k_\alpha > 0$, $k_v > 0, k_o > 0, k_t > 0, k_s > 0$, Ψ_i^i and Φ_i^i are obtained from (3.3.3), and $\hat{g}_i^i$ comes from (1.5.7). For agents 1 and 2 in (5.4.11) we have $\Phi_i^i = 0$. The control law (5.4.11) is completely distributed in the sense that each agent can implement it in its local coordinate system by using only local measurements.

Theorem 5.4.2. *Given a multi-agent system with N single integrator agents (1.5.1), and the distributed control law (5.4.11) under Algorithm 1. Suppose Assumptions 1.5.1 to 1.5.4 and 5.3.1 about the scalar field and the location of obstacles and Remark 2.2.1 are fulfilled. Then, for all $p_i(0) \in \mathbb{R}^n$ and $t \geq 0$, the agents achieve a desired formation that is congruent with p^*, without collision and at the formation center ($p_c(t)$) we have $\hat{g}_c \to 0$ as $t \to \infty$ when $k_s \geq k_t\sqrt{2}e_g$. Then the center of formation is stabilized in a region with distance from the source p_s bounded by $\|(p_s - p_c)\| \leq \frac{-2e_g}{\eta_1}$*

Proof: To show asymptotic stability we choose the Lyapunov function candidate

$$V(p_i) = \sum_{i=1}^{N} \left(\frac{1}{2} k_\alpha \phi_i + \frac{1}{2} k_v \psi_i + k_o V_{ai} + k_t(\bar{\mu}(p_s) - \mu(p_i) \right), \tag{5.4.12}$$

Taking the derivative of (5.4.12) and substituting from (1.5.1) yields

$$\dot{V} = \sum_{i=1}^{N} -u_i^T \left(k_\alpha \Phi_i + k_v \Psi_i - k_o \frac{\partial V_{ai}}{\partial p_i} + k_t g_i \right), \tag{5.4.13}$$

Define $g_i = \hat{g}_i + \varepsilon_i$, $\varepsilon_i \in \mathbb{R}^n$ and by substituting in (5.4.13) yields

$$\dot{V} = \sum_{i=1}^{N} -u_i^T \left(u_i + k_t \varepsilon_i + k_s \cdot \text{sign}(u_i) \right), \tag{5.4.14}$$

thus

$$\dot{V} = -\sum_{i=1}^{N} \|u_i\|^2 - k_t \sum_{i=1}^{N} u_i^T \varepsilon_i - k_s \sum_{i=1}^{N} \|u_i\|_1 . \tag{5.4.15}$$

Note we have

$$\dot{V} \leq -\sum_{i=1}^{N} \|u_i\|^2 + k_t \sum_{i=1}^{N} \|u_i\|_1 \|\varepsilon_i\|_1 - k_s \sum_{i=1}^{N} \|u_i\|_1 . \tag{5.4.16}$$

The remaining part of this proof is similar to the proof of Theorem 5.4.1. ■

5.5 Simulation Results

In this section, the simulation results are presented to verify the functionality and effectiveness of the proposed control laws in the previous section. Consider five agents in a plane. The aim is to achieve a desired formation and to steer the center of formation to the source. The desired formation is a pentagon shape with five sides equal to 15 and angles equal to $3\pi/5$. The initial positions of agents are defined as $p_1 = [25\ 10]^T$, $p_2 = [12\ -10]^T$, $p_3 = [-10\ 40]^T$, $p_4 = [-40\ 10]^T$, $p_5 = [-10\ 10]^T$. The adjacency matrices of the undirected communication graph $\mathcal{G}_s$ and the directed formation graph $\mathcal{G}_f$ are defined as

$$A_s = \begin{bmatrix} 0 & 1 & 1 & 0 & 0 \\ 1 & 0 & 0 & 0 & 1 \\ 1 & 0 & 0 & 1 & 0 \\ 0 & 0 & 1 & 0 & 1 \\ 0 & 1 & 0 & 1 & 0 \end{bmatrix}, \quad A_f = \begin{bmatrix} 0 & 1 & 0 & 0 & 0 \\ 1 & 0 & 0 & 0 & 0 \\ 1 & 1 & 0 & 0 & 0 \\ 0 & 1 & 1 & 0 & 0 \\ 0 & 0 & 1 & 1 & 0 \end{bmatrix}.$$

In all following simulations we assume agent 1 and 2 are the leaders of the formation and the distance neighbor for agent i with $i > 2$ is agent $i-1$ and the angle neighbor of it, is agent $i-2$. The scalar field is defined as

$$\mu(p_i) = A_0 e^{-\left((p_i - p_s)^T H_1 (p_i - p_s)\right)} + A_0 e^{-\left((p_i - p_s)^T H_2 (p_i - p_s)\right)},$$

where $A_0 = 50$, $H_1 = \begin{bmatrix} \frac{1}{2\sigma_{x1}^2} & 0 \\ 0 & \frac{1}{2\sigma_{y1}^2} \end{bmatrix}$, $H_2 = \begin{bmatrix} \frac{1}{2\sigma_{x2}^2} & 0 \\ 0 & \frac{1}{2\sigma_{y2}^2} \end{bmatrix}$, $\sigma_{x1} = 30$, $\sigma_{x2} = 90$, $\sigma_{y1} = 75$, $\sigma_{y2} = 25$. The maximum of the scalar field is located at $p_s = [70\ 70]^T$. In all subsequent simulations the tuning parameters are set to $k_\alpha = 10$, $k_v = 0.15$, $k_o = 0.1$, $k_d = 0.951$, $k_t = 0.1$, $k_s = 0.1$, $R = 8$, $r = 4$. Two scenarios are simulated.

5.5.1 Source Seeking with Single Integrator Agents

In this scenario we apply control law (5.4.11). Agents are modeled as a single integrator. Results are shown in Fig. 5.5.1. As depicted in Fig. 5.5.1, agents achieve a desired formation and maintain it and locate the maximum of the scalar field p_s as well. Fig. 5.5.2 shows the distance and angle errors of the formation. Note that when one agent or an obstacle are inside the detection area of another agent, the avoidance function is activated. As a consequence, the agents change the trajectories to avoid the collisions and the distance and angle errors increase or decrease temporarily, depending on the direction of the repulsive force. In Fig. 5.5.3 the distance between center of formation p_c and the source p_s is shown and as depicted the distance is declining near to zero.

5.5.2 Source Seeking with Double Integrator Agents

In this scenario we apply control law (5.4.1). Agents are modeled as double integrator and $m = 1$ for all agents. Results are shown in Fig. 5.5.4. As presented there, agents

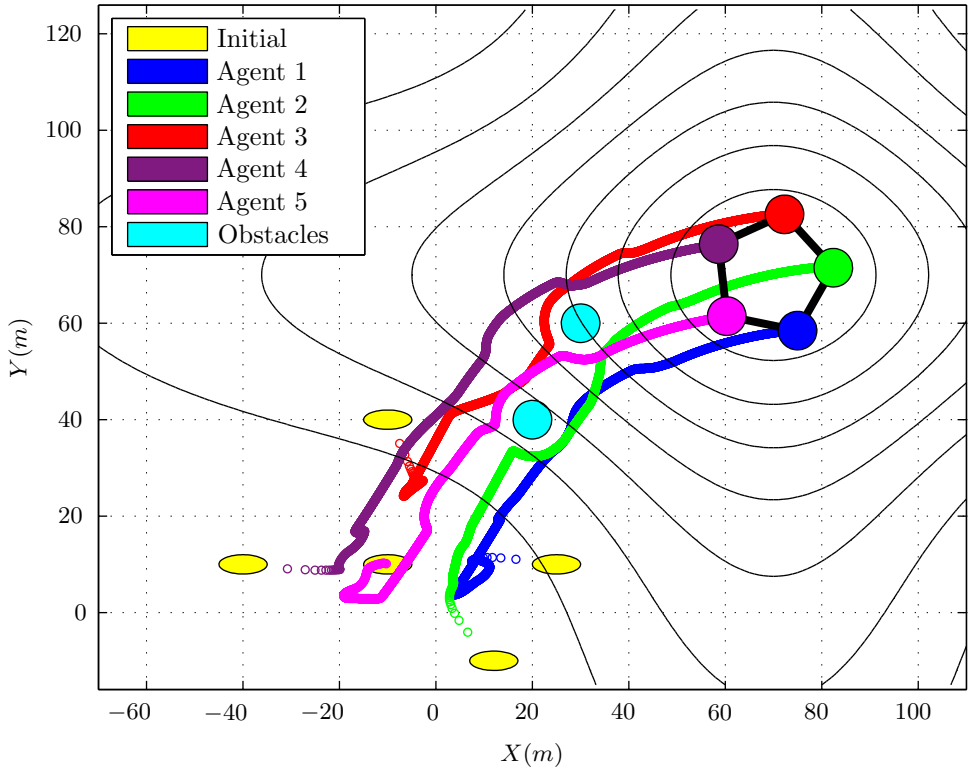

Figure 5.5.1: Formation and source seeking for single integrator agents.

achieve a desired formation and maintain it and locate the maximum of the scalar field p_s as well. Fig. 5.5.5 shows the distance and angle errors in the formation and the absolute value of v_i. In Fig. 5.5.6 the distance between center of formation p_c and the source p_s is shown and as depicted the distance is declining near to zero.

5.6 Conclusion

In this chapter, a new method for source seeking with distance-angle-based formation control is proposed. In this approach, a distributed source seeking algorithm is combined with distance-based formation control and is used to design a control law. The absolute position is not required. Unlike standard source seeking control, in our approach each agent can use its own local coordinate system. That will be helpful in an environment where a common coordinate system is not available. Also the communication among agents is limited and all-to-all communication is not required. We prove asymptotic stability of the system by using Lyapunov-like functions for double integrator and single integrator agents in the presence of obstacles and we show the convergence of the center of formation to the source. The control law has the capability of preventing collision between agents, or agents and static obstacles and steer the center of the formation to the source. The theoretical analysis demonstrates that agents are able to converge to the

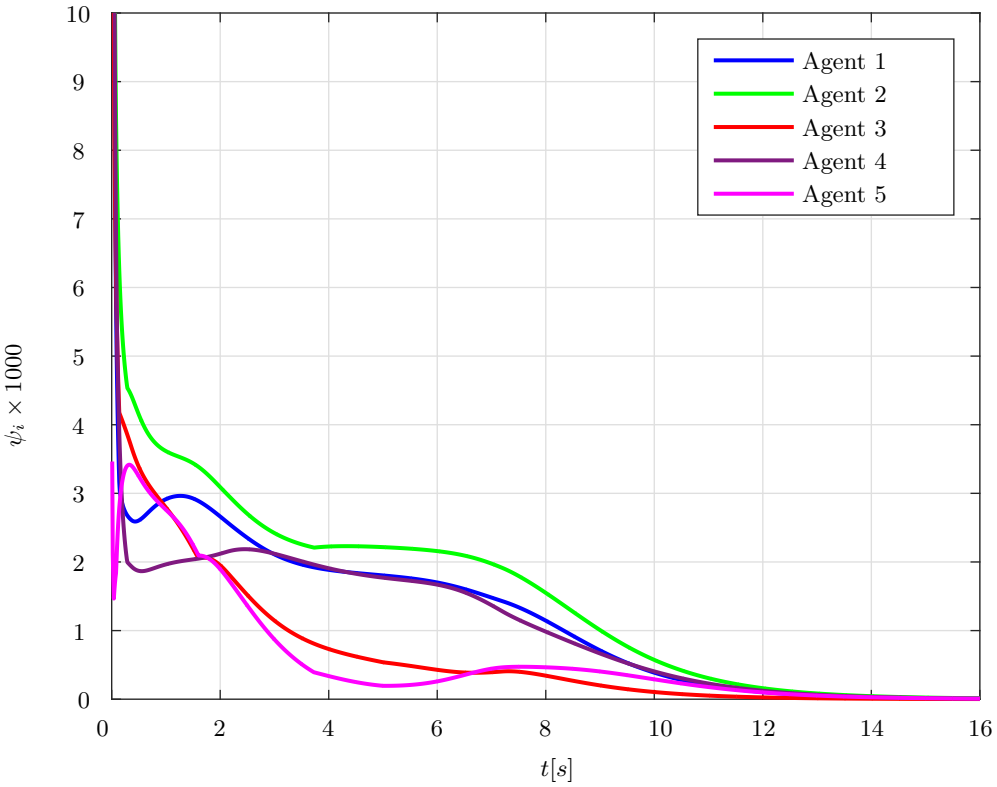

Figure 5.5.2: Distance (ψ_i) errors for single integrator agents

source of the scalar field; stability conditions are proposed and the formation without collision is maintained. Simulations confirm the effectiveness of the proposed algorithms.

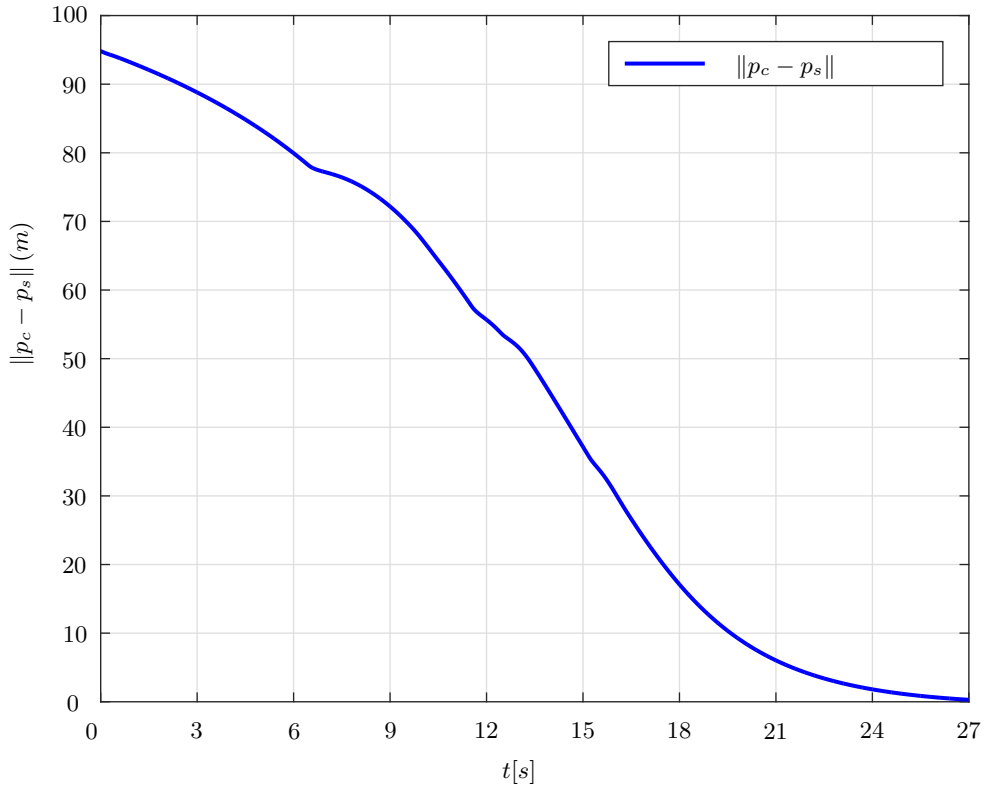

Figure 5.5.3: Distance between source (p_s) and center of formation (p_c) for single integrator agents

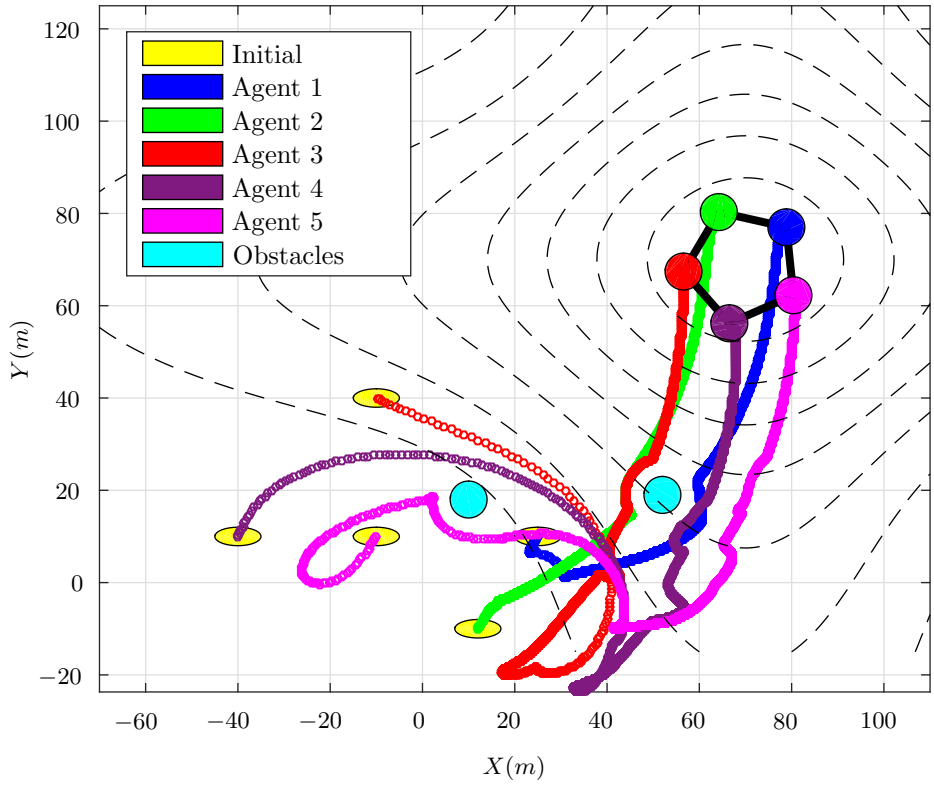

Figure 5.5.4: Formation and source seeking for double integrator agents

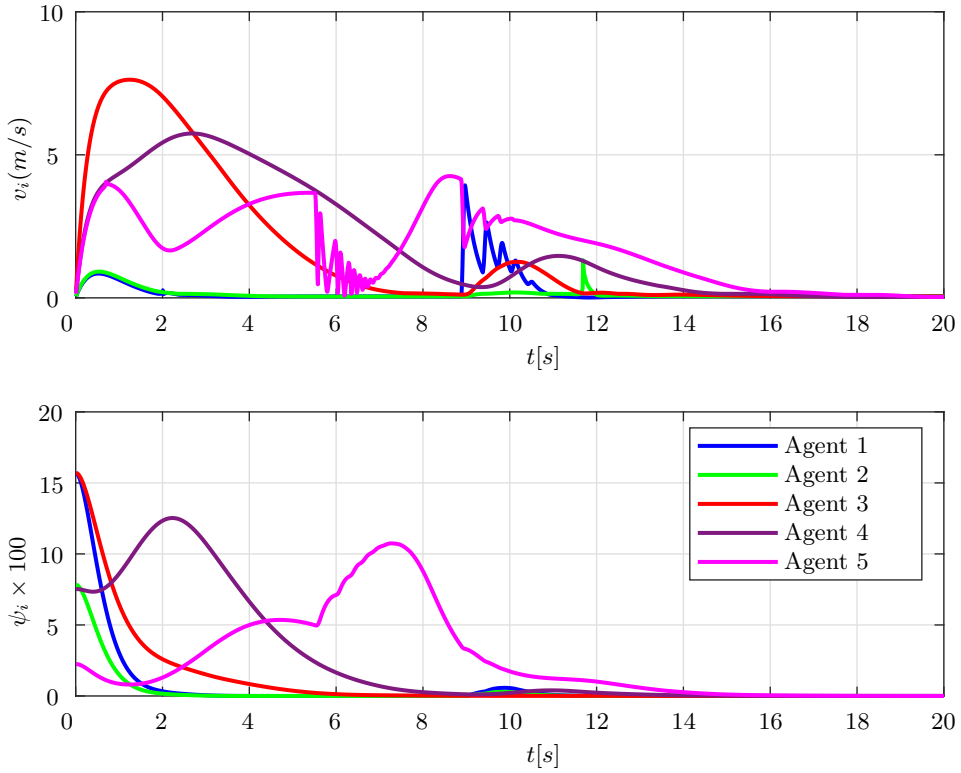

Figure 5.5.5: Distance (ψ_i) error and v_i for double integrator agents.

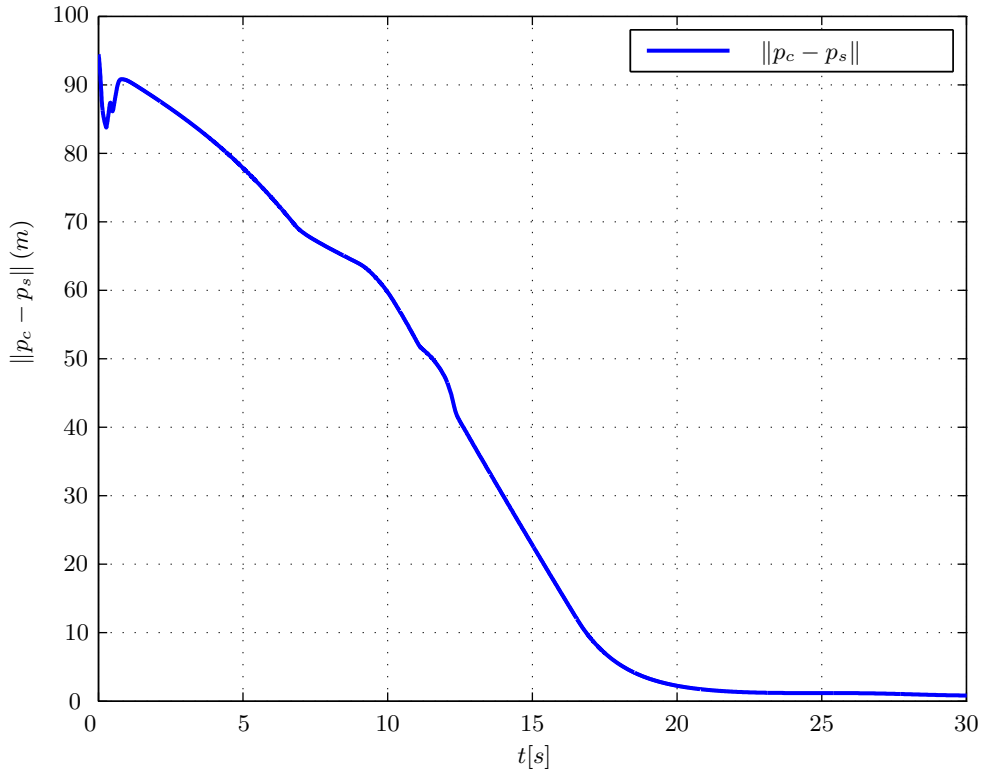

Figure 5.5.6: Distance between source (p_s) and center of formation (p_c) for double integrator agents

Chapter 6

Cooperative Source Seeking Using Non-holonomic Agents

In this chapter, the problem of source seeking with a group of agents subjected to non-holonomic constraints in a distance-based formation is considered. Similar to Chapter (5), agents are equipped with a suitable sensor set to measure the distance to other agents and the strength of a field signal. The formation strategy used in this chapter is the same as in Chapter (5). Simulation results are presented to show the effectiveness of the proposed control laws. The control schemes and algorithms that are proposed in this chapter were published in (Ahmadi Barogh and Werner [2017a]).

6.1 Introduction

In Chapter 5 we address the problem of source seeking using a distance-based formation control without access to the absolute position or a common coordinate system. In this approach, each agent has its own local coordinate system and is equipped with appropriate sensors to detect the distance between itself and its neighbors. The distributed gradient is estimated individually by each agent with respect to its local coordinate system. Similar to the control laws in Chapter 5, in this chapter a proposed distributed control law includes two parts: a formation control component with collision avoidance and a source seeking component. The first part of the control law guarantees that the group of agents achieves the formation and maintains it in the presence of obstacles. The second part forces the group to follow the source seeking objective.

6.2 Outline of This Chapter

The rest of this chapter is arranged in five sections: Section 6.3 provides the problem statement for the source seeking problem. In Section 6.4, we propose a control law that achieves source seeking, and we present conditions for stability of the closed-loop system

for non-holonomic agents in the presence of obstacles. Section 6.5 shows simulation results, and Section 6.6 concludes with a summary.

6.3 Problem Statement

Given $p^* \in \mathbb{R}^{nN}$ as a desired representation of $\mathcal{G}_f$ in n-dimensional space. The communication graph to estimate the gradient at each agent is represented by $\mathcal{G}_s$. The model of the agents is assumed to be the non-holonomic model (1.5.4). Design a distributed control law to force a group of agents to achieve the desired formation based on local information about the distance, and to drive the center of the formation to the source p_s, where $\bar{\mu} = \mu(p_s)$, based on the estimated gradient by each agent. All agents are modeled by identical non-holonomic model (6.4.2). The desired formation of a group of non-holonomic agents is represented by the set

$$E_{p,u} = \left\{ \begin{bmatrix} p^T & u^T \end{bmatrix} \in \mathbb{R}^{4N} : \|p_j - p_i\| = \left\|p_j^* - p_i^*\right\| \atop , u = 0, \forall (i,j) \in \mathcal{E} \right\}, \tag{6.3.1}$$

where $u = [u_1^T, \cdots, u_N^T]$. Therefore $E_{p,u}$ is the set of all formations equivalent to p^*.

6.4 Control Law

In this section a control law to achieve formation and source seeking will be introduced. In addition, asymptotic stability of the formation is proved. We propose a control law in two steps. First, the control law is proposed for the kinematic model of agent i, (1.5.3). The control input for the kinematic model is u_i^i. Second, we take into account the dynamics of non-holonomic agents (1.5.5) and propose an extended control law. The control input for the dynamic model is τ_i^i. We use the following potential function to propose a control law:

$$V_i(p_i) = k_v \psi_i(t) + k_\alpha \phi_i(t), \tag{6.4.1}$$

where $k_v > 0$ and $k_\alpha > 0$ and ψ_i and ϕ_i are obtained from (3.3.2). Define also

$$e_{pi}^i(t) = \begin{bmatrix} e_{xi}^i(t) & e_{yi}^i(t) \end{bmatrix}^T = -\frac{\partial V_i}{\partial p_i^i} - k_o \frac{\partial V_{ai}}{\partial p_i^i} + k_t \hat{g}_i^i(p_i^i) - k_s \cdot \text{sign}(v_i^i C_i^i), \tag{6.4.2}$$

where $k_o > 0, k_t > 0, k_s > 0$, $C_i^i = \begin{bmatrix} \cos(\theta_i^i) & \sin(\theta_i^i) \end{bmatrix}^T$. Define

$$\begin{aligned} \theta_{di}^i(t) &= \arctan(e_{yi}^i(t), e_{xi}^i(t)), \\ e_{\theta i}^i(t) &= \theta_i^i(t) - \theta_{di}^i(t), \\ v_{di}^i(t) &= k_f \sqrt{(e_{xi}^i)^2 + (e_{yi}^i)^2} \cos(e_{\theta i}^i(t)), \\ \omega_{di}^i(t) &= -k_\theta e_{\theta i}^i(t), \end{aligned} \tag{6.4.3}$$

where $k_f > 0$ and $k_\theta > 0$ and Assumption 2.2.1 holds.

6.4.1 Control Law for Kinematic Agent Models

A control law for the kinematic model (1.5.3) is proposed as

$$u_i^i(t) = \begin{bmatrix} v_{di}^i(t) & \omega_{di}^i(t) \end{bmatrix}^T. \tag{6.4.4}$$

From (6.4.4) and (1.5.3) it is obtained that $v_i^i = v_{di}^i$ and $\omega_i^i = \omega_{di}^i$; in the kinematic model the internal dynamics of (1.5.4) are ignored. The following theorem states the convergence of the proposed control law to the source. The proposed control law with a distance-based formation is stated in Algorithm 1.

Theorem 6.4.1. *Given a multi-agent system of N non-holonomic kinematic model agents (1.5.3), and the distributed control law (6.4.4) under Algorithm 1. Suppose that Assumptions 1.5.1 to 1.5.4 and 5.3.1 about the scalar field and the location of obstacles and Remark 2.2.1 are fulfilled. Then, for all $p_i(0) \in \mathbb{R}^n$, $i = 1, \cdots, N$ and $t \geq 0$, the agents achieve a desired formation that is equivalent with p^*, without collision and in the formation center, $p_c(t)$, we have $\hat{g}_c \to 0$ as $t \to \infty$ when $k_s \geq k_t\sqrt{2}e_g$. The center of formation is stabilized in the region with bounded distance from the source p_s as $\|(p_s - p_c)\| \leq \frac{-2e_g}{\eta_1}$.*

Proof: We will present the proof in two steps. First, stability of the formation is shown. Then source seeking is addressed. We have

$$\dot{v}_c = \frac{1}{N}\sum_{1}^{N} \dot{v}_i, \tag{6.4.5}$$

where v_c is the velocity of center of formation. To show asymptotic stability we use the following Lyapunov function candidate

$$W = \sum_{i=1}^{N}\left(\frac{1}{4}k_v\psi_i + \frac{1}{4}k_\alpha\phi_i + V_{ai} + \frac{1}{2}\lambda(\theta_i - \theta_{di})^2 + k_t(\bar{\mu}(p_s) - \mu(p_i))\right), \tag{6.4.6}$$

where V_i and V_{ai} come from (6.4.1) and (2.2.15) respectively. Without loss of generality, we assume $k_f = 1$, $k_\theta = 1$ and $k_o = 1$. Taking the derivative of (6.4.6) yields

$$\begin{aligned}\dot{W} = \sum_{i=1}^{N}\Bigg(&\frac{1}{4}k_v\sum_{k\in\mathcal{N}_i}\left(\frac{\partial\psi_{ik}^T}{\partial p_i}\dot{p}_i + \frac{\partial\psi_{ik}^T}{\partial p_k}\dot{p}_k\right) + \frac{1}{4}k_\alpha\sum_{k\in\mathcal{N}_i}\left(\frac{\partial\phi_{ik}^T}{\partial p_i}\dot{p}_i + \frac{\partial\phi_{ik}^T}{\partial p_k}\dot{p}_k\right)\\ &+ k_o\frac{\partial V_{ai}^T}{\partial p_i}\dot{p}_i + \lambda(\theta_i - \theta_{di})(\dot{\theta}_i - \dot{\theta}_{di}) - k_t g_i^T\dot{p}_i\Bigg).\end{aligned} \tag{6.4.7}$$

The graph $\mathcal{G}_f$ is connected and undirected and therefore from (3.3.3) we obtain

$$\dot{W} = \sum_{i=1}^{N}\left(-\left(k_v\Psi_i + k_\alpha\Phi_i - k_o\frac{\partial V_{ai}}{\partial p_i}\right)^T\dot{p}_i - k_t g_i^T\dot{p}_i + \lambda(\theta_i - \theta_{di})(\dot{\theta}_i - \dot{\theta}_{di})\right). \tag{6.4.8}$$

Assume $g_i = \hat{g}_i + \varepsilon_i$ and $\varepsilon_i \in \mathbb{R}^2$. Substituting from (6.4.2) we have

$$\dot{W} = \sum_{i=1}^{N} \Big(- (e_{pi} + k_t \varepsilon_i + k_s \cdot \text{sign}(v_i C_i))^T \dot{p}_i + \lambda(\theta_i - \theta_{di})(\dot{\theta}_i - \dot{\theta}_{di}) \Big). \tag{6.4.9}$$

From (6.4.9),(6.4.3),(1.5.3) we have

$$\dot{W} = \sum_{i=1}^{N} \Big(- e_{pi}^T C_i v_i - \left(k_s \cdot \text{sign}(v_i C_i) + k_t \varepsilon_i\right)^T C_i v_i - \lambda \omega_i (\omega_i - \dot{\theta}_{di}) \Big), \tag{6.4.10}$$

and

$$e_{pi}^T C_i = e_{xi} \cos(\theta_{di} + e_{\theta i}) + e_{yi} \sin(\theta_{di} + e_{\theta i}). \tag{6.4.11}$$

From (6.4.3) and (6.4.11) we obtain

$$e_{pi}^T C_i = \sqrt{e_{xi}^2 + e_{yi}^2} \cos(e_{\theta i}) = v_{di}. \tag{6.4.12}$$

Substituting (6.4.12) in (6.4.10) we have

$$\begin{aligned} \dot{W} = \sum_{i=1}^{N} \Big(& - v_i^2 - \lambda(\omega_i^2 - \omega_i \dot{\theta}_{di}) \\ & - \left(k_s \left\| C_i v_i \right\|_1 + k_t \varepsilon_i^T C_i v_i\right) \Big). \end{aligned} \tag{6.4.13}$$

From (6.4.3) we have

$$\dot{\theta}_{di} = v_i D_i, \tag{6.4.14}$$

where

$$D_i = \frac{e_{xi} \frac{\partial e_{yi}}{\partial p_i}^T C_i - e_{yi} \frac{\partial e_{xi}}{\partial p_i}^T C_i}{e_{xi}^2 + e_{yi}^2}.$$

Substituting (6.4.14) in (6.4.13) yields

$$\dot{W} = \sum_{i=1}^{N} \Big(- u_i^T \mathcal{X}_i u_i - \left(k_s \left\| C_i v_i \right\|_1 + k_t \varepsilon_i^T C_i v_i\right) \Big), \tag{6.4.15}$$

where

$$\mathcal{X}_i = \begin{bmatrix} 1 & -\frac{1}{2}\lambda D_i \\ -\frac{1}{2}\lambda D_i & \lambda \end{bmatrix}. \tag{6.4.16}$$

According to $\varepsilon_i = g_i - \hat{g}_i$ and from the norm inequalities, we have

$$-\varepsilon_i^T C_i v_i \leq \left\| g_i - \hat{g}_i \right\|_1 \left\| C_i v_i \right\|_1 \leq \sqrt{2} \left\| g_i - \hat{g}_i \right\| \left\| C_i v_i \right\|_1. \tag{6.4.17}$$

Considering Assumption 1.5.2 and by applying the inequality (6.4.17) we have

$$\dot{W} \leq -\sum_{i=1}^{N} \left(u_i^T \mathcal{X}_i u_i + k_s \left\| C_i v_i \right\|_1 (k_s - k_t \sqrt{2} e_g) \right). \tag{6.4.18}$$

In (6.4.18), by using a Schur complement it is possible to show that for $\lambda < \frac{4}{D_i^2}$ we have $\mathcal{X}_i > 0$ and by applying the condition that $k_s \geq k_t \sqrt{2} e_g$, we have $\dot{W} \leq 0$ and the stability is proved. To show asymptotic stability, the equilibrium point of $\dot{W} = 0$ is analyzed. From Equation (6.4.15) and due to $\dot{W} = 0$ we have $u_i \to 0$ as time goes to infinity for all $i = 1 \cdots N$ and, $e_{pi} \to 0$. Then from Remark 2.2.1 it is concluded that in the equilibrium point, $\frac{\partial V_{ai}}{\partial p_i} = 0$ and the collision avoidance is guaranteed for all agents. Therefore $\Psi_i \to 0$ and $\Phi_i \to 0$ as $t \to \infty$. Then from $\Psi_i \to 0$ it is concluded that $(d_{ik}^{*2} - d_{ik}^2)^2 \to 0$ and therefore $d_{ik} \to d_{ik}^*$ and asymptotic stability of system is established. Thus in the equilibrium points of $\dot{W} = 0$ we have $v_i, \psi_{ik}, \phi_{ik} = 0$ for $\forall i, k$. Therefore $\begin{bmatrix} p^T & u^T \end{bmatrix} \in E_{p,u}$ when $t \to \infty$. Now $\dot{v}_i \to 0$ from (6.4.5) we have that $\dot{v}_c \to 0$ and therefore from (6.4.5) and Remark 5.3.1 we have that $\hat{g}_c \to 0$ as $t \to \infty$. Finally we show that the distance between p_c and p_s is bounded. The Taylor series expansion of $\bar{\mu}(p_s)$ around p_c is

$$\bar{\mu}(p_s) = \mu(p_c) + (p_s - p_c)^T \nabla \mu(p_c) + \frac{1}{2}(p_s - p_c)^T \nabla^2 \mu(p_c)(p_s - p_c). \tag{6.4.19}$$

From Assumption 1.5.2, we obtain

$$\bar{\mu}(p_s) \leq \mu(p_c) + (p_s - p_c)^T \nabla \mu(p_c) + \frac{1}{2} \left\| (p_s - p_c) \right\|^2 \eta_1,$$

and we have

$$\bar{\mu}(p_s) - \mu(p_c) \leq \left\| (p_s - p_c)^T \nabla \mu(p_c) \right\| + \frac{1}{2} \left\| (p_s - p_c) \right\|^2 \eta_1.$$

From Remark 5.3.1 and considering the fact that $\hat{g}_c \to 0$ it follows that $\|\nabla \mu(p_c)\| \leq e_g$ as $t \to \infty$. Note that according to the fact that $\bar{\mu}(p_s)$ is a global maximum we have $\bar{\mu}(p_s) - \mu(p_c) \geq 0$, and from Assumption 1.5.2, $\eta_1 < 0$ therefore $\|(p_s - p_c)\| \leq \frac{-2e_g}{\eta_1}$. ■

6.4.2 Control Law for Dynamic Agent Models

In order to take into account the system dynamics (1.5.5), the following control law is proposed

$$\begin{aligned} \tau_{1i}^i &= k_1(v_{di}^i - v_i^i), \\ \tau_{2i}^i &= k_2(\omega_{di}^i - \omega_i^i), \end{aligned} \tag{6.4.20}$$

where $k_1, k_2 > 0$ and v_{di}^i and ω_{di}^i are from (6.4.3) with e_{pi}^i from (6.4.2).

Theorem 6.4.2. *Given a multi-agent system with N non-holonomic agents (1.5.5), and the distributed control law (6.4.20) under Algorithm 1. Suppose that Assumptions 1.5.1*

to 1.5.4 and 5.3.1 about the scalar field and the location of obstacles and Remark 2.2.1 are fulfilled. Then, for all $p_i(0) \in \mathbb{R}^n$ and $t \geq 0$, the agents achieve a desired formation that is equivalent with p^*, without collision, and at the formation center, $p_c(t)$, we have $\hat{g}_c \to 0$ as $t \to \infty$ when $k_s \geq k_t\sqrt{2}e_g$. Then the center of formation is stabilized in the region with bounded distance from the source p_s as $\|(p_s - p_c)\| \leq \frac{-2e_g}{\eta_1}$.

Proof: The errors of linear and angular velocity are defined as

$$\delta_i = \begin{bmatrix}\delta_{1i} & \delta_{2i}\end{bmatrix}^T = \begin{bmatrix}v_i - v_{di} & \omega_i - \omega_{di}\end{bmatrix}^T. \tag{6.4.21}$$

By substituting (6.4.21) and (6.4.20) in (1.5.4) we have

$$m_i\dot{\delta}_{1i} + k_1\delta_{1i} = -m_i\dot{v}_{di},$$
$$l_i\dot{\delta}_{2i} + k_2\delta_{2i} = -l_i\dot{\omega}_{di}.$$

Then it follows that

$$M_i\dot{\delta}_i + K\delta_i = -M_i\dot{u}_{di}, \tag{6.4.22}$$

where $K = \begin{bmatrix}k_1 & 0\\ 0 & k_2\end{bmatrix}$ and $u_{di} = \begin{bmatrix}v_{di} & \omega_{di}\end{bmatrix}^T$ and M_i is as (1.5.4). Without loss of generality, we assume $k_f = 1$, $k_\theta = 1$ and $k_o = 1$. From (6.4.3) and (1.5.4) we obtain

$$\dot{v}_{di} = \frac{\partial v_{di}}{\partial q_i}^T R_i u_i,$$
$$\dot{\omega}_{di} = k_\theta(\dot{\theta}_{di} - \omega_i). \tag{6.4.23}$$

Then (6.4.14) and (6.4.23) yield

$$\dot{u}_{di} = O_i u_i, \tag{6.4.24}$$

where

$$O_i = \begin{bmatrix}\frac{\partial v_{di}}{\partial q_i}R_i\\ \begin{bmatrix}D_i & -1\end{bmatrix}\end{bmatrix}_{2\times 2}.$$

Substituting (6.4.24) in (6.4.22) results in

$$M_i\dot{\delta}_i + K\delta_i = -M_iO_iu_i. \tag{6.4.25}$$

To show asymptotic stability, the candidate Lyapunov function is taken as

$$F(t) = \beta F_1(t) + F_2(t),$$

where

$$F_1 = \sum_{i=1}^{N}\left(\frac{1}{4}k_v\psi_i + \frac{1}{4}k_\alpha\phi_i + V_{ai} + \frac{1}{2}\lambda(\theta_i - \theta_{di})^2 + k_t(\bar{\mu}(p_s) - \mu(p_i))\right),$$

$$F_2 = \frac{1}{2}\sum_{i=1}^{N}\left(m_i\delta_{1i}^2 + l_i\delta_{2i}^2\right), \tag{6.4.26}$$

and $\lambda, \beta > 0$ and ψ_i and ϕ_i and V_{ai} obtained from (3.3.2) and (2.2.15). By taking the derivative, we have

$$\dot{F} = \beta\dot{F}_1 + \dot{F}_2. \tag{6.4.27}$$

Let us assume $g_i = \hat{g}_i + \varepsilon_i$ and therefore from from (3.3.3), (6.4.2), (6.4.3), (1.5.4) and (6.4.21) and similar to the proof of Theorem 6.4.1 we have

$$\dot{F}_1 = \sum_{i=1}^{N}\Bigg(- e_{pi}^T C_i v_i - (k_s \cdot \text{sign}(v_i C_i) + k_t\varepsilon_i)^T C_i v_i + \lambda(\delta_{2i} - \omega_i)(\dot{\theta}_i - \dot{\theta}_{di})\Bigg). \tag{6.4.28}$$

From (6.4.21) and by substituting (6.4.12) in (6.4.28) we obtain

$$\dot{F}_1 = \sum_{i=1}^{N}\Bigg(\delta_{1i}v_i - v_i^2 + \lambda(\omega_i\delta_{2i} - \omega_i^2 - \delta_{2i}\dot{\theta}_{di} + \omega_i\dot{\theta}_{di}) - (k_s\left\|C_i v_i\right\|_1 + k_t\varepsilon_i^T C_i v_i)\Bigg). \tag{6.4.29}$$

Substituting (6.4.14) in (6.4.29) yields

$$\dot{F}_1 = \sum_{i=1}^{N}\Bigg(- u_i^T\mathcal{X}_i u_i + u_i^T\begin{bmatrix}1 & -\lambda D_i\\ 0 & \lambda\end{bmatrix}\delta_i - (k_s\left\|C_i v_i\right\|_1 + k_t\varepsilon_i^T C_i v_i)\Bigg), \tag{6.4.30}$$

where $\mathcal{X}_i$ is calculated as (6.4.16). From (6.4.26), the derivative of F_2 is obtained as

$$\dot{F}_2 = \sum_{i=1}^{N}(m_i\delta_{1i}\dot{\delta}_{1i} + l_i\delta_{2i}\dot{\delta}_{2i}). \tag{6.4.31}$$

From (6.4.25) and (6.4.31) we have

$$\dot{F}_2 = \sum_{i=1}^{N}(-\delta_i^T K\delta_i - \delta_i^T M_i O_i u_i). \tag{6.4.32}$$

After substituting (6.4.30) and (6.4.32) in (6.4.27) and developing, we obtain

$$\dot{F} = -\sum_{i=1}^{N}\left(Z_i^T\mathcal{Q}_i Z_i + (k_s\left\|C_i v_i\right\|_1 + k_t\varepsilon_i^T C_i v_i)\right), \tag{6.4.33}$$

where $\mathcal{Q}_i = \begin{bmatrix}K & B_i\\ B_i^T & \beta\mathcal{X}_i\end{bmatrix}$ and $B_i = \frac{1}{2}\left[M_i O_i - \beta\begin{bmatrix}1 & 0\\ -\lambda D_i & \lambda\end{bmatrix}\right]$ and $Z_i^T = \begin{bmatrix}\delta_i^T & u_i^T\end{bmatrix}$. For $\lambda < \frac{4}{D_i^2}$ we have $\mathcal{X}_i > 0$. By using the Schur complement and from the results of (Gouvea et al. [2010]) and (Pereira et al. [2011]), we can conclude that $\exists\beta$ such that $\mathcal{Q}_i > 0$. Similar to the proof of Theorem 6.4.1 is possible to show that $k_s \geq k_t\sqrt{2}e_g$ implies $\dot{F} \leq 0$. The remaining part of this proof is similar to the proof of Theorem 6.4.1. ■

Remark 6.4.1. *In this chapter, all results are based on Remark 2.2.1 and in the final formation, all agents are out of obstacles protecting region. However, in some circumstances is not fulfilled. For example, if obstacles are located very close to the source. In that case, an incorrect equilibrium point is created, and the formation errors do not converge to zero.*

6.5 Simulation Results

In this section, simulation results are presented to verify the functionality and effectiveness of the proposed control laws in the previous section. Consider five agents in a $2D$ plane. The aim is to achieve a desired formation and to steer the center of formation to the source. The desired formation is a pentagon shape with five sides equal to 15 and angles equal to $3\pi/5$ and $p^* = \begin{bmatrix}12.13 & 0 & 0 & 8.81 & -12.13 & 0 & -7.5 & -10.81 & 7.5 & -10.81\end{bmatrix}$. The initial positions of agents are defined as $p_1 = [40\ 10]^T$, $p_2 = [12\ 20]^T$, $p_3 = [20\ 40]^T$, $p_4 = [-40\ 0]^T$, $p_5 = [-10\ -10]^T$. The adjacency matrix $\mathcal{G}_s$ is defined as

$$A = \begin{bmatrix}0 & 1 & 0 & 1 & 1\\ 1 & 0 & 1 & 0 & 1\\ 0 & 1 & 0 & 1 & 0\\ 1 & 0 & 1 & 0 & 1\\ 1 & 1 & 0 & 1 & 0\end{bmatrix}.$$

The scalar field

$$\mu(p_i) = A_0 e^{-\left((p_i-p_s)^T H_1 (p_i-p_s)\right)} + A_0 e^{-\left((p_i-p_s)^T H_2 (p_i-p_s)\right)},$$

where $A_0 = 50$, $H_1 = \begin{bmatrix}\frac{1}{2\sigma_{x1}^2} & 0\\ 0 & \frac{1}{2\sigma_{y1}^2}\end{bmatrix}$, $H_2 = \begin{bmatrix}\frac{1}{2\sigma_{x2}^2} & 0\\ 0 & \frac{1}{2\sigma_{y2}^2}\end{bmatrix}$, $\sigma_{x1} = 30$, $\sigma_{x2} = 90$, $\sigma_{y1} = 75$, $\sigma_{y2} = 25$. The maximum of the scalar field is located at $p_s = [70\ 70]^T$. In all subsequent simulations the tuning parameters are set to $k_f = 0.01$, $k_\theta = 0.1$, $k_v = 0.15$, $k_o = 0.1$, $k_t = 0.7$, $k_s = 0.001$, $R = 8$, $r = 4$, $k_1 = 1$, $k_2 = 1$, $l_i = 1$, $m_i = 1$ for $i = 1 \cdots 5$.

6.5.1 Non-Holonomic Agents with Dynamic Model

In this section we apply control law (6.4.20). Agents are modeled by the non-holonomic dynamic model (1.5.5). Results are shown in Fig. 6.5.1. As depicted in Fig. 6.5.1, agents achieve a desired formation and maintain it and locate the maximum of scalar field p_s as well. Fig. 6.5.2 shows the formation errors considering the formation and v_i. Note that when one agent or an obstacle is inside the detection area of another agent, the avoidance function is activated. As a consequence, the agents change their trajectories to avoid collisions and the formation errors increase or decrease temporarily, depending on the direction of the repulsive force. As shown in Fig. 6.5.1 agent 3 encounters an obstacle at time 12s and tries to pass it without collision. Therefore the repulsive force is increased for agent 3 and the value of distance error for this agent is increased because avoiding collision has a higher priority than maintaining the desired formation for each agent. By increasing the value of the distance error, the velocity of the corresponding agent also is increased temporarily.

In Fig. 6.5.3 the distance between the center of formation p_c and the source p_s is shown and as depicted the distance is declining near to zero.

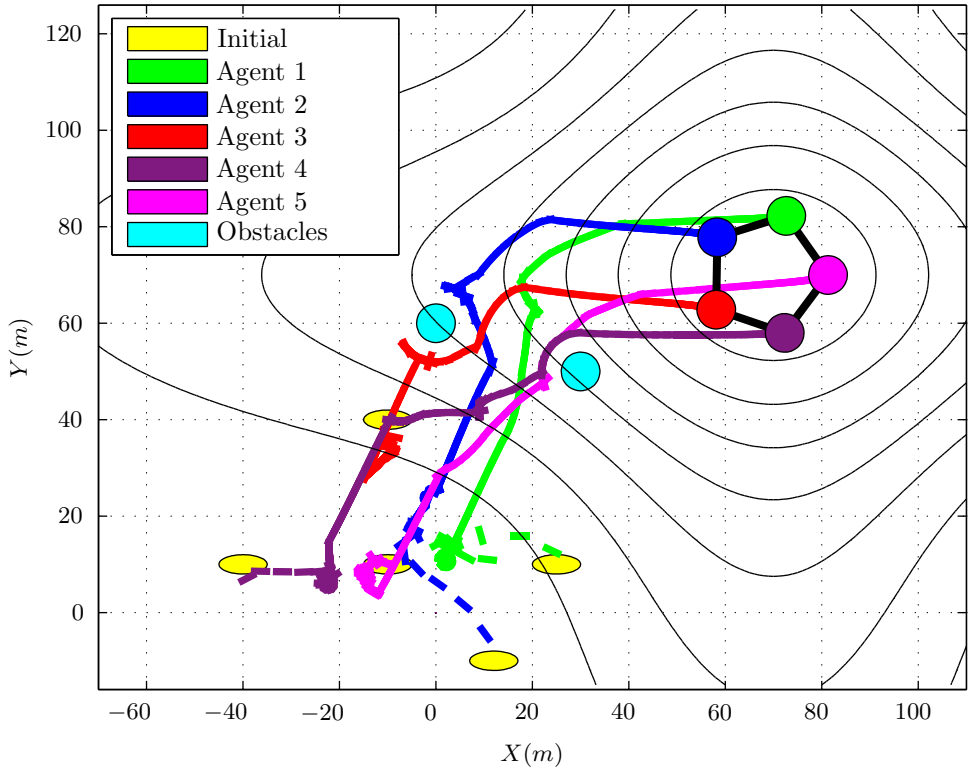

Figure 6.5.1: Formation and source seeking for non-holonomic agents

6.6 Conclusion

In this chapter, a new method for source seeking with distance-based formation control without access to global positioning is proposed for non-holonomic agents. A distributed source seeking algorithm is combined with distance-based formation control to design a control law. Unlike most of the known source seeking control methods, in our approach, each agent can use its own local coordinate system and the absolute position is not required. In some cases such as indoor or underwater environments, this method is useful because of lack of access to GPS or the nonavailability of a common coordinate system. We propose an algorithm and prove asymptotic stability of the system by using Lyapunov-like functions for non-holonomic agents with both kinematic and dynamic models in the presence of obstacles. Each agent detects the signal strength of a scalar field with its local sensors and receives information from neighbors, enabling it to estimate the gradient locally. Therefore, each agent only needs to have limited communication with its neighbors and all-to-all communication is not required. Agents do not need to rotate in a circular path, which reduces energy consumption and the possibility of collision and also a particular formation shape such as circular is not required. The theoretical analysis demonstrates that agents are able to converge to the source of the scalar field. Stability conditions are proposed and it is shown that the formation without collision is maintained. Simulations confirm the effectiveness of the proposed algorithms.

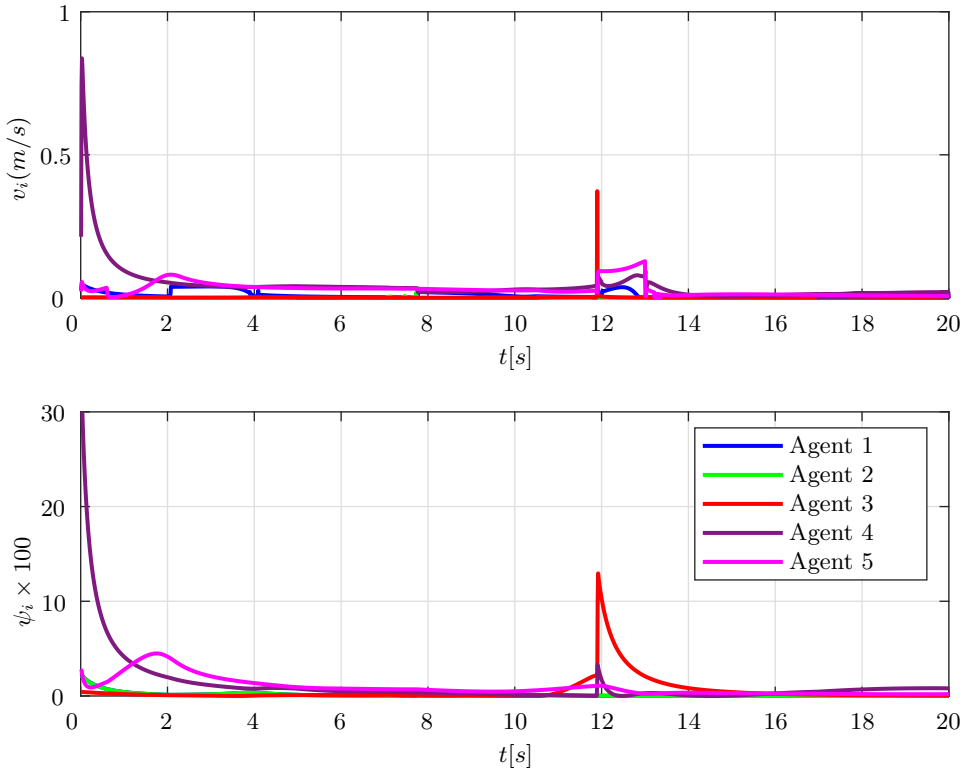

Figure 6.5.2: Formation (ψ_i) errors and v_i

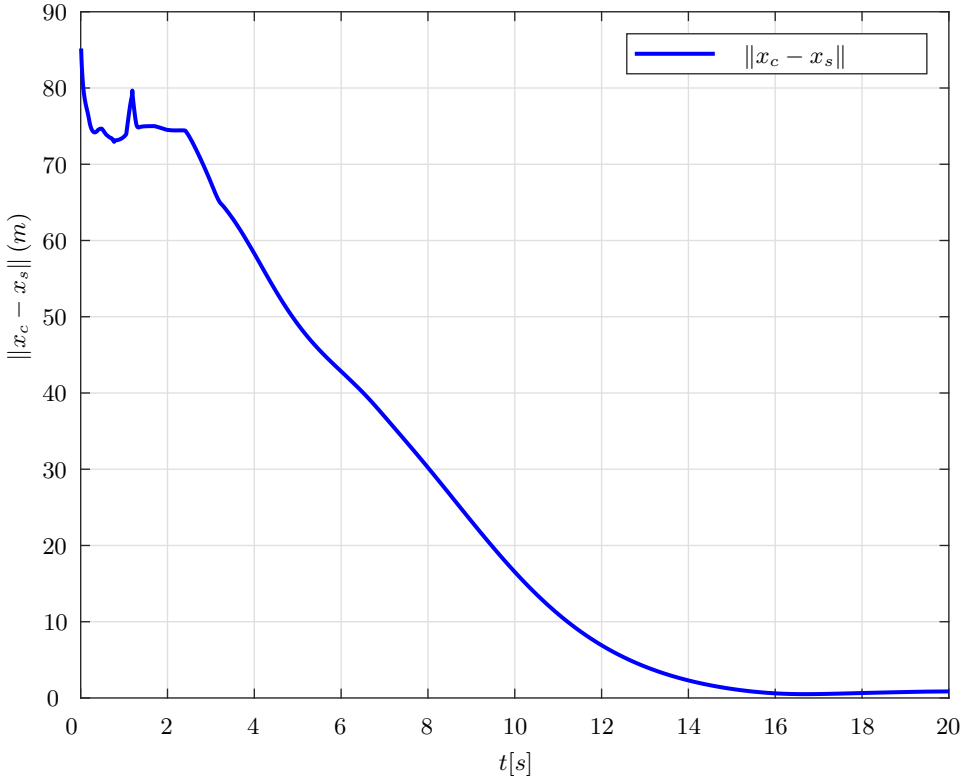

Figure 6.5.3: Distance between source (p_s) and center of formation (p_c)

Chapter 7

Implementation

This chapter presents the experimental validation of the proposed control laws for source seeking with distance angle-based formation control. Experimental results reported here were obtained in one master project and one master thesis (Menck [2017]) and (Kiefer [2015]) which were concluded in the context of the research reported in this thesis.

7.1 Introduction

In this chapter, we presented the implementation of source seeking with distance angle-based formation control. A group of wheeled robots is equipped with infrared sensors; they are trying to find a source of light in an environment by using the multi-agent source seeking algorithms which were proposed in previous chapters. To detect the distance between robots, a camera is mounted on the ceiling which can capture all robots and obstacles' positions. An image processing program was developed to detect the distances between robots; these distances are sent to the corresponding robots. The implementation of the proposed control laws consists of several parts. Wheeled robots were developed with hardware and local controllers; moreover, an image processing software platform was implemented on a PC to detect the distances. All robots have wireless communication with a PC to receive the distances between themselves and their neighbors.

A summary of the utilized hardware will be given in Section 7.2. Then the software used will be explained in Section 7.3. I Section 7.4 the results of simulation and experiments are presented and Section 7.5 concludes with a summary.

7.2 Hardware

The hardware needed for the implementation mainly consists of wheeled robots. A robot and its components are introduced briefly here.

7.2.1 Wheeled Robots

One such robot is depicted in Fig. 7.2.1. The main parts, numbered according to Fig. 7.2.1, are

1. A Romeo V2 board,
2. A battery pack,
3. Two wheels with one motor and encoder each,
4. A triangular marker,
5. An XBee Pro module,
6. Four infrared sensors.

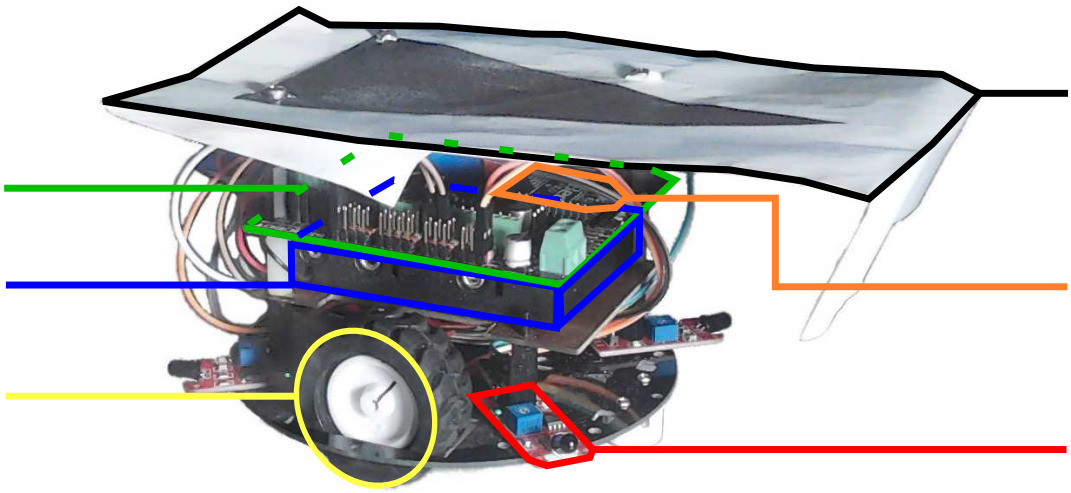

Figure 7.2.1: Image of a wheeled robot. (Menck [2017])

A microcontroller and the motor controller, both part of the Romeo V2 board, calculate the input voltage to each of the motors according to the local controller software. Once a wheel moves, a rotation encoder situated below the motor is used to calculate the current velocity of the robots. Each rotation encoder has two sensors, allowing it to calculate the speed of the revolution as well as its direction.

Communication with the PC is achieved through an XBee Pro module. The baud rate is 38400. The marker on top of the robot, a simple sheet of paper with a black triangle printed on it, is used to allow the PC to detect the robots using image processing with data from the camera. The robots can drive at up to about 0.6 m/s under normal conditions,

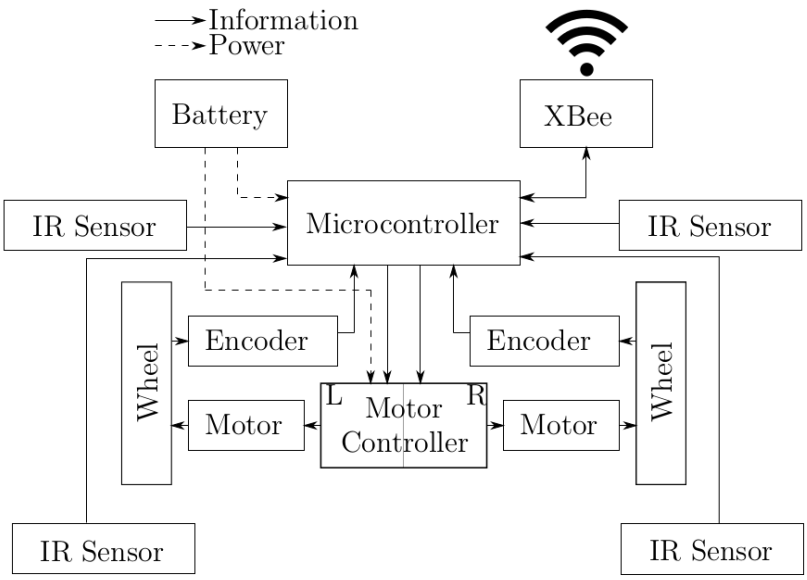

Figure 7.2.2: Schematic of a wheeled robot used in experiments. (Kiefer [2015])

while being able to accelerate very quickly, reaching their top speed easily in less than one second depending on the local controller settings. Due to their small size and the fact that they have only two wheels they can rotate very quickly (Menck [2017]).

7.2.2 Camera

To detect the distance between robots, a camera system was used here. The camera was mounted on the ceiling and captured the environment. The camera was connected to the pc via a USB port. It was a full HD camera with $1920 * 1080$ pixels resolution. The frame rate of the used camera was 15 frames per second.

7.2.3 PC and Components

A PC acts as a central entity that takes care of communication between the agents of the formation, which simplifies the setup of the employed communication. More importantly, a PC is needed to connect with the camera and run an image processing program. The PC then runs the program described in Section 7.3, using the OpenCV library to calculate the robots' positions and rotation in the plane and employing the control law to calculate target velocities for each robot. As a next step, the robots' target velocities are sent to the robots using the Xbee Explorer USB on which an Xbee Pro is placed. The schematic shape for the PC and robots communications is shown in Fig. 7.2.3 (Menck [2017]).

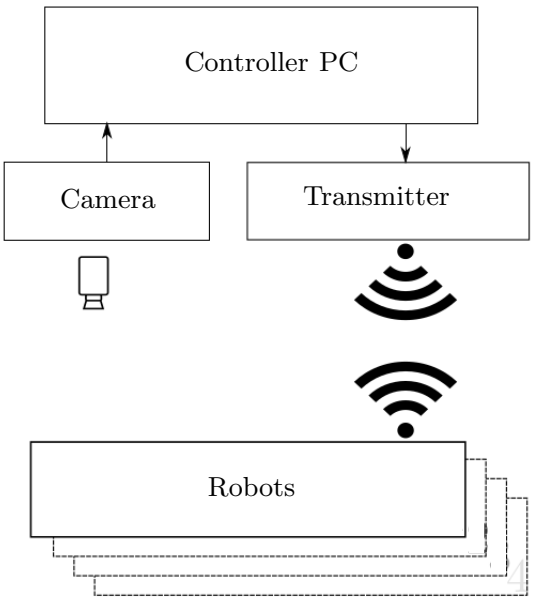

Figure 7.2.3: Schematic of the setup (adapted from (Meiners [2014])

7.3 Software

The software used can be divided into two parts: local controllers of the robots and the PC software. The local controller of a robot has two different modes, one for the kinematic model and one for the dynamic model as they were defined in Section 1.5.3.

Controller for the Kinematic Model
The entire kinematic controller is made up of two independent controllers, one for the linear and one for the angular velocity. They are PID controllers based on the measured speed and angular velocity by the robot.

Controller for the Dynamic Model
Like with the kinematic model, there are two separate PID controllers, one for the linear and one for the angular acceleration. The reference input to the control loop is now represented by $\boldsymbol{\tau}_i$ according to Equation 1.5.2. On top of that, there is a $\frac{d}{dt}$ block after the encoder which calculates the numerical derivative of the velocity v_n and the angular velocity ω_n in step n using the backward difference formula, resulting in the linear acceleration $\dot{v}_n$ and the angular acceleration $\dot{\omega}_n$. More sophisticated backward difference formulas from (Bard [2011]) that use multiple last steps were tested, but the simple formulas above proved to be the most robust to noise and as a consequence the most accurate for this implementation (Menck [2017]).

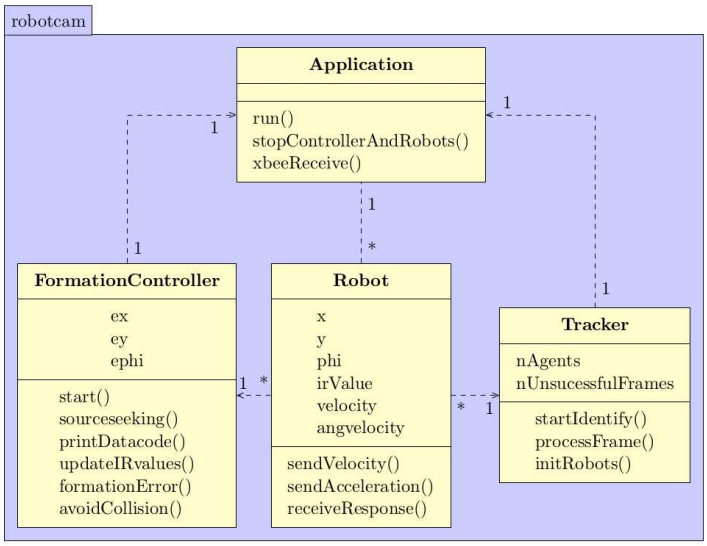

Figure 7.3.1: Incomplete UML class diagram of the most important parts of the program (Menck [2017])

7.3.1 PC Software

The control laws from Chapter 6 are implemented on a PC in addition, the PC handles image processing of pictures from the camera and is responsible for communication among the robots. Among other tasks, it also stores data of the experiment and records videos for further analyses (Menck [2017]).

The control law from Chapter 6 is implemented in C++ using the C++ *Eigen* library for linear algebra calculations. An simplified class diagram of the entire PC code is given in Fig. 7.3.1. The main loop run() of the implementation is part of the class Application, which accesses other classes, the most important ones of which are:

- *FormationController* is the class in which the control laws from Chapter 6 are implemented. Using the robots positions, their infrared values and other information, it calculates a set of new desired linear and angular velocities.

- The *Robot* class exists once for every robot in the formation. It contains information that is individual for each robot, such as their position, orientation in the plane, and their current infrared values. The class also handles communication over the XBees with the robots to send as well as receive information.

- The *Tracker* class handles image processing using the library OpenCV. It uses pictures from the USB camera to calculate each robot's position and orientation in the plane.

7.4 Results

7.4.1 Experiments

In this section experimental results are presented with different control and communication strategies. For the following three sets of results, one of the above parameters is changed each time while the rest remains as in Section 7.4.2. Each result is presented with three different sets of controller gains aside from the case with different communication topologies.

Table 7.1: Standard controller gains according to Chapter 6.

gain	value
k_v	3.53
k_a	9900
k_o	1750
k_t	101
k_f	0.1220
k_θ	180

7.4.2 Distance-Angle-Based Control with All-to-All Communication

Results for kinematic distance-angle-based controllers with all-to-all communication are presented with three sets of different parameters for the gains k_v and k_a from Equation 6.4.20 as well as the gain k_t from Equation 6.4.20.

Increasing the gains k_v and k_a causes the formation controller to use more control efforts, while increasing k_t means the gradient contribution has a higher absolute value. The former means that it is likely the formation will be achieved quicker while the latter will probably cause faster convergence towards the source. Assuming the above is correct, decreasing the gains should have the opposite effect and slow the system down.

The three sets of gains were used as listed in Table 7.2. The gain values are chosen experimentally and some physical restrictions such as maximum motor speed and the accuracy of motor encoder to count the wheel revolution, limit the maximum values for the gains.

The formation consists of three agents arranged in an equilateral triangle with a goal distance of 0.6m between each robot and its neighbor and is depicted in Fig. 7.4.1. Robots 1 and 2 are the leaders of the formation. Therefore, according to Chapter 4, they are their distance neighbors such that $\mathcal{D}_1 = \{2\}$ and $\mathcal{D}_2 = \{1\}$. The third robot is a follower and uses robot 1 as its distance neighbor and agent 2 as an angle neighbor, meaning $\mathcal{D}_3 = \{1\}$ and $\mathcal{A}_3 = \{2\}$. The distance d_{23} is not explicitly enforced by any robot.

Table 7.2: Controller gains for the kinematic distance-angle based all-to-all communication case.

name	k_v	k_a	k_t
high	7.02	19650	200
medium	3.53	9900	101
low	1.74	4900	50.4

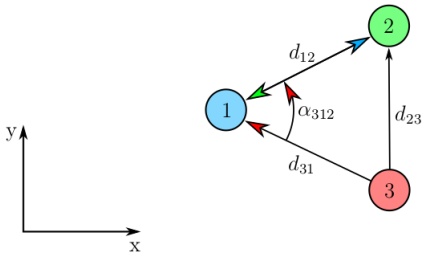

Figure 7.4.1: Formation used for three robots in the distance-angle-based case.

Experimental results of this experiment are displayed in Fig. 7.4.2. The upper graph shows the distance of the robot formation's center to the source of the scalar field, i.e. the light bulb. As expected, the high control gains make the formation converge faster towards the source than the other two cases, of which the lowest gains unsurprisingly cause the slowest convergence towards the source. Selected images of the source seeking with medium gains are pictured in Fig. 7.4.3. Green circles around the robots mark the detection and avoidance radii while the yellow arrows show the direction of the robots. The initial position as shown in Fig. 7.4.3 and the position of the light bulb are approximately the same as used in the simulation and will remain the same for all experiments done with three robots. Fig. 7.4.6 reveals why the robot formation cannot fully reach the light source, as otherwise collision with the lamp would occur. Therefore simulation results about the distance of the formation towards the source will be cut off at $1m$ distance as has been done in Fig. 7.4.2. The limited space around the lamp is also the reason why the formation errors tend to increase again after the source has mostly been reached, since the formation cannot fully reach the source and begins moving erratically.

Another reason for the increase in formation errors that sometimes occurs towards the end is the increase in the gradient as the formation approaches the light bulb. The infrared values rapidly increase as the robots get closer to the lamp, meaning that the formation increases in velocity as it approaches it. The average velocity of the formation with three different sets of gains is pictured in Fig. 7.4.7. Infrared values over the distance to the source are depicted in Fig. 7.4.7.

The medium set of gains causes the formation to assemble quickly and retains it better over the rest of the simulation than the high set of gains, while the low set of gains causes

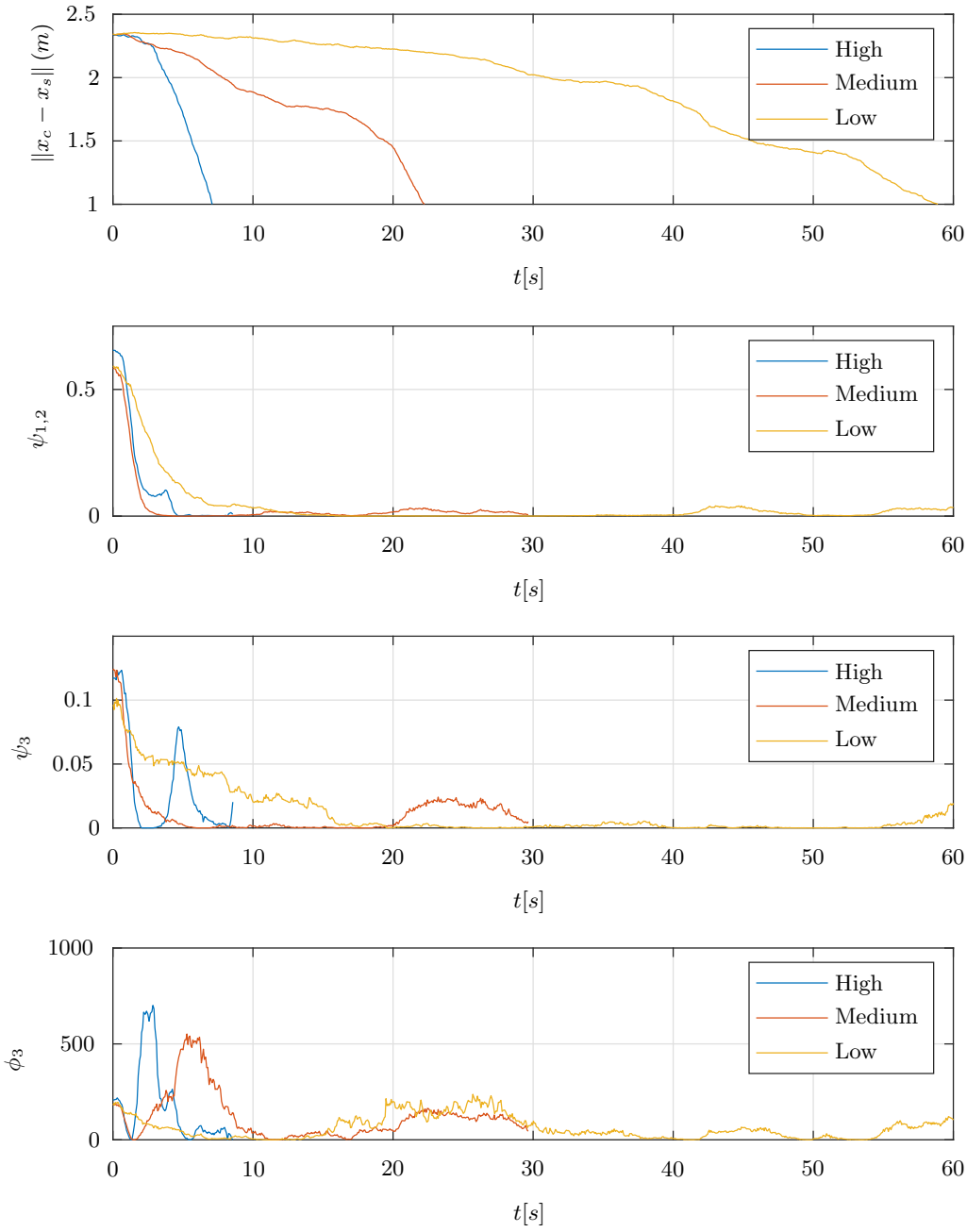

Figure 7.4.2: Distance between the formation center and source $||x_c - x_s||$, distance errors $\psi_{1,2}$, distance errors ψ_3 and angle errors ϕ_3 plotted over time t (Section 7.4.2)

slow speed of the formation's assembly but provides smooth movement over the rest of the experiment (Menck [2017]).

Figure 7.4.3: Robots' location in time = 0s

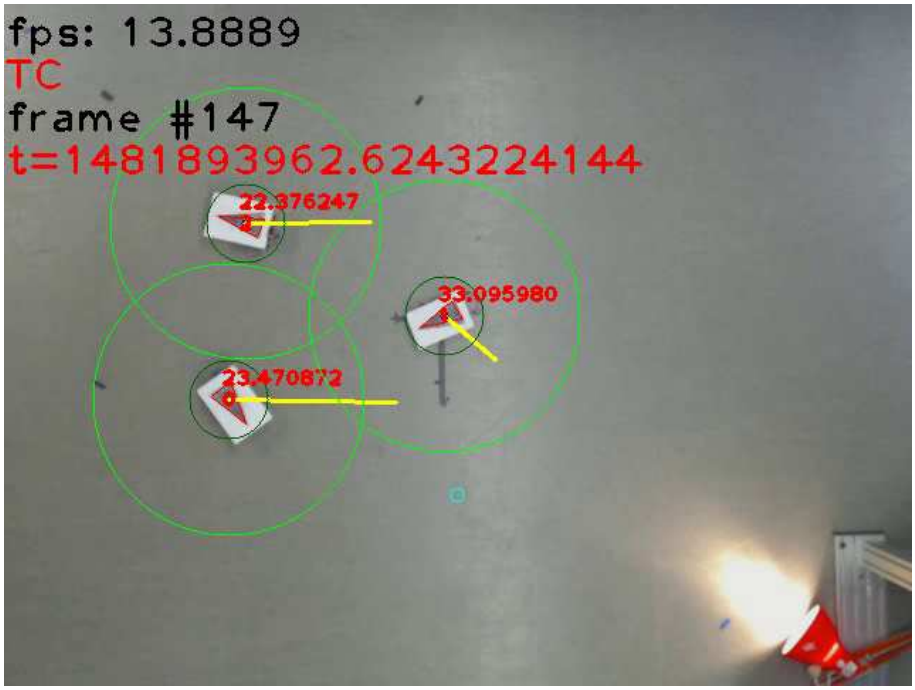

Figure 7.4.4: Robots' location in time = 10s

7.4.3 Distance-Based Control with All-to-All Communication

The main difference between this section and Section 7.4.2 is the fact that this one uses the purely distance-based control law of Chapter 6. Other than that, the robot models

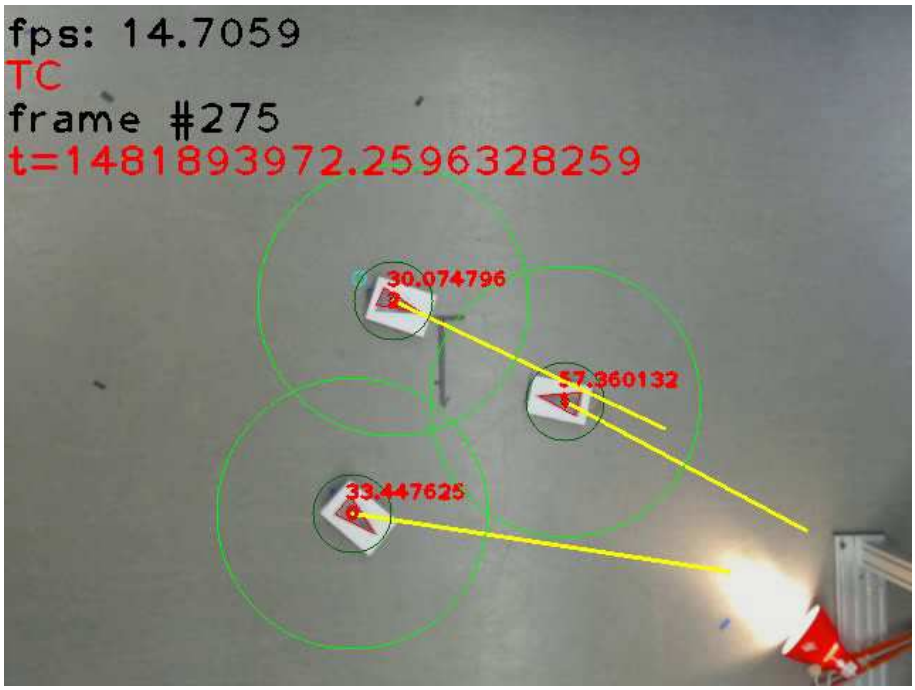

Figure 7.4.5: Robots' location in time = 20s

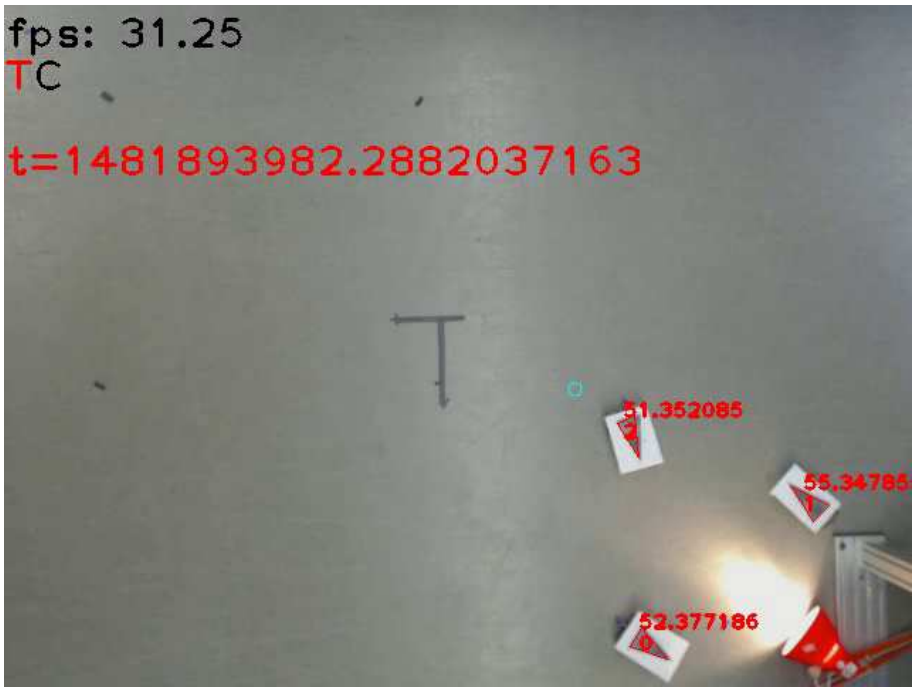

Figure 7.4.6: Robots' location in time = 30s

are still kinematic and there is still all-to-all communication between them as is necessary in the case of three robots.

The formation used is depicted in Fig. 7.4.8. Each agents uses the two other agents in the formation as its distance neighbors, such that the set of distance neighbors of agent

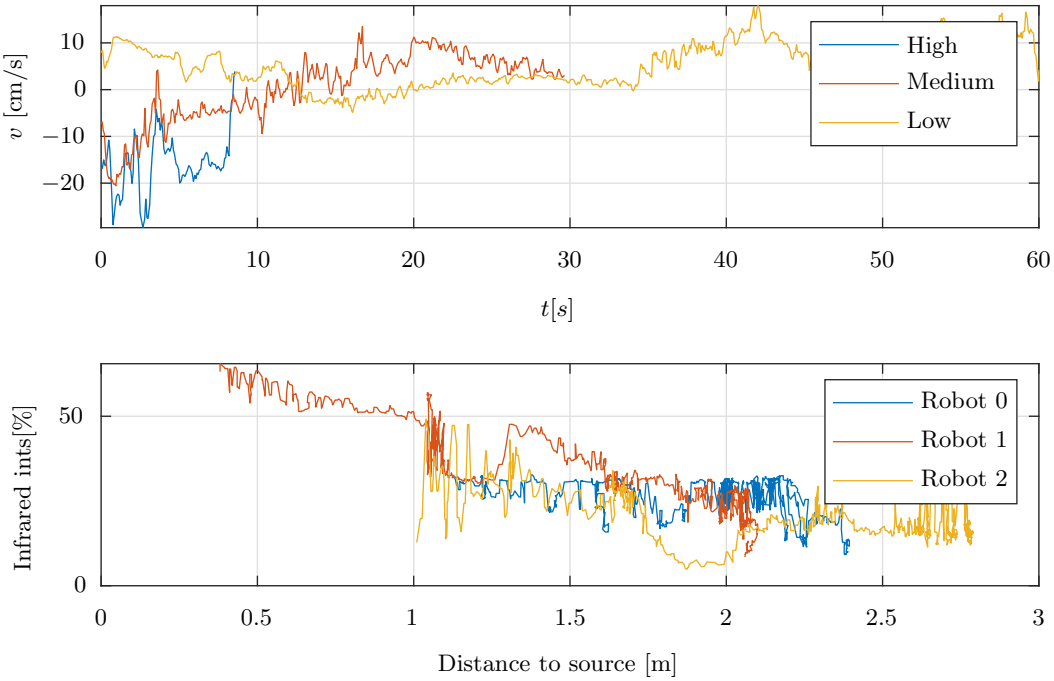

Figure 7.4.7: Average velocity v of the formation and infrared values for the low gains case plotted over the distance to the source (Section 7.4.2)

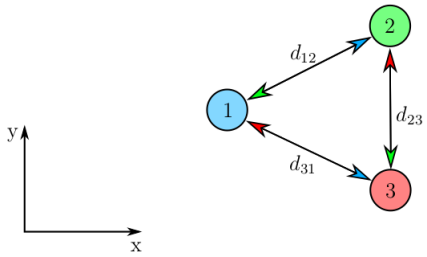

Figure 7.4.8: Formation with three robots in the distance-based case.

i consists of $\mathcal{D}_i = \{1, 2, 3\} \setminus i$ with $i = 1, 2, 3$. The formation achieved this way is an equilateral triangle with a side length of 0.6m. The three sets of gains that were used to achieve this are shown in Table 7.3.

Table 7.3: Controller gains for the kinematic distance based all-to-all communication case.

name	k_v	k_t
high	$0.7020 \cdot 10^{-3}$	200
medium	$0.3530 \cdot 10^{-3}$	101
low	$0.1740 \cdot 10^{-3}$	50.4

Experimental results are plotted in Fig. 7.4.9. Similar to the previous section, the source convergence is as expected, with the highest gains causing the fastest convergence while the lowest gains cause the slowest convergence. Because of the nature of the formation in which all robots have two distance neighbors under the same conditions, the errors ψ_i look very much alike with the exception of ψ_3 because agent 3 was closer to the other robots in its initial position. The errors seem to converge faster than in the distance-angle-based case, which is however due to the definition of the angle error in the distance-based case. The distance error is defined as $\psi_{ik}(t) = \frac{1}{2} \cdot (d_{ik}^2(t) - d_{ik}^{*2}(t))^2$, unlike the distance error in the distance-angle based case which is defined as $\psi_i(t) = (d_{ki}(t) - d_{ki}^*)^2$. Since the distances d_{ik} are squared in the former before they are subtracted, the error appears smaller as their distance is lower than 1m. This difference in definitions is also the reason why k_v is substantially smaller than it was in the angle-distance based case (Menck [2017]).

7.4.4 Formation for Dynamic Model

The difference between this section and Section 7.4.2 lies in the different local controllers used for the robots. They are now following the dynamic model, not the kinematic one as before. The formation otherwise is the same as that used in Section 7.4.2. The different values for k_1 and k_2 are shown in Table 7.4. As expected, the set of high gains causes the

Table 7.4: Controller gains for the dynamic distance-angle based all-to-all communication case

name	k_1	k_2
high	16239	1650
medium	8045	827
low	4273	416

formation to approach the light bulb faster while the formation takes the longest if the low set of gains is used. Similar to the cases with kinematic models, using the high set of gains causes higher spikes in the error graphs due to the increased speed that goes along with high controller gains. Unlike in the previous experiments, however, the angle error ϕ_3 of robot 3 is higher for the low gain case than for the medium one. This is due to the fact that using very low gains on the kinematic model causes the acceleration setpoint to be rather low, meaning that it may be too low for the robot to overcome friction and turn properly in time (Menck [2017]).

7.4.5 Distance-Based Controller with Different Communication

This section looks at an angle-distance-based formation control with kinematic robots under different communication types. Because the minimum number of robots in a plane

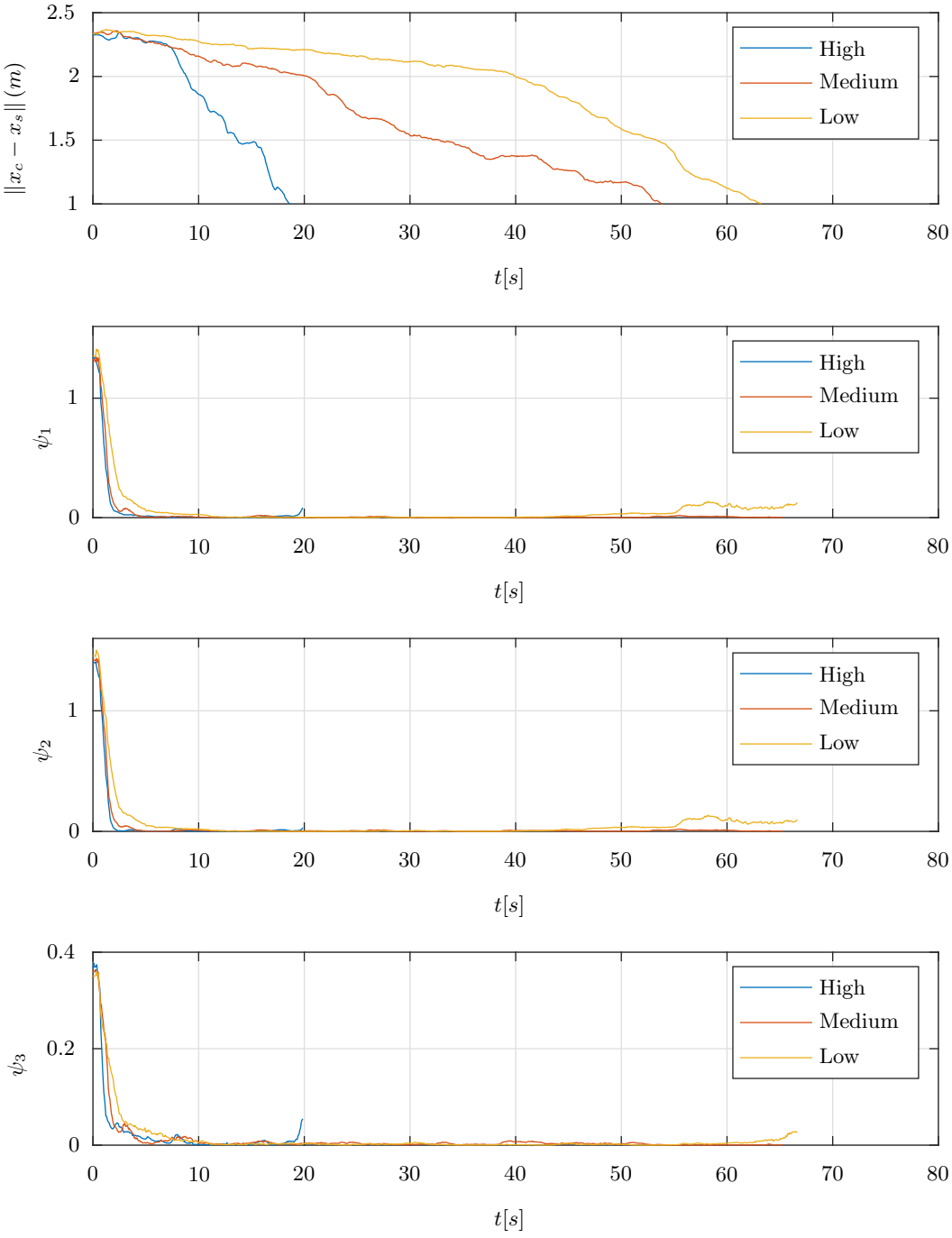

Figure 7.4.9: Distance between formation and source and distance angle errors.

that is needed for the gradient estimation in this work is three robots, here we consider four robots.

The formation control setup used in the following is depicted in Fig. 7.4.11. Robots

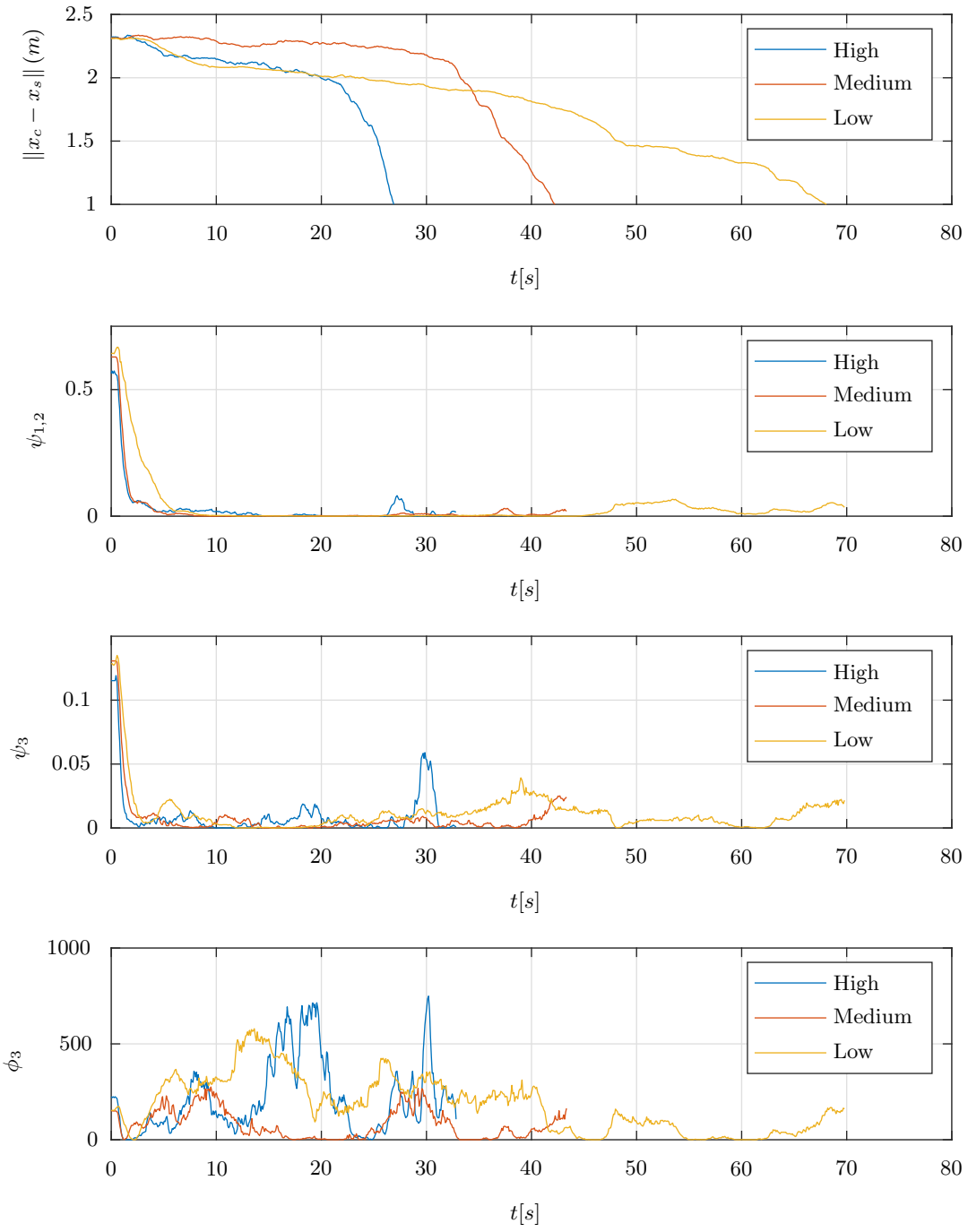

Figure 7.4.10: Distance between the formation center and source $||x_c - x_s||$, distance errors $\psi_{1,2}$, distance errors ψ_3 and angle errors $\phi 3$ plotted over time t (Section 7.4.4)

1 and 2 are the leaders of the formation and therefore only see each other as distance neighbours, i.e. $\mathcal{D}_1 = \{2\}$ and $\mathcal{D}_2 = \{1\}$. The third robot uses robot 2 as its distance neighbor and robot 1 as its angle neighbor, which is slightly different from the previous

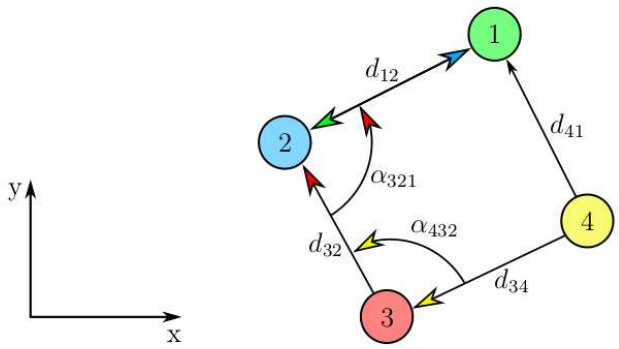

Figure 7.4.11: Formation with four robots in the distance-angle-based (Section 7.4.5)

experiments since now $\mathcal{D}_3 = \{2\}$ and $\mathcal{A}_3 = \{1\}$. Robot 4 which is new uses robot 3 as its distance neighbor and robot 2 as its angle neighbor, meaning $\mathcal{D}_4 = \{3\}$ and $\mathcal{A}_4 = \{2\}$. The distance d_{41} is not explicitly enforced by any robot.

Two different communication setups will be used:

- For **full communication**, there is only one possible communication variant, which can be described by the adjacency matrix

$$\mathbf{A}_{full} = \begin{pmatrix} 0 & 1 & 1 & 1 \\ 1 & 0 & 1 & 1 \\ 1 & 1 & 0 & 1 \\ 1 & 1 & 1 & 0 \end{pmatrix}, \tag{7.4.1}$$

  meaning that every robot communicates with every single other robot.

- The **limited communication** setup used was chosen as

$$\mathbf{A}_{lim} = \begin{pmatrix} 0 & 1 & 0 & 1 \\ 1 & 0 & 1 & 0 \\ 0 & 1 & 0 & 1 \\ 1 & 0 & 1 & 0 \end{pmatrix}, \tag{7.4.2}$$

  which means that every robot in the formation communicates only with those two robots in the corners next to him but not the one opposite to him.

In Fig. 7.4.12, for each of the setups, three results with identical conditions are displayed. The error ψ_{avg} is the average distance error of all four robots while the error ϕ_{avg} is the average angle error of robots 3 and 4 in the formation.

The results of the full communication case are evidently more consistent than those of the limited communication one. Using full communication, all robots reach the goal in under 15 seconds while formation errors remain low.

The limited communication results are very inconsistent. Though the light bulb is reached in under 30 seconds in all cases, the duration until the source is found varies a lot.

Moreover, the formation errors become very high in some of the experiments. The reason for this is the fact that using limited communication, the robots do not all have the same set of data to use for their gradient estimation. Therefore their estimated gradients can vary much more than those of the full communication case, resulting in them moving in different directions. This is why the errors increase specifically as the formation comes closer to the source, since the gradient is higher here such that the effect of the differences in movement directions is intensified (Menck [2017]).

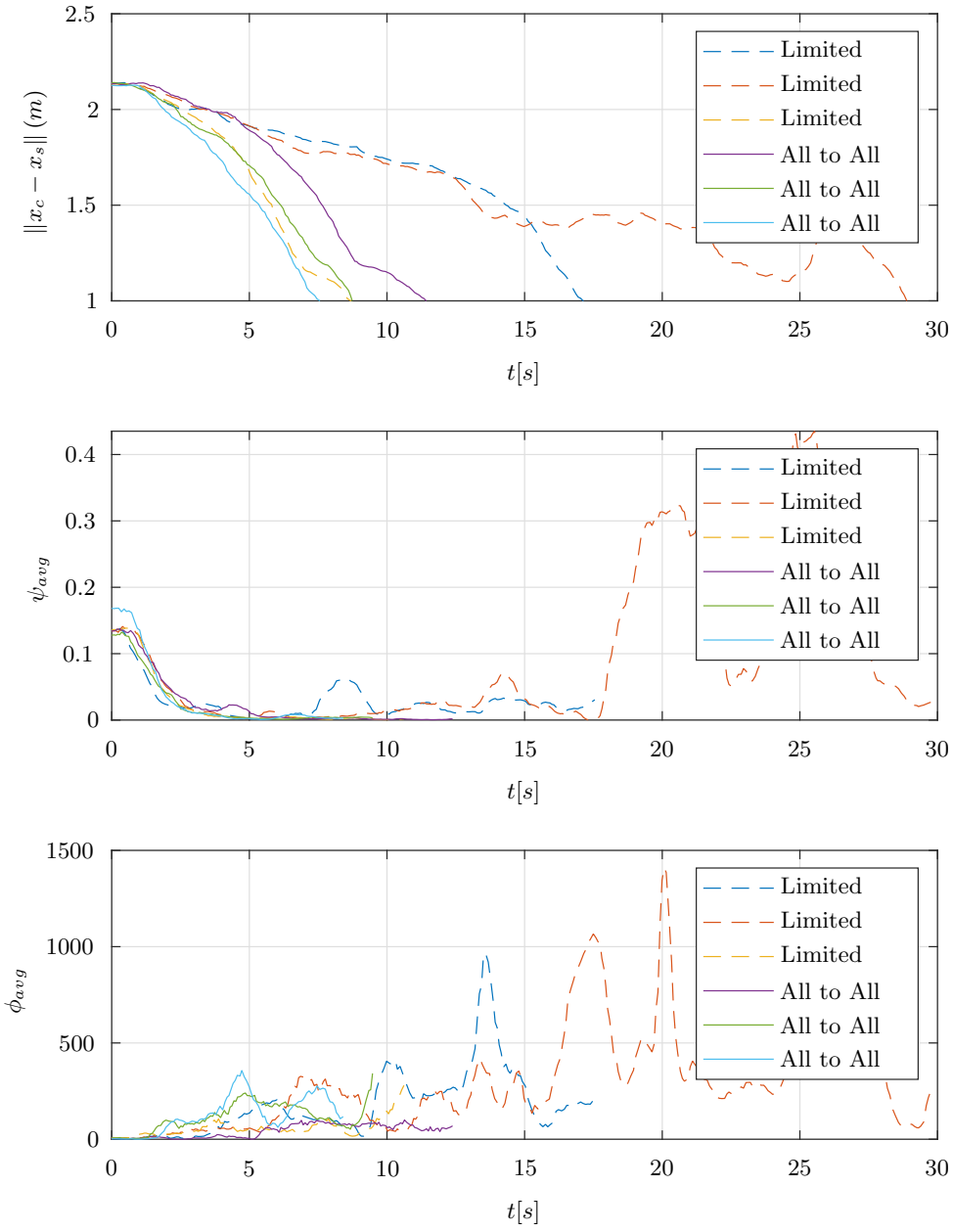

Figure 7.4.12: Distance between the formation center and source $||x_c - x_s||$, average distance errors ψ_{avg} and average angle errors ϕ_{avg} plotted over time t (Section 7.4.5)

7.5 Conclusion

In this chapter, experimental results about the implementation of the proposed control laws for source seeking with non-holonomic agents are presented. In order to implement the source seeking strategy, a group of wheeled robots was implemented. Each robot is equipped with infrared sensors to detect the intensity of light in the environment. The source is a bulb of light and the scalar field is the intensity of the light in the environment. The distance between robots is detected via a camera which is located on top and with image processing software distances are calculated and then transferred via wireless communication to the corresponding robots. Each robot has a local controller to control the velocity of each wheel. The distributed source seeking and formation control scheme works at a high level in each robot to steer the robot to the desired formation and then to lead the whole formation toward the source of light which is located in the corner of the area. Regarding the results of experimental implementation, robots first achieve the desired formation and then move toward the source, and the center of formation is stabilized close to the light source.

Chapter 8

Conclusions and Outlook

In this thesis, distributed algorithms to solve both formation control and source seeking problems for a multi-agent system have been presented. To tackle formation control, two different algorithms based on a displacement or distance-based formation, have been proposed. Then by a combination of distance-based formation control with source seeking a novel distributed algorithm for multi-agent source seeking has been developed. The distributed algorithm consists of three parts, formation control, collision avoidance, and a source-seeking trajectory controller. The local formation controller in each agent uses its local coordinate system to achieve and maintain the formation. The local collision avoidance schemes use measurements captured to generate an avoidance force. The local source-seeking controller uses information from neighbors to estimate the local gradient.

The main new feature in all proposed approaches is implementing the source seeking and formation control algorithms in each agent individually. This feature can be very useful when because of environmental restrictions, there is no access to global positioning. Examples are tunnels, underwater, in roofed places, or underground, where there is no GPS active and each agent should maintain the formation based on local information.

The dynamic models of agents considered in the proposed approaches are single and double integrator and nonlinear, non-holonomic dynamic models.

Experimental validation of the source-seeking approach on a physical wheeled robots shows the effectiveness of proposed controllers. In the experimental platform, the robots only know their distances with their neighbors, and based on that and the measurement of light intensity captured via infrared sensors, each non-holonomic wheeled robot maintains the formation and moves toward the source of light.

All mentioned algorithms are presented with stability analysis, which shows that under certain assumptions the multi-agent system can move toward the scalar field's source by maintaining the formation without collision.

8.1 Future Directions

In this work these issues were not considered:

- **Noise and disturbances:**
  According to natural environment signals are corrupted with different sorts of disturbances, therefore, the problem of noise and disturbances needs to be considered in the real environment.
- **Multiple extremum in scalar field:**
  Scalar field in the real environment can have multiple maxima. In order to find all local maximums and also locate the global maximum, some solutions should be considered.
- **Time variant scalar field:**
  The scalar field can be variable in the real environment. In other words, the source can be moved in the environment, and therefore some solutions need to be applied to avoid closed loops and infinite movement of agents.
- **LTI agent model:**
  In addition to the integrator model and non-holonomic model, other agent models such as general LTI models need to be taken into account and control laws for them provided. The kinematic model that is used in this thesis for non-holonomic dynamics is unicycle kinematic, which can be extended to the bicycle model.

Bibliography

Ahmadi Barogh, S., Rosero, E., and Werner, H. (2015). Formation control of non-holonomic agents with collision avoidance. In *American Control Conference (ACC)*, pages 757–762.

Ahmadi Barogh, S. and Werner, H. (2016a). Cascaded formation control using angle and distance between agents with orientation control (part 1). In *UKACC International Conference on Control*, pages 1–6.

Ahmadi Barogh, S. and Werner, H. (2016b). Cascaded formation control using angle and distance between agents with orientation control (part 2). In *UKACC International Conference on Control*, pages 7–12.

Ahmadi Barogh, S. and Werner, H. (2017a). Cooperative source seeking with distance-based formation control and non-holonomic agents. *IFAC World Congress*, 50(1):7917–7922.

Ahmadi Barogh, S. and Werner, H. (2017b). Cooperative source seeking with distance-based formation control and single-integrator agents. *IFAC World Congress*, 50(1):7911–7916.

Al-Abri, S., Maxon, S., and Zhang, F. (2018). Integrating a pca learning algorithm with the susd strategy for a collective source seeking behavior. In *American Control Conference (ACC)*, pages 2479–2484.

Al-Abri, S., Wu, W., and Zhang, F. (2019). A gradient-free three-dimensional source seeking strategy with robustness analysis. *IEEE Transactions on Automatic Control*, 64(8):3439–3446.

Al-Abri, S. and Zhang, F. (2022). A distributed active perception strategy for source seeking and level curve tracking. *IEEE Transactions on Automatic Control*, 67(5):2459–2465.

Anderson, B. D. O., Yu, C., Fidan, B., and Hendrickx, J. M. (2008). Rigid graph control architectures for autonomous formations. *IEEE Control Systems*, 28(6):48–63.

Atanasov, N., Ny, J. L., and Pappas, G. (2014). Distributed algorithms for stochastic source seeking with mobile robot networks. *ASME Journal of Dynamic Systems, Measurement, and Control*, 137(3):031011–9.

Baillieul, J. and Suri, A. (2003). Information patterns and hedging brockett's theorem in controlling vehicle formations. In *IEEE Conference on Decision and Control (CDC)*, volume 1, pages 556–563.

Bandyopadhyay, S., Chung, S.-J., and Hadaegh, F. Y. (2017). Probabilistic and distributed control of a large-scale swarm of autonomous agents. *IEEE Transactions on Robotics*, 33(5):1103–1123.

Bard, G. V. (2011). Numerically estimating derivatives during simulations. In *International Conference on Modelling, Simulation, and Visualization Methods (MSV'11)*, pages 341–347.

Biggs, N., Biggs, N. L., and Norman, B. (1993). *Algebraic Graph Theory*. Number 67. Cambridge university press.

Bishop, A. (2011). A very relaxed control law for bearing-only triangular formation control. In *IFAC World Congress*, pages 5991–5998.

Bishop, A., Summers, T., and Anderson, B. (2013). Stabilization of stiff formations with a mix of direction and distance constraints. In *IEEE International Conference on Control Applications (CCA)*, pages 1194–1199.

Biyik, E. and Arcak, M. (2007). Gradient climbing in formation via extremum seeking and passivity-based coordination rules. In *IEEE Conference on Decision and Control (CDC)*, pages 3133–3138.

Brinon-Arranz, L., Schenato, L., and Seuret, A. (2016). Distributed source seeking via a circular formation of agents under communication constraints. *IEEE Transactions on Control of Network Systems*, 3(2):104–115.

Brinon-Arranz, L., Seuret, A., and Canudas-de Wit, C. (2011). Collaborative estimation of gradient direction by a formation of AUVs under communication constraints. In *IEEE Conference on Decision and Control (CDC) and European Control Conference (ECC)*, pages 5583–5588.

Brinon-Arranz, L., Seuret, A., and de Wit, C. C. (2014). Cooperative control design for time-varying formations of multi-agent systems. *IEEE Transactions on Automatic Control*, 59(8):2283–2288.

Chen, J., Sun, D., Yang, J., , and Chen, H. (2010). Leader-follower formation control of multiple non-holonomic mobile robots incorporating a receding-horizon scheme. *Int J Robot Res*, 29(6):727–747.

Chen, Y.-Q. and Wang, Z. (2005). Formation control: a review and a new consideration. In *IEEE/RSJ International Conference on Intelligent Robots and Systems*, pages 3181–3186.

Consolini, L., Morbidi, F., Prattichizzo, D., and Tosques, M. (2008). Leader-follower formation control of nonholonomic mobile robots with input constraints. *Automatica*, 44(5):1343–1349.

Consolini, L., Morbidi, F., Prattichizzo, D., and Tosques, M. (2009). Stabilization of a hierarchical formation of unicycle robots with velocity and curvature constraints. *IEEE Transactions on Robotics*, 25(5):1176–1184.

Dimarogonas, D. and Johansson, K. (2008). On the stability of distance-based formation control. In *IEEE Conference on Decision and Control (CDC)*, pages 1200–1205.

Dimarogonas, D. V. and Kyriakopoulos, K. J. (2007). On the rendezvous problem for multiple nonholonomic agents. *IEEE Transactions Automat. Contr.*, 52(5):916–922.

Dong, W. and Farrell, J. A. (2008). Cooperative Control of Multiple Nonholonomic Mobile Agents. *IEEE Transactions Automat. Control.*, 53(6):1434–1448.

Dorfler, F. and Francis, B. (2010). Geometric analysis of the formation problem for autonomous robots. *IEEE Transactions on Automatic Control*, 55(10):2379–2384.

Eren, T. (2012). Formation Shape Control Based on Bearing Rigidity. *International Journal of Control*, 85(9):1361–1379.

Fabbiano, R. (2015). *Collaborative source-seeking control*. PhD thesis, Université Grenoble Alpes.

Fabbiano, R., de Wit, C. C., and Garin, F. (2014). Distributed source localisation with no position information. In *European Control Conference (ECC)*, pages 569–574.

Fabbiano, R., Garin, F., and Canudas-de Wit, C. (2018). Distributed source seeking without global position information. *IEEE Transactions on Control of Network Systems*, 5(1):228–238.

Farrell, J. A., Pang, S., and Li, W. (2005). Chemical plume tracing via an autonomous underwater vehicle. *IEEE Journal of Oceanic Engineering*, 30(2):428–442.

Fidan, B., Gazi, V., Zhai, S., Cen, N., and Karatas, E. (2013). Single-view distance-estimation-based formation control of robotic swarms. *IEEE Transactions on Industrial Electronics*, 60(12):5781–5791.

G. Leitmann, G. and Skowronski, J. (1977). Avoidance Control. *Optimization Theory and Applications*, 23(4):581–591.

Gazi, V. and Passino, K. M. (2004). Stability analysis of social foraging swarms. *IEEE Transactions on Systems, Man, and Cybernetics, Part B (Cybernetics)*, 34(1):539–557.

Gonzalez, A. M. and Werner, H. (2014). LPV formation control of non-holonomic multi-agent systems. *IFAC World Congress*, 47(3):1997–2002.

Gonzlez, A., Arags, R., Lpez-Nicols, G., and Sags, C. (2019). Formation control synthesis in local frames under communication delays and switching topology: An lmi approach. In *American Control Conference (ACC)*, pages 5328–5333.

Gouvea, J., Pereira, A., Hsu, L., and Lizarralde, F. (2010). Adaptive formation control of dynamic nonholonomic systems using potential functions. In *American Control Conference (ACC)*, pages 230–235.

Hutchinson, M., Oh, H., and Chen, W.-H. (2017). A review of source term estimation methods for atmospheric dispersion events using static or mobile sensors. *Information Fusion*, 36:130–148.

Jadbabaie, A., Lin, J., and Morse, A. (2003). Coordination of groups of mobile autonomous agents using nearest neighbor rules. *IEEE Transactions Automatic Control*, 48(6):988–1001.

Kiefer, M. (2015). *Design and Implementation of a Formation Control Scheme for Wheeled Robots in a Plane*. Master's Thesis, Institute of Control Systems, Hamburg University of Technology, Hamburg, Germany.

Kostić, D., Adinandra, S., Caarls, J., van de Wouw, N., and Nijmeijer, H. (2010). Saturated control of time-varying formations and trajectory tracking for unicycle multi-agent systems. In *IEEE Conference on Decision and Control (CDC)*, pages 4054–4059.

Krick, L., Broucke, M., and Francis, B. (2008). Stabilization of infinitesimally rigid formations of multi-robot networks. In *IEEE Conference on Decision and Control (CDC)*, pages 477–482.

Lawton, J., Beard, R. W., and Young, B. J. (2003). A decentralized approach to formation maneuvers. *IEEE Transactions Robot. Automat.*, 19(6):933–941.

Lazna, T., Gabrlik, P., Jilek, T., and Zalud, L. (2018). Cooperation between an unmanned aerial vehicle and an unmanned ground vehicle in highly accurate localization of gamma radiation hotspots. *International Journal of Advanced Robotic Systems*, 15(1):1–16.

Li, G., St-Onge, D., Pinciroli, C., Gasparri, A., Garone, E., and Beltrame, G. (2019). Decentralized progressive shape formation with robot swarms. *Autonomous Robots*, 43(6):1505–1521.

Li, S., Kong, R., and Guo, Y. (2014). Cooperative distributed source seeking by multiple robots: Algorithms and experiments. *IEEE/ASME Transactions on Mechatronics*, 19(6):1810–1820.

Lin, Z., Francis, B., and Maggiore, M. (2005). Necessary and sufficient graphical conditions for formation control of unicycles. *IEEE Automatic Control*, 50(1):121–127.

Listmann, K., Masalawala, M., and Adamy, J. (2009). Consensus for formation control of nonholonomic mobile robots. In *IEEE International Conference on Robotics and Automation, ICRA '09.*, pages 3886–3891.

Mastellone, S., Stipanovic, D. M., Graunke, C. R., Intlekofer, K. A., and Spong, M. W. (2008). Formation control and collision avoidance for multi-agent non-holonomic systems: Theory and experiments. *Int. J. Robotics Research*, 27(1):107–126.

Mateo, D., Kuan, Y. K., and Bouffanais, R. (2017). Effect of correlations in swarms on collective response. *Scientific Reports*, 7(1):1–11.

Meiners, F. (2014). *Implementation and Experimental Validation of Formation Control for Non-Holonomic Vehicles*. Master's Project, Institute of Control Systems, Hamburg University of Technology, Hamburg, Germany.

Menck, O. (2017). *Implementation of Formation Control with Source Seeking for Non-Holonomic Agents*. Master's Project, Institute of Control Systems, Hamburg University of Technology, Hamburg, Germany.

Mesbahi, M. and Egerstedt, M. (2010). *Graph Theoretic Methods in Multiagent Networks*. Princeton University Press, Princeton and Oxford.

Montijano, E., Zhou, D., Schwager, M., and Sagues, C. (2014). Distributed formation control without a global reference frame. In *American Control Conference*, pages 3862–3867.

Moore, B. J. and Canudas-de Wit, C. (2010). Source seeking via collaborative measurements by a circular formation of agents. In *American Control Conference (ACC)*, pages 6417–6422.

Ogren, P., Fiorelli, E., and Leonard, N. E. (2004). Cooperative control of mobile sensor networks:Adaptive gradient climbing in a distributed environment. *IEEE Transactions Automat. Contr.*, 49(8):1292–1302.

Oh, K.-K. and Ahn, H.-S. (2014). Distance based undirected formations of single integrator and double integrator modeled agents in n dimensional space. *International Journal of Robust and Nonlinear Control*, 24(12):1809–1820.

Oh, K.-K., Park, M.-C., and Ahn, H.-S. (2012). A survey of multi-agent formation control: Position-, displacement-, and distance-based approaches. *Gist DCASL TR*, 2.

Oh, K.-K., Park, M.-C., and Ahn, H.-S. (2015). A survey of multi-agent formation control. *Automatica*, 53:424–440.

Olfati-Saber, R., Fax, J., and Murray, R. (2007). Consensus and cooperation in networked multi-agent systems. *Proceedings of the IEEE*, 95(1):215–233.

Olfati-Saber, R. and Murray, R. M. (2004). Consensus problems in networks of agents with switching topology and time-delays. *IEEE Transactions Automat. Contr.*, 49(9):1520–1533.

Park, M.-C. and Hyo-Sung, A. (2015). Distance-based control of formation with orientation control. In *IEEE Conference on Decision and Control (CDC)*, pages 2199–2204.

Pereira, A. R., Gouvea, J. A., Lizarralde, F. C., and Hsu, L. (2011). Formation adaptive control for nonholonomic dynamic agents: Regulation and tracking. *IFAC Proceedings Volumes*, 44:8969–8974.

Queralta, J. P., Gia, T. N., Tenhunen, H., Westerlund, T., Qingqing, L., and Zou, Z. (2019a). Distributed progressive formation control with one-way communication for multi-agent systems. In *IEEE Symposium Series on Computational Intelligence (SSCI)*, pages 2012–2019.

Queralta, J. P., Mccord, C., Gia, T., Tenhunen, H., and Westerlund, T. (2019b). Communication-free and index-free distributed formation control algorithm for multi-robot systems. 151:431–438.

Rabbat, M. and Nowak, R. (2004). Distributed optimization in sensor networks. In *Third International Symposium on Information Processing in Sensor Networks. IPSN*, pages 20–27.

Ren, W. (2006). Consensus based formation control strategies for multi-vehicle systems. In *American Control Conference (ACC)*, pages 6–11.

Rosero, E. and Werner, H. (2014). Cooperative source seeking via gradient estimation and formation control (part 1). In *UKACC International Conference on Control*, pages 628–633.

Sadowska, A., Huijberts, H., Kostic, D., van de Wouw, N., and Nijmeijer, H. (2011). Formation control of unicycle robots using the virtual structure approach. In *Advanced Robotics (ICAR), 15th International Conference on*, pages 365–370.

Sadowska, A., Kostic, D., van de Wouw, N., Huijberts, H., and Nijmeijer, H. (2012). Distributed formation control of unicycle robots. In *IEEE International Conference on Robotics and Automation (ICRA)*, pages 1564–1569.

Senga, H., Kato, N., Ito, A., Niou, H., Yoshie, M., Fujita, I., Igarashi, K., and Okuyama, E. (2007). Development of spilled oil tracking autonomous buoy system. In *OCEANS 2007*, pages 1–10.

Spears, W. M., Spears, D. F., Hamann, J. C., and Heil, R. (2004). Distributed, physics-based control of swarms of vehicles. *Autonomous Robots*, 17(137):428–442.

Sun, Z. and Anderson, B. D. O. (2015). Rigid formation control with prescribed orientation. In *IEEE International Symposium on Intelligent Control (ISIC)*, pages 639–645.

Tran, V.-H. and Lee, S.-G. (2011). A stable formation control using approximation of translational and angular accelerations. *International Journal of Advanced Robotic Systems*, 8(1):65–75.

Turgeman, A., Datar, A., and Werner, H. (2019). Gradient free source-seeking using flocking behavior. In *American Control Conference (ACC)*, pages 4647–4652.

Turgeman, A. and Werner, H. (2017). Mission control - combined solutions for source seeking and level curve tracking in a time-varying field. In *American Control Conference (ACC)*, pages 4268–4273.

Verginis, C. K., Nikou, A., and Dimarogonas, D. V. (2017). Position and orientation based formation control of multiple rigid bodies with collision avoidance and connectivity maintenance. In *IEEE Conference on Decision and Control (CDC)*, pages 411–416.

Wang, J.-W., Guo, Y., Fahad, M., and Bingham, B. (2019). Dynamic plume tracking by cooperative robots. *IEEE/ASME Transactions on Mechatronics*, 24(2):609–620.

Wu, W. and Zhang, F. (2012). Robust cooperative exploration with a switching strategy. *IEEE Transactions on Robotics*, 28(4):828–839.

Yamaguchi, H. (2002). A distributed motion coordination strategy for multiple non-holonomic mobile robots in cooperative hunting operations. In *IEEE Conference on Decision and Control (CDC)*, volume 3, pages 2984–2991.

Zhang, C., Siranosian, A., and Krstic, M. (2007). Extremum seeking for moderately unstable systems and for autonomous vehicle target tracking without position measurements. *Autonomous Robots*, 43(10):1832–1839.

Zhang, F. and Leonard, N. E. (2010). Cooperative filters and control for cooperative exploration. *IEEE Transactions on Automatic Control*, 55(3):650–663.

Zhao, S. and Zelazo, D. (2015). Bearing-based formation stabilization with directed interaction topologies. In *IEEE Conference on Decision and Control (CDC)*, pages 6115–6120.

Zhaoa, S., Linb, F., Pengb, K., Chena, B., and Lee, T. (2014). Distributed control of angle-constrained cyclic formations using bearing-only measurements. *Systems and Control Letters*, 63:12–24.

Symbols and Abbreviations

MAS	Multi-Agent System
$\hat{g}_i(t)$	Estimated gradient in agent i
$\mathcal{L}$	Laplacian matrix
λ_1	First eigenvalue of matrix $\mathcal{L}$
G_f	Formation graph
G_s	Source seeking communication graph
$\mathcal{A}$	Adjacency matrix
$\mathcal{N}_i$	Neighbor set of agent i
$\mathcal{V}$	Node set of graph
μ	Scalar field value
ω_i	Angular velocity of agent i
Ψ^i	Distance error for agent i
Φ^i	Angle error for agent i
$\|.\|$	Euclidean norm
R_i	Non holonomic matrix of agent i
M_i	Mass and inertia moment of agent i
v_i	Speed of agent i
τ_i	Torque input of agent i
$\mathbb{R}^2$	2D plane
θ_i	Orientation of agent i
k_θ	Angular velocity gain
k_v	Speed gain
V_{ai}	Collision Avoidance function
p^i	Position of agent i in its own coordinate system
k_o	Collision avoidance gain
k_t	Source seeking gain
k_s	Sign function gain
k_f	Formation gain
k_s	Sign function gain
p_s	Source position
p_c	Formation center
$sgn(.)$	Sign function

Publications

- Ahmadi Barogh, Siavash, Rosero, Esteban and Werner, Herbert. "Formation control of non-holonomic agents with collision avoidance", *American Control Conference (ACC)*, July, 2015: pp. 757-762
- Ahmadi Barogh, Siavash and Werner, Herbert. "Cascaded formation control using angle and distance between agents with orientation control (part 1)", *UKACC International Conference on Control*, August, 2016: pp. 1-6
- Ahmadi Barogh, Siavash and Werner, Herbert. "Cascaded formation control using angle and distance between agents with orientation control (part 2)", *UKACC International Conference on Control*, August, 2016: pp. 7-12
  - **The Best Paper Award in UKACC International Conference**
- Ahmadi Barogh, Siavash and Werner, Herbert. "Cooperative source seeking with distance-based formation control and singe-integrator agents", *IFAC World Congress*, July, 2017: pp. 7911-7916
- Ahmadi Barogh, Siavash and Werner, Herbert. "Cooperative source seeking with distance-based formation control and non-holonomic agents", *IFAC World Congress*, July, 2017: pp. 7917-7922